Elucidation of WISP3 function in human mesenchymal stem cells and chondrocytes

Dissertation zur Erlangung des
naturwissenschaftlichen Doktorgrades
der Bayerischen Julius-Maximilians-Universität Würzburg

vorgelegt von
Sylvia Hondke

geboren in Potsdam

Würzburg, 2014

Einreichung _____ in Würzburg

Mitglieder der Promotionskommission

Vorsitzender	Prof. Dr. Markus Engstler
1. Gutachter	Prof. Dr. Norbert Schütze
2. Gutachter	Prof. Dr. Manfred Alsheimer

Tag des Promotionskolloquiums _____ in Würzburg

Doktorurkunde ausgehändigt am: _____ in Würzburg

Hiermit erkläre ich, dass ich die vorliegende Dissertation selbstständig verfasst und keine anderen als die angegebenen Hilfsmittel genutzt habe. Alle wörtlich oder inhaltlich übernommenen Stellen habe ich als solche gekennzeichnet. Ich versichere außerdem, dass ich die vorliegende Dissertation nur in diesem und keinem anderen Promotionsverfahren eingereicht habe und, dass diesem Promotionsverfahren keine endgültig gescheiterten Promotionsverfahren vorausgegangen sind.

Würzburg, den 16.10.2014

Sylvia Hondke

Table of Contents

List of Figures

List of Tables

Acknowledgment

I like to thank my supervisor Prof. Norbert Schütze for the possibility to conduct my PhD Thesis at the Orthopaedic Center for Musculoskeletal Research located at the Orthopaedic Clinic of Würzburg. Moreover, giving me the chance to present part of my data at national and international conferences.

Furthermore, my gratitude goes to Prof. Manfred Alsheimer for accepting the position as my second supervisor enabling the dissertation at the Faculty of Biology at the University of Würzburg.

I am greatly indepted to Prof. Franz Jakob for the helpful discussions and visions concerning my work as well as the support during the discussion of this work. Additionally, I would like to thank his lab, Monika Hofmann and the orthopaedic physicians for their helpfull cooperation in many aspects.

Without the other PhD students in my lab, my research and everyday life would not have been what it was. I would like to thank Meike Simann, Julia Dotterweich, Bettina Hafen and Solange LeBlanc for vivid discussions, encouragement, coffee breaks when needed, help in and outside the lab. Moreover, I'm grateful for any help during microarray experiments to Katrin Schlegelmilch and other laboratory problems to Tatjana Schilling. I would also like to thank the technical assistants Viola Zehe, Susanne Wiesner, Beate Geyer and Jutta Schneidereit who supported my work and created an excellent working atmosphere inspite of the difficulties we faced.

I am very grateful to Claudia Semprich for all the corrections concerning language and clear arrangements of this thesis.

At the end, I am deeply indepted to my parents and brother who always believed and supported me in every way they could. At last, my gratitude goes to my boyfriend Felix who endured my doubts and worries always assuring me that everything will be fine in the end.

Abstract

WISP3 is a member of the CCN family which comprises six members found in the 1990's: **C**ysteine-rich, angiogenic inducer 61 (CYR61, CCN1), **C**onnective tissue growth factor (CTGF, CCN2), **N**ephroblastoma overexpressed (NOV, CNN3) and the Wnt1 inducible signalling pathway protein 1-3 (WISP1-3, CCN4-6). They are involved in the adhesion, migration, mitogenesis, chemotaxis, proliferation, cell survival, angiogenesis, tumorigenesis, and wound healing by the interaction with different integrins and heparan sulfate proteoglycans. Until now the only member correlated to the musculoskeletal autosomal disease Progressive Pseudorheumatoid Dysplasia (PPD) is WISP3. PPD is characterised by normal embryonic development followed by cartilage degradation over time starting around the age of three to eight years. Animal studies in mice exhibited no differences between knock out or overexpression compared to wild type litter mates, thus were not able to reproduce the symptoms observed in PPD patients. Studies *in vitro* and *in vivo* revealed a role for WISP3 in antagonising BMP, IGF and Wnt signalling pathways. Since most of the knowledge of WISP3 was gained in epithelial cells, cancer cells or chondrocyte cell lines, we investigated the roll of WISP3 in primary human mesenchymal stem cells (hMSCs) as well as primary chondrocytes.

WISP3 knock down was efficiently established with three short hairpin RNAs in both cell types, displaying a change of morphology followed by a reduction in cell number. Simultaneous treatment with recombinant WISP3 was not enough to rescue the observed phenotype nor increase the endogenous expression of WISP3. We concluded that WISP3 acts as an essential survival factor, where the loss resulted in the passing of cell cycle control points followed by apoptosis. Nevertheless, Annexin V-Cy3 staining and detection of active caspases by Western blot and immunofluorescence staining detected no clear evidence for apoptosis. Furthermore, the gene expression of the death receptors TRAILR1 and TRAILR2, important for the extrinsic activation of apoptosis, remained unchanged during WISP3 mRNA reduction. Autophagy as cause of cell death was also excluded, given that the autophagy marker LC3 A/B demonstrated to be uncleaved in WISP3-deficient hMSCs. To reveal correlated signalling pathways to WISP3 a whole genome expression analyses of WISP3-deficient hMSCs compared to a control (scramble) was performed. Microarray analyses exhibited differentially regulated genes involved in cell cycle control, adhesion, cytoskeleton and cell death. Cell death observed by WISP3 knock down in hMSCs and chondrocytes might be explained by the induction of necroptosis through the BMP/TAK1/RIPK1 signalling axis. Loss of WISP3 allows BMP to bind its receptor activating the Smad 2/3/4 complex which in turn can activate TAK1 as previously demonstrated in epithelial cells. TAK1 is able to block caspase-dependent apoptosis thereby triggering the assembly of the necrosome resulting in cell death by necroptosis.

Together with its role in cell cycle control and extracellular matrix adhesion, as demonstrated in human mammary epithelial cells, the data supports the role of WISP3 as tumor suppressor and survival factor in cells of the musculoskeletal system as well as epithelial cells.

Zusammenfassung

WISP3 ist ein Mitglied der CCN-Familie, die aus sechs Familienmitgliedern besteht und in den 1990er Jahren endeckt wurde: **C**ysteine-rich, angiogenic inducer 61 (CYR61, CCN1), **C**onnective tissue growth factor (CTGF, CCN2), **N**ephroblastoma overexpressed (NOV, CNN3) und den Wnt1 inducible signalling pathway protein 1-3 (WISP1-3, CCN4-6). Die CCN-Proteine sind durch ihre Interaktion mit verschiedenen Integrinen und Heparansulfaten involviert in die Regulation der Adhäsion, der Migration, der Mitogenese, der Chemotaxis, der Proliferation, des Zellüberlebens, der Angiogenese, der Tumorgenese und der Wundheilung. WISP3 ist momentan das einzige Mitglied, das direkt mit einer muskuloskelettalen Erkrankung, der Progressiven Pseudorheumatoiden Dysplasie (PPD), assoziiert wird. PPD ist charakterisiert durch eine normale embryonale Entwicklung mit fortschreitender Knorpeldegeneration beginnend im Alter von drei bis acht Jahren.

Tierversuche mit knock out oder Überexpression von WISP3 in Mäusen waren nicht in der Lage die Symptome der Erkrankung nachzustellen, da keine Unterschiede im Vergleich zu den Wurfgeschwistern beobachtbar waren. *In vitro* und *in vivo* Studien offenbarten eine antagonisierende Rolle für WISP3 im BMP, IGF und Wnt Signalweg. Da die meisten Informationen über WISP3 jedoch in Epithel- und Krebszellen sowie immortalisierten Chondrozytenzelllinien generiert wurden, untersuchten wir die Rolle von WISP3 in primären humanen mesenchymalen Stammzellen (hMSZs) und primären Chondrozyten.

Der WISP3 knock down wurde mit drei short hairpin RNAs in beiden Zelltypen etabliert und wies eine veränderte Zellmorphologie sowie eine reduzierte Zellzahl auf. Knock down mit gleichzeitiger rekombinanter WISP3-Behandlung konnte den beobachteten Phänotyp sowie den Zellverlust nicht retten und auch eine Änderung der endogenen Genexpression von WISP3 war nicht zu detektieren. Schlussfolgernd muss WISP3 ein wichtiger Überlebensfaktor sein, dessen Verlust zur Überschreitung von Zellzyklus-Kontrollpunkten führt, was in Apoptose mündet. Apoptosenachweise wie Annexin V-Cy3 Färbung, Immunfluoreszenzfärbung und Western blot für aktive Caspasen lieferten keine positiven Beweise für diese Form des Zelltodes. Auch die Genexpression der Todesrezeptoren TRAILR1 und TRAILR2, wichtig für die extrinsische Aktivierung der Apoptose, zeigte kein verändertes Expressionsmuster in WISP3-defizienten hMSZs. Autophagie als Zelltod wurde ebenfalls ausgeschlossen, nachdem im Western Blot kein gespaltene Form des Autophagiemarkers LC3 A/B zu detektieren war. Um die Rolle von WISP3 beim Zelltod weiter zu entschlüsseln, wurden Genom-Expressionsanalysen von WISP3-defizienten hMSZs im Vergleich zu Kontroll-hMSZs angefertigt. Die Analysen ergaben unterschiedlich regulierte Gene vor allem in den Bereichen Zellzyklus-Regulation, Adhäsion, Zytoskelett und Zelltod. Der durch WISP3-Verlust ausgelöste Zelltod kann möglicherweise durch die Aktivierung der Nektroptose über den BMP/TAK1/RIPK1 Signalweg erklärt werden. Es ist bekannt, dass WISP3 BMP4 bindet und so dessen Bindung an den Rezeptor verhindert. Bei WISP3 Verlust bindet BMP4 an seinen Rezeptor und aktiviert den Smad 2/3/4 Komplex der wiederum TAK1 phosphoryliert, wie zuvor in Epithelzellen demonstriert. TAK1 ist in der Lage die Caspase-induzierte Apoptose zu blockieren und auf diese Weise die Bildung des Nekrosomes auszulösen, welches zum Zelluntergang durch Nekroptose führt.

Zusammen mit seiner Rolle in der Zellzyklus-Kontrolle und der extrazellulären Matrixadhäsion, die in humanen Brustepithelialzellen nachgewiesen wurden, unterstützen diese Daten eine Rolle für WISP3 als Tumorsuppressor und Überlebensfaktor in Zellen des Epithel und des muskuloskelettalen Systems.

Part I

Introduction

Chapter 1

WISP3 - member of the CCN family

1.1 Structure and function

Matricellular proteins serve a non-structural function in the extracellular matrix (ECM), thereby influencing the adhesion, migration, proliferation, differentiation and apoptosis of cells. Their expression is characterised by high expression levels during development, injury and repair, while the expression decreases in adult tissue [1]. SPARCs, thrombospondins and CCNs form a multifamily, where members are composed of different protein domains but can be grouped by their function [2]. Among them is the CCN family which was discovered in the 1990's and named after the first three discovered members: **C**ysteine-rich, angiogenic inducer, 61 (CYR61), **C**onnective tissue growth factor (CTGF) and **N**ephroblastoma overexpressed (NOV) [3]. The family comprises six members, which were named after their discovery date: CCN1 (Cyr61, O'Brien et al. 1990 [4]), CCN2 (CTGF, Bradham et al. 1991 [5]), CCN3 (NOV, Joliot et al. 1992 [6]) and the last members CCN4-CCN6 (Wnt1 inducible signalling pathway protein 1-3, Pennica et al. 1998 [7]). They emerged approximately 40 million years ago [8] and show a highly conserved nucleotide sequence homology of 30-50 % [9] as well as an amino acid homology of 40-60 % [10]. The cysteine-rich 348 to 381 amino acid long proteins [8] contain 38 conserved cysteines [9], which make up nearly 10 % of the overall weight [11].

Every member of the family consists of five exons each coding for one protein domain. Exon one codes for the signal peptide, followed by the insulin-like growth factor binding protein-like domain (IGFBP), the von-Willebrand factor type C repeat domain (VWC), the trombospondin type-1 repeat domain (TSP-1) and the cysteine-knot containing domain (CT) - missing in WISP2 [9]. Some of the functions are covered by a single protein domain, while others need the interaction of two or more protein domains. The VWC domain is needed for oligomerisation, while cell attachment is achieved by the TSP-1 domain and the CT domain on the other hand is involved in the dimerisation process [8]. The hinge region, between the VWC and TSP-1 domain, is highly susceptible to protease cleavage [12] and displays varying amino acid sequences among the CCN members (Figure 1) [8]. Therefore the hinge region is thought to be necessary for truncated protein formation [9].

After thorough search for a specific receptor [2] it is now accepted that the CCN proteins mainly orchestrate their actions by binding integrins and heparan sulfate proteoglycans (HSPG). Furthermore, it was found that binding of integrins often occurs outside the conserved motifs found in integrins e.g. RGD-motif [10]. CCN proteins interact with the integrins $\alpha 2\beta 1$, $\alpha 5\beta 1$, $\alpha 6\beta 1$, $\alpha v\beta 5$, $\alpha IIb\beta 3$, $\alpha M\beta 2$, $\alpha D\beta 2$ and $\alpha v\beta 3$ [13]. As for HSPG, some of the family members bind to syndecan 4, biglycan, decorin and perlecan [10] as well as vitronectin and fibronectin [14], thereby positively or negatively influencing Wnt [8], bone morphogenic protein (BMP) and transforming growth factor beta (TGFβ) signalling pathways [2] leading to their modifying role in a broad spectrum of cell biological functions like adhesion, mitogenesis, migration, chemotaxis, cell survival, differentiation, angiogenesis, chondrogenesis, tumorigenesis and wound healing [9].

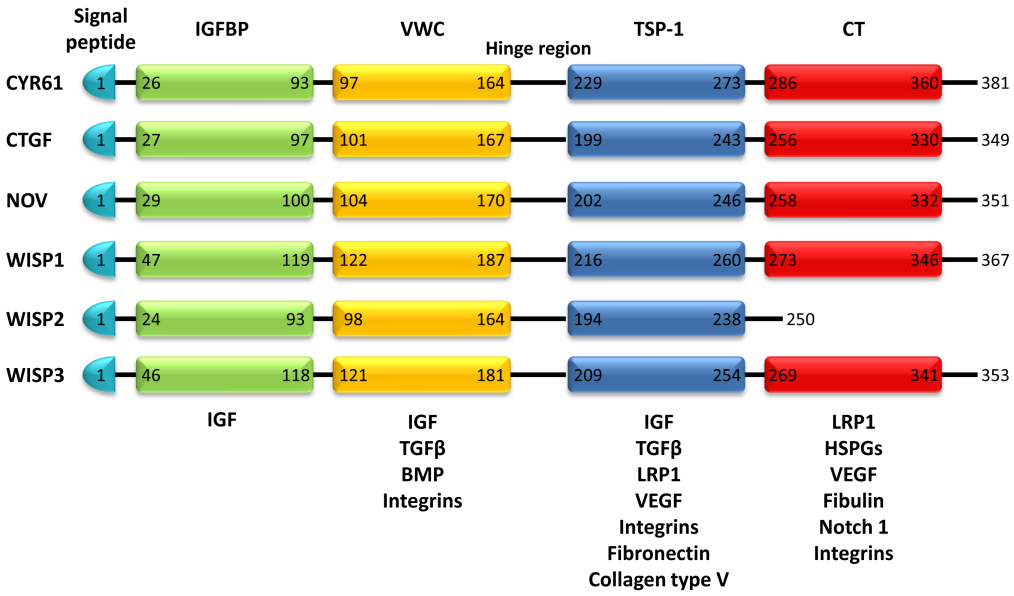

Figure 1 Scheme of CCN protein family domain structure.
CCN proteins display a length of 348 to 381 amino acids, except for WISP2 which lacks the CT domain. The protein starts with a signal peptide (light blue) of 25-30 amino acids followed by the IGFBP domain (green), the VWC domain (yellow) which is connected to the TSP-1 domain (blue) by a highly variable hinge region and is completed by the CT domain (red). The CCN proteins possess a 40-60 % amino acid homology with 38 conserved cysteine residues which make up for 10 % of the protein mass [9]. Underneath the protein domains possible interaction partners are listed (IGF - insulin-like growth factor, TGFβ - transforming growth factor beta, BMP - bone morphogenic protein, LRP1 - low density lipoprotein receptor-related protein 1, VEGF - vascular endothelial growth factor, HSPG - heparan sulfate proteoglycan). The illustration combines the data presented in the following reviews [11, 13].

1.2 Deregulation of CCN in cancer

Due to their broad cellular interactions, it is no surprise that the CCN family is also involved in tumorigenesis and cancer. Deregulated expression levels in cancer or tumours were found in the following tissues and organs - breast, colon, gall bladder, stomach, ovarian, pancreas, prostate, brain, liver, lung, blood, skin and cartilage. Their presence can partly be explained by their angiogenic potential [13].
Moreover, some of the members are able to support survival signals. As seen for CYR61, which is upregulated in breast cancer cells and leads to an increased expression of anti-apoptotic XIAP (X-linked inhibitor of apoptosis) [15]. Since CYR61 is able to suppress the tumour growth of non-small lung cancer [16] as well as multiple myeloma cells thereby preventing bone resorption [17], the function of CCN proteins seems to be cell type specific.
In case of CTGF, 27 types of cancers are correlated with its change of expression in which an overexpression is mostly linked to poor survival rates except for lymphoma and gall bladder cancer where the survival rate is increased [18]. Altogether, the overexpression might improve angiogenesis since it is known to bind angiogenic regulators e.g. vascular endothelial growth factors (VEGFs) [19] or support invasion of new tissue environment due to interaction with adhesion molecules e.g. perlecan [20] and integrin α5β1 [2].
NOV, a relevant protein in skeletogenesis and antagonist of CTGF, is overexpressed in bone metastases and induces osteoclastogenesis via receptor activated NFκB ligand (RANKL) [21]. On the other hand, loss of WISP2 as well as WISP3 triggers epithelial-mesenchymal transition (EMT) in breast cancer cells contributing to the invasiveness of the cancer [22, 23]. WISP3 possesses an adenine mononucleotide sequence (9 adenines) in the coding region prone to mutations with changes in this region found in 31 % of colorectal cancer and in 11 % of gastric cancer [21]. Moreover, 80 % of inflammatory breast cancer

patients revealed a loss of WISP3 [24].

1.3 WISP3 in chondrogenesis and osteogenesis

In context to the musculoskeletal system CCN proteins are involved in the regulation of chondrogenesis and osteogenesis orchestrating TGFβ and BMP signalling. CYR61 is able to induce the expression of BMP2 via its binding to integrin αvβ3 [25] leading to an increase of chondrogenic marker expression [9] supporting the differentiation of mesenchymal stem cells (MSCs) into chondrocytes as seen in mouse MSCs [26].
CTGF on the other hand, is elevated in hypertrophic chondrocytes, calcified cartilage, ribs and vertebral column during embryogenesis [11]. This protein fine tunes osteogenesis by negative regulation of BMP signalling as demonstrated by CTGF knock out mice with an increase in osteoblast maturation and mineralisation [27]. However, double knock out of CYR61 and CTGF delays the osteogenesis of long bones and enlarges hypertrophic chondrocytes [2].
Additionally, NOV knock out mice exhibited abnormal skeletal development due to increased chondrogenesis and osteogenesis [28] in the same way as CTGF knock outs do [29]. Nevertheless, CTGF induces the expression of the chondrogenic markers aggrecan and collagen type II while NOV reverses this function [30].
WISP1 directly supports BMP2 induced osteogenesis by integrin αvβ3 binding as revealed by overexpression in bone marrow stroma cells (BMSC) where anti-integrin αvβ3 antibodies blocks BMP2 binding to BMSC [31]. In contrast, WISP3 is downregulated during chondrogenesis and osteogenesis [32] while in another study the overexpression in a chondrocyte cell line results in an increased protein level of aggrecan and collagen type II as well as mRNA level of SOX9 [33].
Elevated WISP3 protein expression was observed in damaged cartilage as well as in osteoarthritic cartilage [34] supporting the role for WISP3 in cartilage homoeostasis. In chondrosarcoma cells elevated levels of WISP3 allow cell migration by the increased expression of the intracellular adhesion molecule 1 (ICAM1) due to interaction of WISP3 to integrin αvβ3 and integrin αvβ5 followed by focal adhesion kinase (FAK) phosphorylation and the mitogen activated kinase kinase 1 and -2 (MEK1,-2) as well as c-Jun activation [35]. Chondrogenesis is supported by the insulin-like growth factor 1 (IGF1) [36] and controlled by WISP3 as demonstrated in the chondrocyte cell line C28I2 where it decreased the IGF1 secretion about 50 % [37]. Administration of WISP3 suppresses IGF-dependent collagen type X expression as well as alkaline phosphatase activity [37], markers for hypertrophy in cartilage [38].

1.4 Progressive Pseudorheumatoid Dysplasia

WISP3 is the only family member correlated to a disease affecting the musculoskeletal system known as the autosomal recessive Progressive Pseudorheumatoid Dysplasia (PPD). PPD is a rare disease with a prevalence of one in a million in the United Kingdom [39] and located to 2 cM on chromosome 6q22 [40]. Hurvitz *et al.* performed sequence analyses of WISP3 from different PPD patients, leading to the discovery of various mutations in this gene, mostly causing frame shifts resulting in protein truncation or failure of protein production [40]. Up until now 23 different mutations have been discovered [41]. The disease is characterised by a normal embryonic development and progressed cartilage loss starting in the first life decade, stiffness of all joints, motor weakness, knobby appearance of interphalangeal joints (IPJ) and articular pain [41].
Several animal studies were performed to reveal the function of WISP3 in PPD, surprisingly the animal models were not able to mirror the symptoms observed during the disease. Kutz *et al.* created a WISP3 knock out mouse where the IGFBP domain is fused to a β-galactosidase resulting in a truncated protein since the other domains are lost [42]. The mice were undistinguishable from their wild type litter mates

[42] and the same applied to WISP3 overexpressing mice [43]. Only the WISP3 knock out in zebrafish exhibited smaller mandibular and altered pharyngeal cartilage while the overexpression disturbed the dorsal-ventral patterning [44]. The studies revealed the direct binding of BMP4 and the low density lipoprotein receptor-related protein 6 (LRP6) as well as frizzled class receptor 8 (FZD8) to WISP3 thereby blocking Wnt and BMP signalling [42, 44]. The results raise the question as to how close the animal models really display the situation in PPD patients since their life span is much lower. Moreover, mice, human, and zebrafish WISP3 was introduced into the human embryonic kidney cell line HEK293T displaying a cleaved form for the mice and human WISP3 protein while zebrafish WISP3 was secreted as full length protein [44]. Thus, the truncated protein forms might still allow partial activity through the existing protein domains. Hence, the animal models reveal some aspects of WISP3 signalling pathway but are not an appropriate way to identify its role in human.

Nevertheless, only one study to this day examined articular chondrocytes isolated from a PPD patient revealing an increase in proliferation and a low apoptosis rate while the matrix metalloproteinases 1 (MMP), -3 and -13 are downregulated [45]. Overexpression studies in the chondrocyte cell lines TC28a2 and C28I2 show induced expression of chondrogenic markers [33] while mutations adapted from PPD patients caused a change in WISP3 protein distribution and delayed the collagen type II secretion into the ECM [46].

Chapter 2

Determination of cell fate

2.1 Cell cycle control

Additional roles for WISP3 signalling were found in cell cycle control where a knock down of WISP3 increases cyclin-dependent kinase 1 (CDK1), cell division cycle 25A (CDC25A) and -C as well as cyclin D1 in human mammary epithelial cells [47]. Moreover, reexpression of WISP3 in the WISP3-deficient human breast cancer cell line SUM149 induced the expression of the cell cycle inhibitors $p27^{kip1}$ and $p21^{Waf1}$ [23].

Cell cycle control is an important process to guarantee the correct replication of the genome. Thus, it is not surprising that it is tightly controlled at every interface between the cell cycle checkpoints. To undergo mitosis, a cell will grow during G1 phase before entering S phase, where DNA is replicated, followed by ongoing growth in G2 phase resulting in the entry of the mitotic phase. Main cell cycle checkpoints are in between G1 and S phase (G1/S) as well as at the transition from G2 into the mitosis (G2/M) [48]. The cell cycle is mainly regulated by cyclins and cyclin-dependent kinases (CDK). These form complexes that regulate genes like retinoblastoma (Rb), which in turn blocks the activity of E2F proteins that are involved in the regulation of genes controlling the progression of S phase as well as apoptosis related genes like apoptotic peptidase activating factor 1 (APAF1) [49].

In fact, there are numerous connections between cell cycle arrest and cell death. In case of DNA damage, p53 arrests the cell cycle at the G1/S checkpoint by activating $p21^{waf1}$ which in turn inhibits the CDK4-CDK6 complex [50]. Two studies have revealed that the absence of p53 and p21 in tumour cells accelerates their entry into mitosis [51, 52]. The G2/M checkpoint is controlled by CDK2 whose activity is either activated by CDC25C mediated dephosphorylation or inhibited by Wee which phosphorylates CDK2 [48]. To remove the checkpoint, CDC25C is bound to 14-3-3 proteins, leading to nuclear export, stabilising the phosphorylation at CDK1 [53, 54]. Defects in cell cycle control can result in programmed cell death, gene mutation, chromosome damage and aneuploidy which in turn favour tumorigenesis [53].

2.2 Cell death

From this point of view, cell death is a crucial process that allows the proper regulation of cell development, growth and damage to support cellular homoeostasis. Especially in embryogenesis removal of cells is fundamental for the development of a functional organism. [55]. Dysfunction of this process may cause uncontrolled growth as seen in cancer [56]. A broad spectrum of cell death forms exists: most prevalent apoptosis, necrosis and autophagy.

It is well known that the first three members of the CCN family are able to induce TNFα-dependent apoptosis in a NFκB-independent way [57]. CYR61 can trigger cytochrome C release by ROS induced activation of the p38 mitogen-activated protein kinase (MAPK) [58]. Furthermore, WISP1 blocks p53 activated apoptosis by the phosphorylation of Bad which decreases the pro-apoptotic Bim/Bad complex and increases the anti-apoptotic Bcl-x_L/Bax complex. This seems to be coupled to Akt signalling, a survival pathway, since increased Bcl-x_L expression needs Akt phosphorylation [59]. Additionally, WISP3 knock down in the mammary epithelial cell lines MCF10A and HME allowed survival under serum-deprived conditions by the upregulation of Akt1 [47]. Hence, apoptosis was observed when WISP3 was re-expressed in SUM149 cells, which lack endogenous WISP3, together with a decrease in the proliferative markers cyclin E and the proliferating cell nuclear antigen (PCAN) [23].

2.2.1 Apoptosis

The term 'apoptosis' was introduced by Kerr *et al.* in 1972, to describe morphogenic changes observed during cell death [60] and further described a controlled cell death also referred to as programmed cell death. First phenotypic changes during apoptosis are phosphatidylserine translocation from the inner to the outer plasma membrane, shrinkage of cells, membrane blebbing, chromatin condensation followed by internucleosomal DNA fragmentation and development of apoptotic bodies. There is no universal trigger but a broad range of stimuli that induce apoptosis depending on the cell type [61].
The initiation of apoptosis is divided into intrinsic or extrinsic depending on the signalling cascade that is activated. The later is initiated by death receptors, mostly of the tumour necrosis factor (TNF) family, binding their specific extracellular ligands, thereby inducing the assembly of the death induced signalling complex (DISC) [62]. DISC is composed of the receptor's Fas-associated via death domain (FADD) as well as the pro-caspases 8 and -10 which are then activated [63]. These initiator caspases in turn activate the effector caspases 3, -6 and -7 which further cleave target proteins like lamin A and poly (ADP-ribose) polymerase (PARP) [64]. It is thought that the extrinsic pathway alone is not sufficient to induce apoptosis to its full extent [65].
Nevertheless, the extrinsic pathway also triggers the intrinsic signalling cascade by the activation of BH3 interacting domain death agonist (Bid) which then translocates to the mitochondrion and induces mitochondrial outer membrane permeabilisation (MOMP) [66], a key event in the intrinsic pathway. The integrity of the mitochondrion is mostly regulated by the Bcl-2 family [61] which is divided into three groups: the multidomain anti-apoptotic proteins (Bcl-2, Bcl-x_L, Mcl-1), the pro-apoptotic BH3-only proteins (Bid, Bad, NOXA, PUMA) and the multidomain pro-apoptotic proteins (Bax, Bak) [67]. The first group binds pro-apoptotic proteins thereby preventing MOMP, while the last group orchestrates the development of membrane pores [68]. The BH3-only proteins are needed for the multimerisation of Bax and Bad [69, 70] as well as the counteraction of anti-apoptotic proteins by the activation of Bax-like proteins e.g. Bid [71, 68]. Bad, Bax as well as Bid and Bcl-x_L are able to create pores in the mitochondrial membrane causing MOMP [72, 73, 74] which results in the release of apoptotic proteins into the cytoplasm [75].
The apoptosome, a wheel-shaped complex, is built up of cytochrome C, Apaf1 and ATP [76]. Cytochrome C released from the mitochondrion together with ATP triggers the activation and oligomerisation of Apaf1 monomers [76, 77]. Caspase 9 is mostly found as a monomer with low activity [78] and is only activated upon dimerisation as reported by Boatright *et al.* [79]. The assembled wheel-shaped complex binds caspase 9 [80] which then cleaves the effector caspases 3, -6 and -7 as well as the initiator caspases 8 and -10 [81, 64, 82]. The caspases further cleave target proteins amplifying the 'death signal' in a wide range of signalling cascades leading to the above mentioned apoptotic phenotypic changes.

2.2.2 Caspase-independent cell death

In case of disrupted caspase function another signalling pathway must substitute for the loss of apoptosis since the simultaneous knock out of caspase 3 and -9 in mice showed a normal embryonic development [83]. Another study demonstrated, that instead of the caspases, MOMP is essential for programmed cell death since 90 % of Bak and Bax deficient mice ($Bak^{-/-}$ and $Bax^{-/-}$) died prenatally unable to undergo coordinated cell death [84].
Chipuk *et al.* defined caspase-independent cell death (CICD) as proceeding cell viability loss, with sustained inhibition or disruption of caspase function, triggered by pro-apoptotic conditions [85]. CICD is mainly characterised by partial or no chromatin condensation as well as no DNA laddering while some markers of apoptosis are still present like shrinkage of the nucleus and loss of membrane potential [86]. Other changes include vacuolated cytoplasm, ribosome aggregation, swelling of mitochondrial membrane, no apoptotic bodies, sometimes loss of attachment and contradictory staining results for Annexin V [85].

It is still under debate as to which point CICD really exists *in vivo* since most studies were carried out *in vitro* with caspase inhibitors that are known to interfere with other proteases too [87].

2.2.3 Necrosis

Apoptosis was the only form of cell death thought to be a regulated process while necrosis was categorised as uncontrolled [88] before it became clear that there were defined patterns. Necrosis is characterised by rapid swelling of the cell resulting in rupture of the membrane and organelle break down [89]. A signalling pathway activated by TNF-like cytokines in the presence of caspase inhibition leads to necrosis [90] and that can be further divided in several subtypes like necroptosis, mitochondrial permeability transition-dependent regulated necrosis (MPT-RN) and parthanos [91].
Necroptosis is characterised by the assembly of the necrosome that is composed of RIPK3 and MLKL [92], which can be triggered by death receptors, damaged DNA [93] as well as TLR and further factors [94]. It is hypothesised that following activation the complex translocates to the plasma membrane causing a Ca^{2+} and Na^{+} influx disturbing the cellular homoeostasis [95].
On the other hand, parthanos displays a hyperactivation of PARP1, an enzyme normally involved in single and double strand DNA break repair [96]. NAD^{+}, a cofactor important for redox reactions [97], is essential for the dissociation of the PARP1 complex from DNA [98]. In case of PAPR1 hyperactivation, the NAD^{+} pool is depleted which leads to reduced ATP synthesis as well as the release of apoptotic inducing factors (AIF). Release of apoptotic proteins can also be observed in MPT-RN, caused by the influx of water through the inner mitochondrial membrane thereby disrupting the transmembrane potential [91].

2.2.4 Autophagy

A cell death form that was recognised later was the lysosomal autophagy that up until then was thought to only degrade and recycle cell components [99]. This process controls the level of over-produced, long lived or damaged proteins [100] and thereby counteracts cellular stress [101]. Autophagy can be divided in three subtypes: microautophagy, chaperon-mediated autophagy (CMA) and macroautophagy, the most common form [102].
In microautophagy cellular content is engulfed in nearby lysosomes by the formation of membrane invaginations [103]. In contrast, CMA is characterised by chaperone actions which specifically bind proteins marked for degradation transporting them to the lysosome, where these proteins become unfolded before entering the lysosome [104]. In macroautophagy, the dominant form, targeted proteins are enclosed in a double membrane vesicle, called autophagosome [105]. The autophagosomes act as cargo vesicles that fuse with the lyosomes where the content is degraded into amino acids and macromolecules by proteases. The recycled molecules are then transported back into the cytoplasm for reuse [106].
A connection between cell death and autophagy was often detected for cancer cells, where the cells undergo cell death due to autophagy in response to chemotherapeutical components [107, 108, 109]. All forms of cell death are interlinked amongst each other [110, 111].

Chapter 3

Aim of the study

CCN proteins are involved in a broad spectrum of signalling pathways like adhesion, migration, proliferation, differentiation and apoptosis. They act as adaptor proteins by binding to a set of integrins and heparan sulfate glycosaminoglycans. WISP3 is the only CCN protein directly correlated to the musculoskeletal disease Progressive Pseudorheumatoid Dysplasia (PPD) due to mutations found in the gene. With regard to the cartilage degradation in PPD, WISP3 is thought to be a regulator of cartilage homoeostasis. Several studies supported that role by the finding that WISP3 induces the expression of chondrogenic markers like collagen type II and aggrecan. Nevertheless, animal models with WISP3 knock out failed to mirror the symptoms seen in PPD patients also overexpression of WISP3 in mice showed no differences compared to their litter mates. The studies shed some light on binding partners and signalling pathways linked to WISP3 but until now most of the *in vitro* work was carried out in cancer cells e.g. breast cancer cells or in chondrocyte cell lines. Thus, to uncover the function of WISP3 in the musculoskeletal system we applied cellular assays and molecular techniques on human primary chondrocytes and human primary mesenchymal stem cells (hMSCs). Here I focused on:

1. Verification of constant endogenous expression in the investigated cell types by RT-PCR and qPCR
2. Influence of WISP3 on proliferation in these cells by recombinant protein treatment with various conentrations for 48 h
3. Reduction of WISP3 mRNA by a shRNA approach in hMSCs and primary chondrocytes
4. Whole genome analyses of WISP3-deficient hMSCs five days past transduction
5. Validation of the received microarray data with the same RNA as well as additional one with molecular approaches
6. Investigation of highlighted signalling pathways from the microarray analyses by molecular approaches
7. Examination of the phenotypic changes by immunohistochemical approaches

The study will help broaden the knowledge of WISP3 signalling in the musculoskeletal system. Thereby it will present possible new interaction partners or signalling pathways as start point for the development of therapeutics for cartilage preservation in PPD patients.

Part II

Material and methods

Chapter 4

Material

4.1 Equipment

Equipment	Supplier
Abimed Single Channel Pipette (10µL, 100µL, 1000µL)	Kinesis GmbH, Langenfeld, Germany
Autoclave Systec VX-75	Systec GmbH, Wettenberg, Germany
BioPhotometer	Eppendorf AG, Hamburg, Germany
Branson Digital Sonifier	Emerson Electrics, Danbury, USA
CFX96 Touch^{TM} Real-time PCR detection system	Bio-Rad Laboratories GmbH, München, Germany
Centrifuge Biofuge Fresco	Thermo Electron LED GmbH, Langenselbold, Germany
Centrifuge Function Line	Thermo Electron LED GmbH, Langenselbold, Germany
Centrifuge Micro FugOne	Thermo Electron LED GmbH, Langenselbold, Germany
CO_2 Incubator CB150	Binder GmbH, Tuttlingen, Germany
CO_2 Incubator Heracell240i	Fisher Scientific GmbH, Schwerte, Germany
Dishwasher	Miele & Cie. KG, Gütersloh, Germany
Drier	Thermo Electron LED GmbH, Langenselbold, Germany
FluorChemQ	Cell Biosciences Inc., Santa Clara, USA
Freezer Economic (-20°C)	Bosch GmbH, Gerlingen-Schillerhöhe, Germany
Freezer II Shin (-80°C)	Nunc GmbH & Co. KG, Wiesbaden, Germany
Fridge Freshcenter	Bosch GmbH, Gerlingen-Schillerhöhe, Germany
Gel documentation system	Vilber Lourmat Deutschland GmbH, Eberhardzell, Germany
Gel electrophoresis Mini Protean 3cell	Bio-Rad Laboratories GmbH, München, Germany
Glas equipment	Schott, purchased from A. Hartenstein, Würzburg, Germany

...continuous on the next page

Equipment	**Supplier**
Glas pipettes	A. Hartenstein, Würzburg, Germany
Heater	Medax, purchased from A. Hartenstein, Würzburg, Germany
Heat shaker TH15	Edmund Bühler GmbH, Hechingen, Germany
Ice machine	Scotsman Ice Systems, Vernon Hills, USA
Laminar air flow box Hera Safe KS12	Thermo Electron LED GmbH, Langenselbold, Germany
Magnetic stirrer	A. Hartenstein, Würzburg, Germany
Microscope AxioVert. A1	Carl Zeiss Jena GmbH, Jena, Germany
PeqStar gradient cycler	PeqLab Biotechnologie GmbH, Erlangen, Germany
PeqStar 2x double block cycler	PeqLab Biotechnologie GmbH, Erlangen, Germany
Perfect Blue semi-dry electroblotter	PeqLab Biotechnologie GmbH, Erlangen, Germany
Peristaltic pump P-1	GE Healthcare Europe GmbH, Freiburg, Germany
pH Meter inolab pH level 1	WTW, purchased from A. Hartenstein, Würzburg, Germany
Pipetboy Acu	IBS Integra Biosciences, Fernwald, Germany
Power Pac300	Bio-Rad Laboratories GmbH, München, Germany
Precision balance SPO51	Scaltec Insturments, purchased by A. Hartenstein, Würzburg, Germany
Sunrise Absorbance reader	Tecan Group, Männedorf, Switzerland
Water bath WB7	Memmert, purchased from A. Hartenstein, Würzburg, Germany

4.2 Consumables

Consumables	Supplier
Cell culture flasks (25 cm^2, 75 cm^2, 175 cm^2)	Greiner Bio-One GmbH, Frickenhausen, Germany
Cell culture flasks (TPP - 25 cm^2, 150 cm^2) (for Sf21 cell cultivation)	Biochrom AG, Berlin, Germany
Cell culture plates (6-, 12-, 24-well)	Greiner Bio-One GmbH, Frickenhausen, Germany
Cell scraper	TTP, purchased from A. Hartenstein GmbH, Würzburg, Germany
Cell stainers (70 µm, 100 µm)	BD Falcon, purchased from A. Hartenstein GmbH, Würzburg, Germany
Centrifugation tubes (15 mL, 50 mL)	Greiner Bio-One GmbH, Frickenhausen, Germany
Cover slipe (24x26 cm)	A. Hartenstein GmbH, Würzburg, Germany
Cryo tubes (1.5 mL)	Greiner Bio-One GmbH, Frickenhausen, Germany
GeneChip HG-U 133 Plus 2.0	Affymetrix UK ltd., High Wycombe, UK
Hi-TrapProtein G HP column (1 cm)	GE Healthcare Europe GmbH, Freiburg, Germany
Lab-Tek chamber slide (4 well chamber)	Nunc, purchased from A. Hartenstein GmbH, Würzburg, Germany
Microcentrifuge tube (1.5 mL)	Greiner Bio-One GmbH, Frickenhausen Germany
Multitips (5 mL)	Eppendorf AG, purchased from A. Hartenstein GmbH, Würzburg, Germany
NucleoSEQ column	Macherey-Nagel GmbH & Co. KG, Düren, Germany
Optical flat cap strips (qPCR)	Biozym Sientific GmbH, Hessisch Oldendorf, Germany
Pasteur pipettes	A. Hartenstein GmbH, Würzburg, Germany
PCR reaction tubes	PeqLab Biotechnologie GmbH, Erlangen, Germany
PCR reaction tube lids	PeqLab Biotechnologie GmbH, Erlangen, Germany
Petri dish	Greiner Bio-One GmbH, Frickenhause, Germany

...continuous on the next page

Consumables	Supplier
Pipette tips (10 µL, 100 µL, 1000 µL)	Brandt, purchased from Laborbedarf Scheller GmbH & Co. KG, Kürnach, Germany
Plastic pipettes (5 mL, 10 mL, 25 mL)	Greiner Bio-One GmbH, Frickenhausen, Germany
Portran nitrocellulose transfer membrane	Whatman GmbH, purchased from A. Hartenstein GmbH, Würzburg, Germany
0.2 mL Low profile 8 well-strips (qPCR)	Biozym Scientific GmbH, Hessisch Oldendorf, Germany
Sterile filter (0.2 µm)	SatoriusStedim purchased from A. Hartenstein GmbH, Würzburg, Germany
Sterile filter tips (10 µL, 100 µL, 1000 µL)	Starlab GmbH, Hamburg, Germany
UVettes	Eppendorf AG, purchased from A. Hartenstein GmbH, Würzburg, Germany
Whatman blot paper	Whatman GmbH, purchased from A. Hartenstein GmbH, Würzburg, Germany

4.3 Reagents

Chemicals and reagents	Supplier
2-Propanol	Carl Roth GmbH & Co. KG, Karlsruhe
Acetic acid	Carl Roth GmbH & Co. KG, Karlsruhe
Acetone	AppliChem, purchased from A. Hartenstein GmbH, Würzburg, Germany
Agar	AppliChem, purchased from A. Hartenstein GmbH, Würzburg, Germany
Ammonium persulfate (APS)	PAA Laboratories GmbH, Pasching, Austria
BioScript reverse transcriptase	Bioline GmbH, Luckenwalde, Germany
Boric acid	Merck KGaA, Darmstadt, Germany
Bovine serum albumin (BSA)	PAA Laboratories GmbH, Pasching, Austeria
Bromphenol blue sodium salt	Carl Roth GmbH & Co. KG, Karlsruhe
Cell lysis buffer (10x)	Cell Signaling Technology Inc., Danvers, USA
Colored reaction buffer (5x)	Bioline GmbH, Luckenwalde, Germany
Collagenase NB4	Serva Electrophoresis GmbH, Heidelberg, Germany
Complete protease inhibitor cocktail	Roche Diagnostics GmbH, Mannheim, Germany

...continuous on the next page

Chemicals and reagents	Supplier
Crystal violet powder	Serva Electrophoresis GmbH, Heidelberg, Germany
Dimethyl sulfoxide (DMSO)	Carl Roth GmbH & Co. KG, Karlsruhe
DMEM/Ham's F12 with L-glutamine	Life Technologies GmbH, Darmstadt, Germany
DMEM High glucose (4.5 g/L)	Life Technologies GmbH, Darmstadt, Germany
DNA ladder (100 bp)	PeqLab Biotechnologie GmbH, Erlangen, Germany
dNTP Set 4x100 µL	Bioline GmbH, Luckenwalde, Germany
Dulbecco's phosphate buffered saline (PBS) powder	Biochrom AG, Berlin, Germany
Ethanol, absolute	AppliChem, purchased from A. Hartenstein GmbH, Würzburg, Germany
Fetal calf serum	Biochrom AG, Berlin, Germany
Gentamycin (10 mg/mL)	Life Technologies GmbH, Darmstadt, Germany
GelRed	Genaxxon BioScience GmbH, Ulm, Germany
Glycerol	Merck KGaA, Darmstadt, Germany
Glycine	AppliChem, purchased from A. Hartenstein GmbH, Würzburg, Germany
Grace's insect medium	Life Technologies GmbH, Darmstadt, Germany
Hexadimethrine bromide (polybrene)	Sigma-Aldrich Chemie GmbH, Schnelldorf, Germany
Hyaluronidase	Serva Electrophoresis GmbH, Heidelberg, Germany
Hydrochloride acid (1 M)	AppliChem, purchased from A. Hartenstein GmbH, Würzburg, Germany
Insect express Sf9-S2 medium	PAA Laboratories GmbH, Pasching, Austria
Kapa SYBR Fast Universal (2x)	Peqlab Biotechnologie GmbH, Erlangen, Germany
L-Ascorbic acid 2-phosphate	Sigma-Aldrich Chemie GmbH, Schnelldorf, Germany
LE agarose	Biozym Scientific GmbH, Hessisch Oberdorf, Germany
Lipofectamine 2000	Life Technologies GmbH, Darmstadt, Germany

...continuous on the next page

Chemicals and reagents	Supplier
MangoTaq™ DNA Polymerase 1000 Units	Bioline GmbH, Luckenwalde, Germany
MISSION pLKO.1 - puro - CMV - TurboGFP™	Sigma-Aldrich Chemie GmbH, Schnelldorf, Germany
MISSION pLKO.1 - puro Empty Vector Control	Sigma-Aldrich Chemie GmbH, Schnelldorf, Germany
N,N,N,N-Tetramethylethylebediamine (TEMED)	Merck KGaA, Darmstadt, Germany
Penicillin/Streptomycin (10,000 U/mL; 10,000 µg/mL)	Life Technologies GmbH, Darmstadt, Germany
Phenylmethansulfonyl fluorid (PMSF - Serin protease inhibitor)	AppliChem, purchased from A.Hartenstein GmbH, Würzburg, Germany
PhosStop phosphatase inhibitor cocktail tablets	Roche Diagnostics GmbH, Mannheim, Germany
PMD2.G	Addgene Europe, Teddingtion, UK
Ponceau S	AppliChem, purchased from A. Hartenstein GmbH, Würzburg, Germany
Primer (forward, revers)	Eurofins GmbH, Ebersberg, Germany
Pronase E	Serva Electrophoresis GmbH, Heidelberg, Germany
Protease Inhibitor Cocktail Tablets: Complete, Mini, EDTA-free	Roche Diagnostics GmbH, Mannheim, Germany
PSPAX2 (packaging plasmid)	Addgene Europe, Teddington, UK
Sodium acetate	AppliChem, purchased from A. Hartenstein GmbH, Würzburg, Germany
Sodium pyruvate	Sigma-Aldrich Chemie GmbH, Schnelldorf, Germany
Trypsin/EDTA (1x)	Life Technologies GmbH, Darmstadt, Germany
Rainbow marker RPN800E	GE Healthcare Europe GmbH, München, Germany
Random hexamer primer	Life Technologies GmbH, Darmstadt, Germany
Roti-Quant (5x)	Carl Roth GmbH & Co. KG, Karlsruhe, Germany
Rotiphorese gel 40	Carl Roth GmbH & Co. KG, Karlsruhe, Germany
Skimmed milk powder	AppliChem, purchased from A. Hartenstein, Würzburg, Germany

...continuous on the next page

Chemicals and reagents	Supplier
Sodium chloride	AppliChem, purchased from A. Hartenstein GmbH, Würzburg, Germany
Sodium dodecyl sulfate (SDS)	Merck KGaA, Darmstadt, Germany
Tris-aminomethane	AppliChem, purchased from A.Hartenstein GmbH, Würzburg, Germany
Triton X-100	Carl Roth GmbH&Co. KG, Karlsruhe, Germany
Trypan blue (0.4 %)	Sigma-Aldrich Chemie GmbH, Schnelldorf, Germany
Tryptone	AppliChem, purchased from A.Hartenstein GmbH, Würzburg, Germany
Tween20	Merck KGaA, Darmstadt, Germany
Yeast extract	AppliChem, purchased from A. Hartenstein GmbH, Würzburg, Germany
Vectashield® mounting medium with DAPI	Vector Laboratories LTD, Peterborough, UK
Water, HPLC grade	Carl Roth GmbH & Co. KG, Karlsruhe, Germany

4.4 Kits

Kits	Supplier
Annexin V-Cy3 Apoptosis Detection Kit Plus	BioVision Inc., Milpitas, USA
BigDye® Terminator v3.1 cycle sequencing kit	Life Technologies GmbH, Darmstadt, Germany
CellTiter Glo® Luminescent Cell Viability Assay	Promega Cooperation, Madison, USA
MISSION® shRNA Bacterial Glycerol Stock	Sigma-Aldrich Chemie GmbH, Schnelldorf, Germany
NucleoBond® Xtra Midi EF	Macherey-Nagel GmbH & Co. KG, Düren, Germany
NucleoSpin® RNA	Machery-Nagel GmbH & Co. KG, Düren,Germany
PlusOne™ Silver Staining Kit, protein	Amersham, purchased from GE Healthcare Europe GmbH, München, Germany
SR FLICA™ in vitro Poly Caspases Kit	ImmunoChemistry Technologies, LLC, Bloomington, USA

...continuous on the next page

Kits	Supplier
Western Bright^{TM} Sirius	Advansta Inc., Menlo Park, USA

4.5 Cell culture media

MSC medium	500 mL DMEM/Ham's F12 + 50 mL FCS + 5 mL penicillin (10,000 U/mL)/streptomycin (10,000 µg/mL) + 555 µL L-ascorbic acid 2-phosphate
Chondrocyte medium	500 mL DMEM/Ham's F12 + 50 mL FCS + 5 mL penicillin (10,000 U/mL)/streptomycin (10,000 µg/mL)
Digestion medium I	20 mL chondrocyte medium + 1 mL Pronase E solution (7.8 %)
Digestion medium II	20 mL chondrocyte medium + 2 mL collagenase NB4 solution (1.25 U/mL) + 1 mL hyaluronidase solution (2000 U/mL)
HEK293T medium	500 mL DMEM High glucose (4.5 g/L) + 50 mL FCS + 5 mL penicillin (10,000 U/mL)/streptomycin (10,000 µg/mL) + 600 µL sodium pyruvate (1M)
HEK293T serum rich medium	80 mL HEK293T medium + 20 mL FCS
Sf21 medium	500 mL Grace's insect medium + 50 mL FCS + 2.5 mL gentamycin (10 mg/mL)

...continuous on the next page

Sf21 protein expression medium	Insect express Sf9-S2

4.6 Cell media supplements

L-Ascorbic acid 2-phosphate	2.5 g L-ascorbic acid 2-phosphate ad 50 mL water, HPLC grade sterile filtered, aliquots stored at -20°C
Pronase E solution	1 g Pronase E ad 12.82 mL sterile PBS aliquots stored at -20°C
Sodium pyruvate	20 mg sodium pyruvate ad 20 mL water, HPLC grade sterile filtered, aliquots stored at -20°C

4.7 Bacterial medium and plates

LB medium	10 g tryptone 5 g yeast extract 10 g sodium chloride ad 1,000 mL bidistilled water
LB agar plates	1,000 mL LB medium + 15 g agar autoclaved before casting the plates

4.8 Short hairpin RNA (shRNA) sequences and controls

Name	shRNA ID	Homology	Sequence ID
shRNA1	TRCN0000033359	Homo sapiens	NM_003880
shRNA2	TRCN0000033360	Homo sapiens	NM_003880
shRNA3	TRCN0000033361	Homo sapiens	NM_003880
shRNA4	TRCN0000033362	Homo sapiens	NM_003880
shRNA5	TRCN0000033363	Homo sapiens	NM_003880
shRNA6	TRCN00003351	Homo sapiens	NM_003882, NM_080838

Name	shRNA sequence [5'-3']
shRNA1	CCGGGCAGCTTTCAACAAGCTACAACTCGAGTTGTAGCTTGTTGAAAGCTGCTTTTTG
shRNA2	CCGGGCGAGTTCAACCAGGTACATTCTCGAGAATGTACCTGGTTGAACTCGCTTTTTG
shRNA3	CCGGCCATTAGATACAACACCTGAACTCGAGTTCAGGTGTTGTATCTAATGGTTTTTG
shRNA4	CCGGGCAGAGAACCTGGAGATATATCTCGAGATATATCTCCAGGTTCTCTGCTTTTTG
shRNA5	CCGGCTTGGATAAGAGATGCTGTATCTCGAGATACAGCATCTCTTATCCAAGTTTTTG
shRNA6	CCGGCTGTGGAGTTTGCATGGACAACTCGAGTTGTCCATGCAAACTCCACAGTTTTG
scramble	CCGGCAACAAGATGAAGAGCACCAACTCGAGTTGGTGCTCTTCATCTTGTTGTTTTT

Name	Vector backbone	Plasmid
vector only	TRC1/1.5	pLKO.1-puro-CMV empty vector
GFP	TRC1/1.5	pLKO.1-puro-CMV-TurboGFP^{TM}

4.9 Solutions for production of recombinant protein

4.9.1 Purification of recombinant protein

PBS pH 7.4	9.55 g PBS ad 1000 mL distilled water
0.1 M Glycine pH 2.2	750 mg glycine ad 100 mL bidistilled water
20% Ethanol	20 mL 99.8% ethanol ad 100 mL bidistilled water

4.9.2 Silver gel staining

Fixation solution	100 mL ethanol 25 mL glacial acetic acid ad to 250 mL distilled water
Sensitizer solution	75 mL ethanol 1.25 mL glutardialdehyde (25% w/v)∗ 10 mL sodium thiosulphate (5% w/v) 17 g sodium acetate ad to 250 mL distilled water
Silver nitrate solution	25 mL silver nitrate (2.5% w/v) 0.1 mL formaldehyde (37% w/v)∗ ad 250 mL distilled water
Develop solution	6.25 g sodium carbonate 0.05 mL formaldehyde (37% w/v)∗ ad 250 mL distilled water
Stopping solution	3.65 g EDTA-Na_2·H_2O ad 250 mL distilled water

∗ immediately added before use

4.10 Solutions for Western blot

4.10.1 Total protein lysate preparation

100 mM PMSF	0.174 g phenylmethylsulfonyl fluoride ad 10 mL dimethyl sulfoxide
Protease inhibitor complete	1 tablet cOmplete ULTRA tablets, mini, EDTA-free ad 2 mL water, HPLC grade aliquots frozen at -20°C
Phosphatase inhibitor PhosStop	1 tablet PhosStop phosphatase inhibitor ad 500 µL water, HPLC grade
Lysis buffer	200 µL 10x Lysis buffer 1540 µL water HPLC grade 80 µL 100 mM PMSF 80 µL Protease inhibitor complete 100 µL Phoshatase inhibitor PhosStop

4.10.2 SDS-PAGE solutions

0.5% Bromophenol blue	0.05 g bromophenol blue ad 10 mL bidistilled water
6x Lämmli buffer	30.275 g tris-aminomethane 7.2 g SDS 18 mL glycerine 1.44 mL 0.5% bromophenol blue solution ad 50 mL bidistilled water∗ ∗ working solution included 10% β-mercaptoethanol
Running gel buffer pH 8.8	36.34 g tris-aminomethane ad 100 mL bidistilled water

...continuous on the next page

Stacking gel buffer pH 6.8	6.1 g tris-aminomethane ad 100 mL bidistilled water
10% APS	1g amino persulfate ad 10 mL bidistilled water aliquots stored at -20°C
10% SDS	10g sodium dodecyl sulfate ad 100 mL bidistilled water
4x Upper puffer	13.6 g tris-aminomethane 57.1 g glycine 4 g SDS ad 1,000 mL bidistilled water
1x Upper buffer	250 mL 4x upper buffer 210 µL β-mercaptoethanol ad 1,000 mL bidistilled water
10x Lower puffer	30.2 g tri-aminomethane 142.8 g glycine ad 1,000 mL bidistilled water
1x Lower buffer	100 mL 10x lower buffer ad 1,000 mL bidistilled water

4.10.3 Western blot solutions

10x Transfer buffer pH 10	30 g tris-aminomethane 144 g glycine ad 1,000 mL bidistilled water
1x Transfer buffer	100 mL 10x transfer buffer 200 mL methanol ad 1,000 mL bidistilled water

...continuous on the next page

Ponceau S solution	2 g Ponceau S 30 g trichloracetic acid 30 g sulfosalicylic acid ad 100 mL distilled water
10x TBS buffer pH 7.6	24.2 g tris-aminomethane 87.66 g NaCl ad 1,000 mL bidistilled water
1x TBST buffer	100 mL 10x TBS buffer 1 mL Tween20 ad 1,000 mL bidistilled water
Stripping buffer	0.985 g tris-aminomethane 20 mL 10% SDS solution ad 100 mL bidistilled water

4.11 Solutions for molecular biology

10x TBE buffer	108 g Ttris-aminomethane 55 g boric acid 9,05 g EDTA ad 1000 mL distilled water
1x TBE buffer	100 mL 10x TBE buffer ad 2000 mL distilled water
1% Agarose	1 g agarose ad 100 mL 1x TBE buffer

4.12 Reverse transcriptase PCR primer sequences

Primer sequence [5' - 3']		T_A [°C]	Product size [bp]	Sequence ID
Eukaryotic translation elongation factor 1 alpha 1 (EEF1A)				
forward	CTGTATTGGATTGCCACACG	54	369	NM_001402.5
reverse	AGACCGTTCTTCCACCACTG			
Ribosomal protein S27a (RPS27A)				
forward	TCGTGGTGGTGCTAAGAAAA	60	141	NM_001135592.2
reverse	TCTCGACGAAGGCGACTAAT			NM_001177413.1
				NM_002954.5
Cysteine-rich, angiogenic inducer 61 (CYR61)				
forward	CAACCCTTTACAAGGCCAGA	54	206	NM_001554.4
reverse	TGGTCTTGCTGCATTTCTTG			
Connective tissue growth factor (CTGF)				
forward	CCTGGTCCAGACCACAGAGT	54	239	NM_001901.2
reverse	ATGTCTTCATGCTGGTGCAG			
Nephroblastoma overexpressed (NOV)				
forward	CTGGATGTGCTACTGCCTGAG	56	214	NM_002514.3
reverse	AGCATGCTGTCCACTCTGTG			
Wnt1 inducible signalling pathway protein 1 (WISP1)				
forward	CAGATGGCTGTGAGTGCTGT			
reverse[1]	AGGACTGGCCGTTGTTGTAG	56	198	NM_003882.3
reverse[2]	ACTGGGCGTTAACATTGGAG	56	264	NM_080838.2

...continuous on the next page

[1] Transcript variant 1

[2] Transcript variant 2

Primer sequence [5' - 3']		T_A [°C]	Product size [bp]	Sequence ID
Wnt1 inducible signalling pathway protein 2 (WISP2)				
forward	GAGTACCCCTGGTGCTGGATG	55	211	NM_003881.2
reverse	GTCTCCCCTTCCCGATACA			
Wnt1 inducible signalling pathway protein 3 (WISP3)				
forward	CTGTGTTACATTCAGCCTTGCGAC	54	337	NM_003880.3
reverse	CTTGGTTTTACAGAATCTTGAGCTC			NM_198239.1
Angiopoietin 1 (ANGPT)				
forward	GAAGGGAACCGAGCCTATTC	52	213	NM_001146.3
reverse	AGCATCAAACCACCATCCTC			NM_001199859.1
Periostin, osteoblast specific factor (POSTN)				
forward	GAATCATCCATGGGAACCAG	52	177	NM_006475.2,
reverse	AGTGACCGTCTCTTCCAAGG			NM_001135936.1
				NM_001286667.1
				NM_001286666.1
				NM_001286665.1
				NM_001135935.1
				NM_001135934.1
Signal transducer and activator of transcription 4 (STAT4)				
forward	TTCCCAAAGACAAAGCCTTC	50	188	NM_003151.3
reverse	CACCGCATACACACTTGGAG			NM_001243835.1
Insulin-like growth factor binding protein 1 (IGFBP1)				
forward	GAGTTTAGCCAAGGCACAGG	52	162	NM_000596.2
reverse	ATCCTCTTCCCATTCCAAGG			

...continuous on the next page

Primer sequence [5' - 3']		T_A [°C]	Product size [bp]	Sequence ID
Prostaglandin-endoperoxide synthase 2 (PTGS2)				
forward	TGGCTACAAAAGCTGGGAAG	55	225	NM_000963.3
reverse	CAGCACTTCACGCATCAGTT			
Cysteine rich transmembrane BMP regulator 1 (chordin-like) (CRIM1)				
forward	ACTGGACTCCATTGCCTCAG	58	189	NM_016441.2
reverse	ACTGTCCACCTGGACTCTGG			
Histidine triad nucleotide binding protein 2 (HINT2)				
forward	CCTACTCCTTGTGGCCAAGC	58	154	NM_032593.2
reverse	TCAACCTGGAGGCCACTG			
Tyrosine 3-monooxygenase/tryptophan 5-monooxygenase activation protein, zeta polypeptide (YWHAZ)				
forward	CGCTGGTGATGACAAGAAAG	55	293	NM_003406.3
reverse	CCGATGTCCACAATGTCAAG			NM_001135700.1
				NM_001135702.1
				NM_001135701.1
				NM_001135699.1
				NM_145690.2
APAF1 interacting protein (APIP)				
forward	CAGGACAAGGAGCATCCAAG	54	211	NM_015957.3
reverse	ATGGCGAAGGTCCACTTATG			
Integrin alpha 6 (ITGA6)				
forward	GGAAACATGGACCTTGATCG	54	182	NM_001079818.1
reverse	TGGAGGCATATCCCACTAGG			NM_000210.2

...continuous on the next page

Primer sequence [5' - 3']		T_A [°C]	Product size [bp]	Sequence ID
Desmoplakin (DSP)				
foward	TGGCAAACGAGACAAATCAG	52	186	NM_004415.2
reverse	TGAACATCTGCAGCCTCTTG			NM_001008844.1
Tumour Necrosis Factor Receptor Superfamily, Member 10A (TRAILR1)				
forward	AGAGAGAAGTCCCTGCACCA	57	154	NM_003844.3
revers	GTCACTCCAGGGCGTACAAT			
Tumour Necrosis Factor Receptor Superfamily, Member 10B (TRAILR2)				
forward	TGCAGCCGTAGTCTTGATTG	55	219	NM_003842.4
revers	TCCTGGACTTCCATTTCCTG			NM_147187.2

4.13 Real-time PCR primer

Primer sequence [5' - 3']		T_A [°C]	Product size [bp]	Sequence ID
TATA box binding protein (TBP)				
forward	TAGAAGGCCTTGTGCTCACC	60	101	NM_001172085.1
reverse	AAGGAGAACAATTCTGGGTTTG			NM_003194.4
Ornithine decarboxylase antizyme 1 (OAZ1)				
forward	TCGGCTGAATGTAACAGAGG	62	103	NM_004152.2
reverse	CACTGTTCGCCAGTTAATGC			
Wnt1 inducible signalling pathway protein 3 (WISP3)				
forward	GCCTGGAACCATTACTACAGC	62	119	NM_003880.3
reverse	GCAGGGAGTCCATTTTGTTG			NM_198239.1

4.14 Software and internet resources

Name	Source
Software	
ABI Prism® Genetic Analyzer	Applied Biosystems Inc., purchased from Life Technologies GmbH, Darmstadt, Germany
CFX Manager Software Version 3.1	Bio-Rad Laboratories GmbH, München, Germany
Gel Analyzer 2010a	http://www.gelanalyzer.com/, Copyright 2010 by Istvan Lazar and Dr. Istvan Lazar
GraphPad Prism Version 6.04	GraphPad Software Inc., LaJolla, USA
Mendeley Desktop Version 1.12.1	Mendeley Ltd., London, UK
Microsoft Office 2007	Microsoft Cooperation, Redmond, USA
Internet resources	
Basic Local Alignment Search Tool (BLAST)	www.ncbi.nlm.nih.gov/BLAST - U.S. National Library of Medicine
GeneCards	www.genecards.org - Copyright © 1996-2014 , Weizmann Institute of Science, Version 3.12.162 19 Aug 2014
National Center for Biotechnology Information (NCBI)	www.ncbi.nlm.nih.gov - U.S. National Library of Medicine
Primer3Plus	http://primer3plus.com/cgi-bin/dev/primer3plus.cgi - Copyright © 2006, 2007 by Andreas Untergasser and Harm Nijveen
PubMed	http://www.ncbi.nlm.nih.gov/pubmed - U.S. National Library of Medicine

Chapter 5

Methods

5.1 Cell culture

Cell culture was performed under humidified 5 % carbon dioxide atmosphere at 37°C, except for the Sf21 insect cell line which was cultured at 27°C in normal non-humidified air.

5.1.1 Mesenchymal stem cell isolation

Human mesenchymal stem cells (hMSCs) were harvested from the cancellous bone of the femur from hip replacement surgery, with informed consents of the patient (average age 62 ± 8; 2 female and 8 male) and the approval of the Ethic Committee of the University of Würzburg. The cancellous bone was once washed with unsupplemented medium which was discarded afterwards. The washing step was repeated until the cancellous bone appeared 'white', while collecting the supernatant. Cells were then centrifuged at 270 xg for 5 min, the supernatant was removed and cells were seeded at a cell density of $4.6 - 5.7 \cdot 10^5$ cells per cm^2. First medium change after 3 to 4 days included a PBS washing step to remove the non-adherent cells. The following medium changes were performed every 4 days.
Stemness character was tested in the lab by osteogenic and adipogenic differentiation.

5.1.2 Primary chondrocyte isolation

Primary human chondrocytes were harvested from the femoral head, with informed consents of the patient (average age 57 ± 16; 3 female and 12 male) and the approval of the Ethic Committee of the University of Würzburg. Chondrocyte chips were sliced from intact parts of the femoral head, collected in unsupplemented medium before cutting them into 1 to 2 mm^2 pieces. These chondrocyte pieces were washed twice with PBS to remove fat before the digestion steps. Sliced chondrocytes were transferred into the digestion medium I and incubated for 1 h at 37°C. Afterwards, medium was exchanged with digestion medium II under stirring conditions at 37°C for 18 to 20 h. The arisen cell suspension was filtered via a 70 µm cell strainer, centrifuged at 481 xg for 5 min and washed twice with PBS. Cells were resuspended in chondrocyte medium and seeded at a density of 8,000 to 10,000 cells per cm^2. First medium change was performed after 3 to 4 days and then repeated every 4 days.

5.1.3 Subcultivation of cells

Cells were passaged at a confluence of 70-100 %. Therefore, they were washed with PBS and detached with 1x Trypsin/EDTA for approximately 5 min at 37°C. The detachment was stopped with growth medium and the cell suspension was centrifuged at 270 xg for 5 min before resuspension and seeding at the desired cell density.

5.1.4 Cultivation of HEK293T cells

HEK293T cells were cultivated up to 90 % confluence before splitting. Cells were detached by washing with PBS, centrifuged at 270 xg for 5 min and resuspended in fresh HEK293T medium followed by seeding at the desired cell density. Medium was changed every 4 days.

5.1.5 Cultivation of Sf21 cells

Sf21 cells were cultivated up to 90 % confluence before splitting. Old medium was removed, 10 mL fresh cultivation medium was added and cells were scraped from the flask bottom. Cells were resuspended in fresh medium and seeded at a ratio of 1:10 into a new flask. Medium change was performed together with splitting of the cells once a week.

5.2 Reduction of WISP3 gene expression

5.2.1 Plasmid production in *E. coli*

Culturing of *E. coli* was performed at 37°C. Transfected *E. coli*, bought as glycerol stocks from Sigma-Aldrich, were streaked out on LB agar plates and incubated for 24 h. Single clones were picked from these plates and further cultured in 2.5 mL LB medium as a 'day culture' for approximately 6-8 h. 2 mL of the day culture were used to inoculate 50 mL LB medium in a baffled flask for 18-20 h overnight. For the harvest, OD_{600} was measured with a photometer and accepted if it was in between 3.0-4.0.

5.2.2 Midi-preparation for plasmids

Midi-Preparation was performed according to the manufacturer's protocol. Briefly, bacterial broth was centrifuged at 6,000 xg for 15 min at 4°C, supernatant was discarded and bacteria were resuspended in RNase buffer. Lysis buffer was added and the solution was inverted constantly for 3 min to allow a homogenous lysis of the cells without disrupting the plasmid DNA. Proteins and plasmids were precipitated with a neutralisation buffer before proteins were removed by a provided paper column on top of the column bed. DNA binds to the column bed while cell debris and proteins were removed by several washing steps. DNA was eluted from the column, mixed with isopropanol to precipitate the DNA and centrifuged at maximal speed for 30 min at 4°C. Afterwards, the supernatant was discarded, the pellet was washed in 70 % ethanol and centrifuged at maximal speed for 5 min at 4°C. Ethanol was removed, the pellet air dried and resuspended in 400 µL DNA-free water. The concentration and purity of the obtained plasmid DNA was determined by photometric measurement of $OD_{260/280}$. Plasmid DNA was only used if purity was in between 1.8-2.0 and stored at -20°C.

5.2.3 Reduction of WISP3 gene expression in hMSCs and primary chondrocytes

Reduction of WISP3 mRNA expression was performed by induction of the cell own RNA interference (RNAi) using a short-hairpin RNA (shRNA) system. The shRNAs were bought as plasmids and were inserted into a lentivirus with the help of HEK293T cells. GFP was also bought to serve as a transfection control for the HEK293T cells as well as the target cells, to monitor the successful transduction.
For virus production HEK293T cells were seeded at a density of $6 \cdot 10^5$cells per well in a 6-well plate. Next day, cells were transfected with 170 µL transfection mix (Table 1) for 24 h, followed by medium change with HEK293T serum rich medium. After another 24 h incubation, supernatant was collected and sterile-filtered (0.2 µm) to remove HEK293T cells. Supernatant, containing viruses plus polybrene (1 mg/mL), was added to the target cells followed by a medium exchange the next day, after that the medium was exchanged every 3 to 4 days. Successful transduction was monitored by GFP exposure with a fluorescence microscope. Reduction of WISP3 gene expression was analysed by reverse transcriptase-polymerase chain reaction (RT-PCR - Section 5.6.4) and subsequent real-time PCR (qPCR - Section 5.6.5).

Table 1 Transfection mix

Transfection mix for 1 sample		Lipofectamin mix for 1 sample	
psPAX2 plasmid DNA	1.8 µg	Lipofectamin® 2000	10 µL
pMD2.G plasmid DNA	0.25 µg	pure DMEM High glucose medium	90 µL
target DNA	2 µg		
Lipofectamin mix	100 µL	incubation for 5 min	
pure DMEM High glucose	ad 180 µL		

5.3 Production of recombinant WISP3-Fc

5.3.1 Plasmids and viruses

Generation of recombinant WISP3-Fc and Fc-Tag is described in Schütze et al. 2007 [112].

5.3.2 Expression in Sf21 cells

Recombinant protein was produced in a baculovirus expression system. Sf21 cells were splitted 1:2, seeded in protein expression medium as described (Section 5.1.5) and infected with approximately 130 µL virus supernatant per 150 cm^2 cell culture flask. The recombinant protein is secreted into the medium, which correlates with a morphological change of the cells. After 6 to7 days, supernatant was harvested and the recombinant protein purified as described (Section 5.3.3).

5.3.3 Purification of the recombinant protein supernatant

Recombinant protein was purified by a HiTrap protein G HP column. All solutions and supernatants were sterile-filtered (0.2 µm) before loaded on the column. For that, the column was equilibrated with PBS (pH 7.4) for 10 min with a flow rate of 1 mL/min. Supernatant containing recombinant protein was collected and centrifuged at 3800 xg for 10 min to remove cells. Afterwards, the supernatant was pumped over the column with a flow rate of 1 mL/min followed by a wash step with PBS for 10 min. To elute the protein from the column, gylcine with an exact pH of 2.2 and a temperature of 23°C was used. 1 mL of the eluate was taken per reaction tube already containing 40 µL 3 M Tris buffer (pH 8.0) to neutralise the solution. Bacterial growth in the protein solution was inhibited by the addition of 3 µL 3 M sodium azide. Immediately after elution of the recombinant protein, the column was washed with PBS for 15 min and sterilised for storage with 20 % ethanol for 10 min. The recombinant protein was stored at 4°C for short term or at -20°C for long term storage.

5.3.4 Silver gel staining

Purity and size of the recombinant protein was checked by a silver staining. Protein samples were prepared as described (Section 5.5.3), loaded alongside a protein full range weight marker onto a 10 % SDS gel and run for approximately 1 h at 150 V. The staining was performed according to the manufacturer's protocol. Briefly, the gel was treated with fixation solution for 30 min followed by 30 min incubation in sensitiser solution. The gel was washed three times with bidistilled water for 5 min, before silver nitrate solution was added for additional 20 min. Development of the silver reaction for 20 min took place after two washing steps for 1 min. The reaction was stopped with a chelating solution for 10 min, followed by three washing steps for 5 min each. The gel was photographed with a Canon Digital camera.

5.3.5 Knock down of WISP3 with simultaneous recombinant WISP3-Fc treatment

Treatment with recombinant WISP3-Fc was carried out to investigate the rescue of the WISP3 knock down in hMSCs. WISP3 knock down was performed as described (Section 5.2.3) and 500 ng/mL WISP3-Fc or 198,6 ng/mL Fc-Tag were added directly with the virus supernatant onto the target cells. Fc-Tag served as control and the concentration was chosen according to the percentage in the recombinant WISP3-Fc. Recombinant protein was renewed with every medium exchange. RNA was harvested at day 6 and the gene expression was analysed by qPCR (Section 5.6.5).

5.4 Assays

5.4.1 FLICA assay

FLICA® provides a sulforhodamine-labelled fluoromethyl peptide inhibitor which allows the detection of active caspases in living cells due to covalent binding to the protein. The assay was performed according to the manufacturer's protocol. Briefly, cells were seeded at a density of 2,000 cells per well in a 4-well chamber slide. Knock down of WISP3 was performed as described (Section 5.2.3). Untreated cells were incubated with 4 mM hydrogen peroxide for 4 h to induce apoptosis serving as positive control. FLICA® was applied to the cells in 290 µL growth medium per well and incubated at 37°C for 1 h. Fresh medium containing Hoechst33342, counterstaining the nuclei, was applied for 5 min at 37°C. Excess dye was removed by three washing steps with wash buffer before fixation of the stained cells. A fluorescence microscope was used to analyse the staining and pictures were taken with the software AxioVision Ref 4.8 immediately after fixation.

5.4.2 Annexin V-Cy3 assay

Annexin V binds phosphatidylserine which is translocated from the inner to the outer membrane of the cell during apoptosis. The assay was performed according to the manufacturer's protocol. Cells were seeded at a density of 2,000 cells per well in a 4-well chamber slide. Knock down of WISP3 was performed as described (Section 5.2.3). Untreated cells were incubated with 4 mM hydrogen peroxide for 4 h to induce apoptosis serving as positive control. Cells were washed three times with 200 µL wash buffer before staining with Annexin V-Cy3 and Hoechst33342 as nucleic counter stain. Stains were visualised under a fluorescence microscope and pictures were taken with the software AxioVision Ref 4.8.

5.4.3 Crystal violet staining

The validation of cell reduction during WISP3 knock down was determined by crystal violet staining, which allows the correlation of dissolved dye to cell number. WISP3 knock down was performed in a 6-well plate as described (Section 5.2.3) and stained with crystal violet at day 6 after transduction. Cells were washed three times with PBS followed by fixation with 5 % glutaraldehyde for 15 min at room temperature. Afterwards, cells were washed as before and stained with 0.1 % crystal violet for 25 min at room temperature. Crystal violet intercalates into the DNA. Excessive dye was removed by washing with distilled water before dissolving the dye with 0.1 % Triton-X solution for 1 h at room temperature at an orbital shaker. 100 µL of dissolved crystal violet-Triton-X solution (1:10) was measured in triplicates against the dissolving solution in a 96-well plate with a wavelength of 540 nm on a plate reader.

5.4.4 Proliferation assay

The influence of WISP3-Fc on the proliferation of hMSCs was investigated using the CellTiter Glo® Luminescent Viability Cell Assay. The assay measures ATP concentration that correlates with metabolic active cells via a luciferase reaction and was performed according to the manufacturer's protocol. Briefly, 2,000 cells per well were seeded into a 96-well plate. Next day, cells were stimulated with 250, 500 and 1,000 ng/mL WISP3-Fc or 397.6 ng/mL Fc-Tag for 48 h. Fc-Tag was used as control and the concentration of Fc-tag was chosen according to its percentage in the recombinant WISP3-Fc with the highest concentration. Luciferase and its corresponding substrate was added, shaken and incubated for 10 min before luminescence measurement in a plate reader. Medium alone served as blank.

5.5 Western blot

5.5.1 Total protein lysate preparation

Cells were harvested by scraping from the cell culture bottom and centrifugation at 270 xg for 5 min. The pellet was resuspended in 100-250 µL lysis buffer and incubated on ice for 10 min with frequent shaking intervals. The suspension was sonicated (10 sec with 1 sec pulse and 1 sec pause at amplitude of 70%) and centrifuged at 13,700 xg for 15 min at 4°C. The supernatant was transferred into a new tube and stored at -20°C or -80°C for long term storage.

5.5.2 Determination of protein concentration

Protein concentration was determined with Bradford assay [113] using Roti®Quant according to the manufacturer's protocol. This colorimetric assay bases on the absorbance shift of Coomassie Brilliant Blue G-250 from its red acidic unbound form towards a blue form. In short, the assay was performed in triplicates, for each replicate 10 µL protein lysate dilution (usually 1:10 to 1:20) was mixed with 200 µL Roti®Quant reagent in a 96-well plate. The plate was measured at 620 nm with a reference wavelength of 405 nm in a plate reader. A standard curve was used for calculation: BSA in PBS for protein lysates (100, 250, 500, 750, 1,000 and 1,500 µg) and in Tris-gylcine solution for recombinant protein produced in Sf21 cells (25, 50, 75, 100, 150 and 250 µg) (Section 5.3.2). Pure buffers were used as blank.

5.5.3 Protein sample preparation

20 to 45 µg protein lysate or 150 to 300 ng recombinant proteins were mixed with Lämmli buffer and denatured at 95°C for 5 min.

5.5.4 SDS PAGE and Western blot

Protein samples and protein weight marker were loaded onto a 10 to 15% SDS gel (Table 2) and run at 150 V for approximately 1 h. The proteins were transferred by a semi-dry blot onto a nitrocellulose membrane at 150 mA per membrane for 2 h. The transfer was confirmed with ponceau S staining and excessive dye was rinsed with distilled water. Afterwards, unspecific binding was blocked with 5 % skimmed milk powder in TBST for 1 h at room temperature. Antibodies were diluted in their corresponding buffer as listed (Table 3). The primary antibody was incubated over night at 4°C, followed by three time washing steps with TBST and the incubation of the secondary antibody for 1 h at room temperature. The membrane was washed three times with TBST before detection of the bands with Western Bright™ Sirius according to the manufacturer's protocol. The bands were captured by a CCD camera system. To determine the housekeeping protein the membrane was stripped for 30 min at 50°C and afterwards washed two times with TBST for 5 min. Successful stripping was confirmed by renewed

incubation with detection reagent. The blockage and incubation of the membrane was performed as described in this section.

Table 2 Composition of SDS

for 2 mini gels of 1.5 mm	10% running gel	15% running gel	5% stacking gel
bidistilled water	12.1 mL	9.6 mL	2.4 mL
40% Rotiphorese® Gel 40 (29:1) acrylamide:bisacrylamide	5 mL	7.5 mL	1 mL
running gel buffer	2.5 mL	2.5 mL	-
stacking gel buffer	-	-	1 mL
10% SDS	200 µL	200 µL	40 µL
10% APS	200 µL	200 µL	40 µL
TEMED	8 µL	8 µL	4 µL

Table 3 Primary and secondary antibodies

primary antibodies

Host	Target	Dilution	Buffer in TBST	Distributor
rabbit	anti caspase 3	1:1,000	5% skimmed milk powder	# 9665, Cell Signaling Technology
rabbit	anti LC3 A/B	1:1,000	5% BSA	#4108, Cell Signaling Technology
mouse	anti GAPDH	1:15,000	5% skimmed milk powder	GTX28245, GeneTex, Inc.

secondary antibodies

Host	Target	Dilution	Buffer in TBST	Distributor
goat	anti rabbit IgG POD	1:2,000	5% skimmed milk powder	#0545, Sigma-Aldrich
goat	anti mouse IgG POD	1:2,000	5% skimmed milk powder	#9917, Sigma-Aldrich

5.6 Molecular biology

5.6.1 RNA isolation

RNA was isolated with the NucleoSpin® RNA kit according to the manufacturer's protocol. In short, cells were harvested by scraping from the culture bottom, centrifuged at 270 xg for 5 min and lysed in appropriate volume of RA1 buffer containing 1% β-mercaptoethanol. If not stated otherwise centrifugation steps were performed at 11,500 xg for 1 min. Viscosity of the lysate was reduced by retaining cell debris on a column by centrifugation and the flow through was mixed with an equal amount of 70% ethanol. Solution was loaded onto a second column to bind nucleic acids, centrifuged and desalted by 350 µL MDB buffer. Afterwards, DNA was degraded by adding 95 µL rDNase per column for 15 min at room temperature. DNase was inactivated by 200 µL RA2 buffer. The column was washed twice, first with 600 µL followed by 250 µL RA3 buffer and a drying centrifugation step at 11,500 xg for 2 min. The RNA was eluted in 20-40 µL nuclease-free water, used immediately or stored at -80°C. Concentration was measured at $OD_{260/280}$ and accepted if the ratio was in between 1.8-2.0.

5.6.2 cDNA synthesis

Since RNA is rather instable, it was reverse transcribed into cDNA for further analysis of gene expression. For cDNA synthesis 1 µg RNA, if possible, was reverse transcribed using a Moloney Murine Leukemia Virus (MMLV) reverse transcriptase. The necessary volume of RNA was mixed with 1 µL random hexamer primers (1 µg/µL) and water (HPLC grade) was added up to 12 µL. The solution was incubated

at 70°C for 5 min, followed by a 5 min incubation step on ice. Afterwards, 8 µL cDNA master mix (Table 4) were added and incubated at room temperature for 10 min before another incubation step at 42°C for 60 min. The reverse transcriptase was heat inactivated at 70°C for 10 min and 30 µL nuclease-free water were added to a total volume of 50 µL. The resulting cDNA was used immediately or stored at -20°C.

Table 4 cDNA master mix

cDNA master mix for 1 sample	
4 µL	reaction buffer
1 µL	10 mM dNTPs
2.75 µL	water, HPLC grade
0.25 µL	200 U/µL BioScript reverse transcriptase

5.6.3 Primer design

Primers were designed using the software Primer3Plus. If possible, primers were chosen spanning the intron-exon junction to exclude contamination with genomic material. The annealing temperature was identified by a temperature gradient. Specificity of the primer was assured by sequencing the PCR product. In case of qPCR, efficiency was verified by a serial dilution of cDNA (1:2, 1:4, 1:8, 1:20, 1:40, 1:400).

5.6.4 Reverse transcriptase-Polymerase chain reaction (RT-PCR)

To investigate gene expression in different experiments a RT-PCR was set up and run according to (Table 5). RT-PCR products and molecular weight marker were loaded onto a 2 % agarose gel, run at 145 V for approximately 1 h. Bands in the gel were visualised by UV-light and recorded by a snapshot with the gel documentation system.

Table 5 RT-PCR pipetting scheme and run protocol

RT-PCR mix for 1 sample	
18.7 µL	water, HPLC grade
6 µL	MangoTaq reaction buffer
1 µL	50 mM $MgCl_2$
1 µL	10 mM dNTPs
1 µL	5 pmol/µL primer forward
1 µL	5 pmol/µL primer reverse
0.3 µL	5000 U/mL MangoTaq polymerase
1 µL	cDNA-template or water, HPLC grade
30 µL	total volume

Step	Temperature
1.	94°C for 3 min
2.	95°C for 45 sec
3.	Anneal.-temp. for 45 sec
4.	72°C for 45 sec
5.	Go to step 2, repeat for x cycles
6.	72°C for 5 min
7.	12°C, store forever

5.6.5 Real-time PCR

Real-time PCR (qPCR) using SYBR green as fluorochrome was used to quantify the gene expression in different experiments. Data was analysed using the method of Pfaffl[114]. Real-time PCR was set up and run according to (Table 6) and (Table 7).

Table 6 qPCR pipetting scheme

qPCR mix for 1 sample	
10 µL	KAPA^{TM} SYBR® FAST qPCR Mastermix (2x) Universal
8 µL	water, HPLC grade
0.5 mL	5 pmol/µL primer forward
0.5 µL	5 pmol/µL primer reverse
1 µL	cDNA (1:4) or water, HPLC grade
20 µL	total volume

Table 7 qPCR run protocol

Step	Temperature
1.	94°C for 3 min
2.	94°C for 10 sec
3.	Anneal.-temp. for 10 sec
4.	72°C for 20 sec + plate read
5.	Go to step 2, repeat for 39 cycles
6.	Melting curve, 65-90°C, increment 0.5°C for 5 sec + plate read

5.6.6 Sequencing

To verify the identity of PCR products they were sequenced by the Sanger sequence method using the BigDye® Terminator v3.1 cycle sequencing kit. The method is based on a termination reaction with unlabelled dNTPs and labelled ddNTPs. In the mix of the labelled ddNTPs every nucleic base is coupled with a different fluorescent dye and terminates the amplification based on a lack of a free 3' OH-group. Due to differing product sizes created by the use of labelled ddNTPs and unlabelled dNTPs, the whole target sequence is covered and can be analysed by capillary electrophoresis. The analysis results in an electropherogram, displaying the determined nucleic base sequence.
For the analysis, the used PCR product must result in only one band on the agarose gel. The sequence PCR was set up and run according to (Table 8) and (Table 9). Free labelled ddNTPs, which can disturb the read out, were removed by binding them on a column. A NucleoSEQ® column was centrifuged at 1133 xg for 30 sec, equilibrated with 600 µL water (HPLC grade) for 30 min and loaded with 20 µL of the sequence PCR product. The column was centrifuged at 1133 xg for 5 min, the flow through was mixed and vortexed with 3 µL 3 M sodium acetate (pH 4.3) and 80 % ethanol. After incubation for 15 min at room temperature, the solution was centrifuged at 16,090 xg for 20 min and the supernatant discarded. 250 µL 70 % ethanol was added, vortexed and centrifuged at 16,090 xg for 10 min. Supernatant was removed and the pellet air dried before resuspension in 30 µL Hi-Di^{TM} formamide. The solution was transferred into a 96-well plate and further processed at the Institute of Human Genetics of the University of Würzburg by Prof. Feichtinger.

Table 8 Sequence PCR pipetting scheme

Sequencing PCR mix for 1 sample	
4 µL	BigDye® Terminator v3.1 Ready Reaction Mix (2.5x)
2 µL	BigDye® Sequencing v3.1 Buffer 5x
1 µL	5 pmol/µL primer (forward or reverse)
1-2 µL	PCR product
ad 20 µL	water, HPLC grade

Table 9 Sequence PCR run protocol

Step	Temperature
1.	94°C for 4 min
2.	94°C for 30 sec
3.	50°C for 1 min
4.	60°C for 1 min
5.	Go to step 2, repeat for 24 cycles
6.	72°C for 5 min
7.	12°C, stored forever

5.6.7 Densitometry

Analyses of gene expressions in RT-PCR was achieved by measuring the density of the received bands by the open source software GelAnalyzer2010a. The values were normalised to the housekeeping gene EEF1A or RPS27A.

5.7 Microarray analyses

Microarray analysis allows to compare a broad spectrum of gene expressions between different experimental setups. Microarray chips are based on the principle that RNA/DNA binds its complementary sequence.
The chip contains single-stranded fragments of thousands of genes spotted on its surface and is incubated with single-strand fluorescence labelled target cRNA. The emission of the fluorescence dye is detected and analysed. Highest emission is reached, if the target cRNA is fully complement to the spotted fragment.
To determine differences between WISP3 deficient cells and control cells, RNA was isolated from WISP3 knock down and scrambled controls in hMSCs (n=3) 5 to 6 days after transduction. Successful down regulation of WISP3 was verified by RT-PCR and RNA quality was checked by RNA gel electrophoresis. Cell culture experiments and RNA isolation were performed by Simone Hilpert. Preparation, staining and scanning of the Affymetrix GeneChip Human Genome-U133 Plus 2.0 were carried out by PD Dr. L. Klein-Hitpass at the Institute of Cell Biology at the University of Duisburg-Essen, Germany. Therefore, arrays were prepared according to the manufacturer's protocol and scanned with the GeneChip scanner 3000.
Analyses of raw data from the microarray were performed by Dr. Alexander Keller and Dr. Katrin Schlegelmilch with the statistical software R using the scripts and normalisations described in [115]. The valdiadtion was run with RNA from the microarray analyses and additional one.

5.8 Statistics

All experiments were performed at least in three biological independent experiments, if not stated otherwise. Graphics and statistics were created and run by GraphPad Prism version 6.04. Significance was tested with the One-Way or Two-Way ANOVA and corrected by Dunnett test except for the microarray validation where the Sidak test was performed. Significance was accepted if $p < 0.05$.

Part III

Results

Chapter 6

Presence of WISP3 in the musculoskeletal system

To get a first impression of the WISP3 levels in the musculoskeletal system the basal expression of WISP3 was investigated in primary chondrocytes and hMSCs (Figure 2). RT-PCR was performed on a set of nine different hMSC donors in passage one. Analyses revealed a stable expression of a specific sequenced WISP3 mRNA band with only slight variations in mRNA expression level (Figure 2b). In primary chondrocytes the same amount of donors in the same passage showed WISP3 mRNA levels similarly expressed with minor differences in mRNA expression level (Figure 2a). Since both cell types exhibited stable WISP3 mRNA expression.

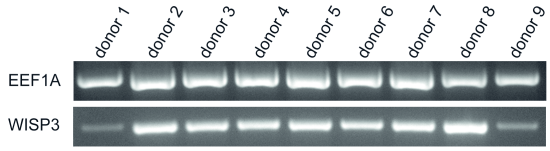

(a) WISP3 expression in primary chondrocytes.

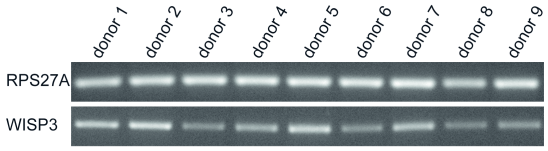

(b) WISP3 expression in hMSCs.

Figure 2 WISP3 mRNA expression in different primary chondrocyte and hMSC donors.
Cells were cultured in passage one for about two weeks before RNA isolation. WISP3 mRNA expression was analysed by RT-PCR and RPS27A or EEF1A served as housekeeping genes.

Chapter 7

Recombinant WISP3-Fc

7.1 Production of recombinant WISP3-Fc

For evaluation of effects caused by WISP3, experiments were performed with WISP3-Fc and the control Fc-Tag, since recombinant protein in comparison to overexpression allows precise control over the applied concentrations. The purity of the recombinant proteins were tested in two concentrations on a silver gel (Figure 3) beforehand. The Fc-Tag produced a band at approximately 30 kDa, as expected. WISP3-Fc exhibited two bands, a lower band at 52 kDa and a higher at approximately 60-62 kDa. The higher molecular weight band displays the recombinant WISP3-Fc that was used for further analysis.

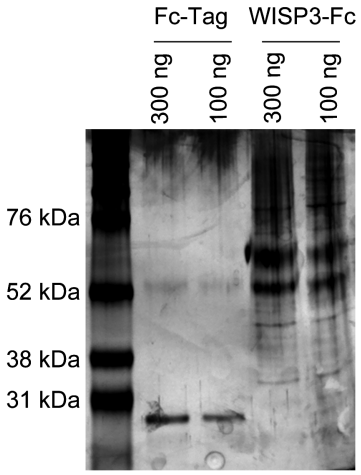

Figure 3 Recombinant WISP3-Fc and Fc-Tag on a silver gel.
Recombinant WISP3-Fc and its respective Fc-Tag were produced in Sf21 cells and purified by affinity chromatography. 100 ng and 300 ng of WISP3-Fc and Fc-Tag were separated in a SDS gel followed by silver staining.

7.2 No effect of WISP3-Fc treatment on proliferation

Since a proliferation effect on hMSCs was described for WISP1, the proliferation rate of hMSCs was analysed after 48 h WISP3-Fc treatment with varying concentrations (Figure 4). No changes in proliferation were detected between the WISP3-Fc treatment and the controls for any of the WISP3-Fc concentrations analysed in the investigated time period.

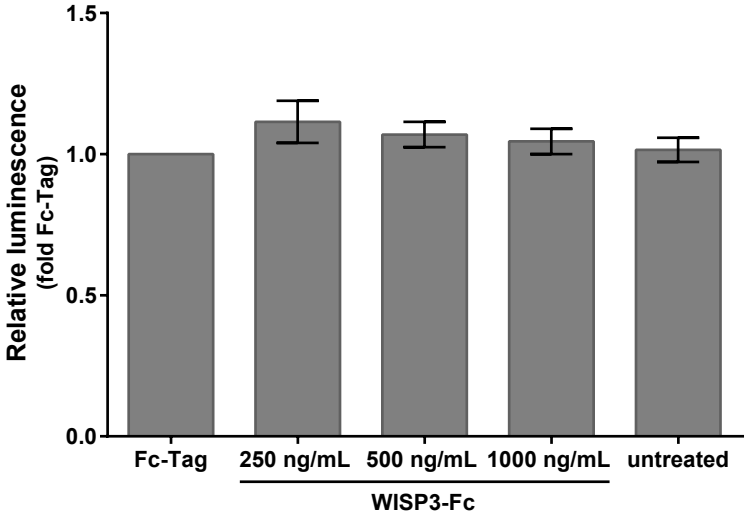

Figure 4 Effect of WISP3-Fc treatment on proliferation of hMSCs after 48 h.
hMSCs were treated with 250, 500 and 1000 ng/mL WISP3-Fc or 397.6 ng/mL Fc-Tag as control for 48 h. Proliferation level was measured with a luminescence assay and normalised to Fc-Tag. Results of four independent experiments are displayed as mean ± standard error of mean (SEM).

Chapter 8

Reduction of WISP3 expression

8.1 Knock down in WISP3-deficient primary chondrocytes and hMSCs

Since the musculoskeletal disease Progressive Pseudorheumatoid Dysplasia correlated to WISP3 is characterised by a preceding cartilage degradation, we investigated the loss of WISP3 in primary chondrocytes and hMSCs. Therefore, WISP3 mRNA expression was reduced by RNA interference with a short-hairpin RNA (shRNA) approach (Figure 5). Five different shRNAs (shRNA1-5) were tested in both cell types, whereas shRNA6 and scramble served as controls. The shRNA6 is a shRNA against another CCN family member and therefore inefficient for WISP3. Scramble displays a general sequence with the same size as the other shRNAs that does not exist in the genome of the investigated organism. In primary chondrocytes four shRNAs (shRNA2-5) showed an explicit down regulation of WISP3 mRNA, whereas shRNA1 displayed only a minor reduction (Figure 5a). The same set of shRNA led to similar results in hMSCs with the same four functional shRNAs (shRNA2-5) remarkably down regulating the WISP3 mRNA expression (Figure 5b). For further experiments either shRNA2, shRNA4 or shRNA5 were used to create a WISP3 mRNA reduction.

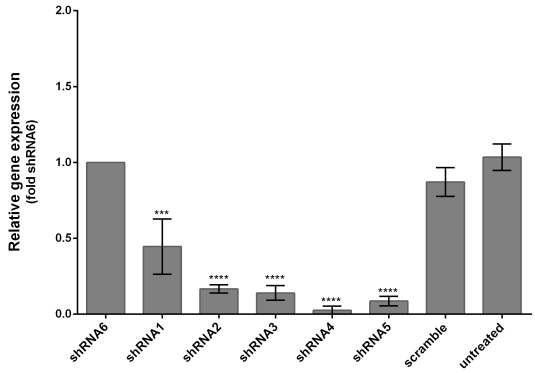

(a) WISP3 expression in primary chondrocytes.

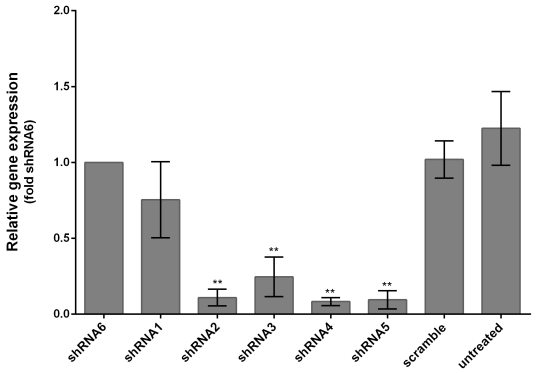

(b) WISP3 expression in hMSCs.

Figure 5 Reduction of WISP3 mRNA expression in primary chondrocytes (a) and hMSCs (b).
WISP3 mRNA expression in primary chondrocytes (a) was analysed with RT-PCR and normalised to the housekeeping gene RPS27A as well as shRNA6. In hMSCs (b) qPCR was performed and the expression was normalised to the housekeeping genes TBP and OAZ1 as well as shRNA6. Results are displayed as mean ± SEM. (n = 4 (a) and n = 3 (b); **** $p < 0.0001$, *** $p < 0.001$, ** $p < 0.01$ and * $p < 0.05$)

8.2 Unaffected CCN family member expression in WISP3 knock down

Since the CCN family members share a high sequence homology, gene expression of all family members was analysed to exclude undesired side effects due to the WISP3 knock down. WISP3 knock down was performed in three hMSC donors with the functional shRNAs (shRNA2, shRNA4 and shRNA5) as well as the corresponding controls. Gene expression was analysed by RT-PCR at day 6 (Figure 6). The expression of WISP3 mRNA was successfully down regulated with all functional shRNAs. The expression of CYR61 was nearly stable with the different shRNAs just as seen for CTGF and WISP2. The expression of NOV and WISP1 mRNA exhibited minor changes in comparison to shRNA6.

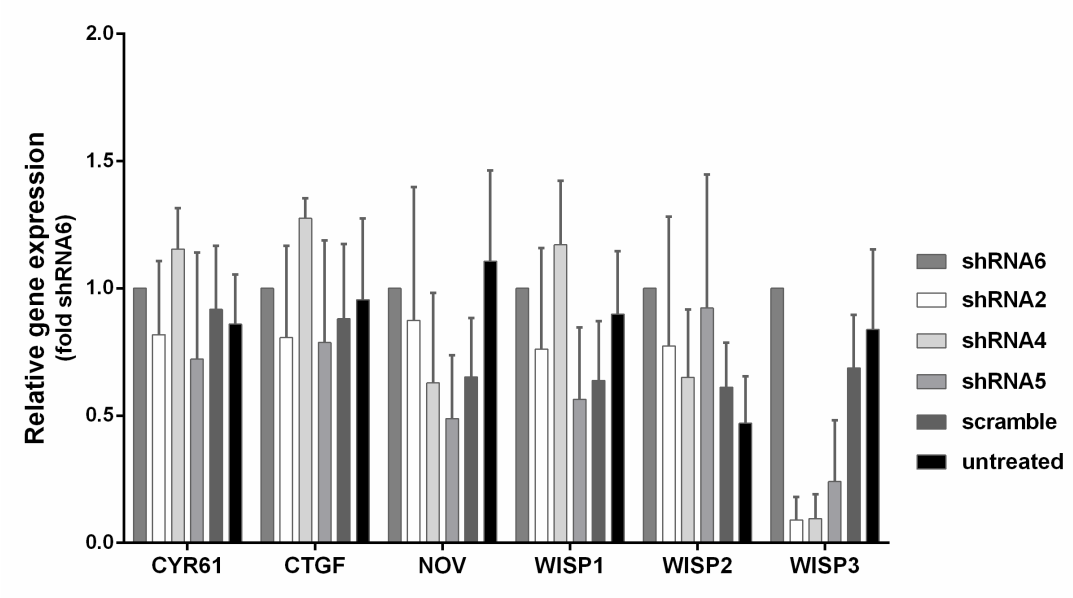

Figure 6 Gene expression of the CCN family members in WISP3-deficient hMSCs at day 6.
WISP3 was knocked down in hMSCs with shRNA2, shRNA4 and shRNA5. Cells were harvested at day 6, RNA was isolated and transcribed before analysing the gene expression with RT-PCR. The expression was normalised to the housekeeping gene RPS27A as well as shRNA6. Bar chart represents the mean ± SEM. (n = 3)

8.3 WISP3 knock down in primary chondrocytes

Reduction of WISP3 was monitored under the microscope and on mRNA level using a shRNA system in primary chondrocytes in a time series over eight days (Figure 9). Successful transduction with the different shRNAs was measured relatively to the positive fluorescence signal of GFP control cells. After 24 h, the first cells exhibited a GFP expression, rising up to 80 % at day eight. Four days after transduction of the cells, first morphological changes were detected in cells treated with shRNA2. There were fewer cells in comparison to the controls. Moreover, these cells showed a more elongated shape and less cell-cell contact. Over time WISP3-deficient cells became more spindle-shaped (day 8) and died in the next seven to ten days (data not shown). Other controls (shRNA6 and scramble) showed no morphological changes over time. Gene expression analyses showed a reduction of WISP3 mRNA at day four that remained nearly unchanged until the end of the investigated period (Figure 7). This proves, that the knock down of WISP3 was successfull in nearly all cells and that untransduced cells did not overgrow the WISP3-deficient cells. Crystal violet staining allowed the indirect analysis of cell number at day eight since the stain intercalates with DNA. Analyses of crystal violet staining exhibited a significant decrease in cell number for WISP3-deficient primary chondrocytes (shRNA2) in comparison to the controls (Figure 8).

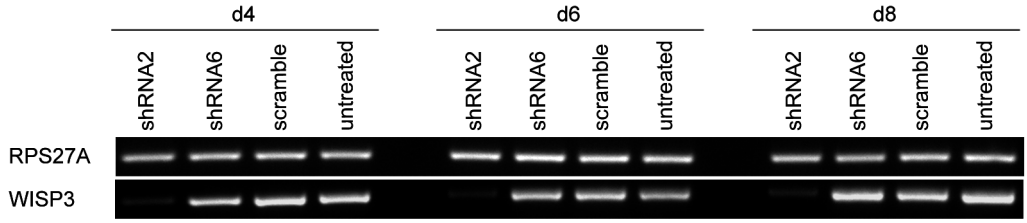

Figure 7 WISP3 gene expression in WISP3-deficient primary chondrocytes.
Reduction of WISP3 mRNA was performed with shRNA2, while shRNA6 and scramble served as controls. RPS27A was used as housekeeping gene.

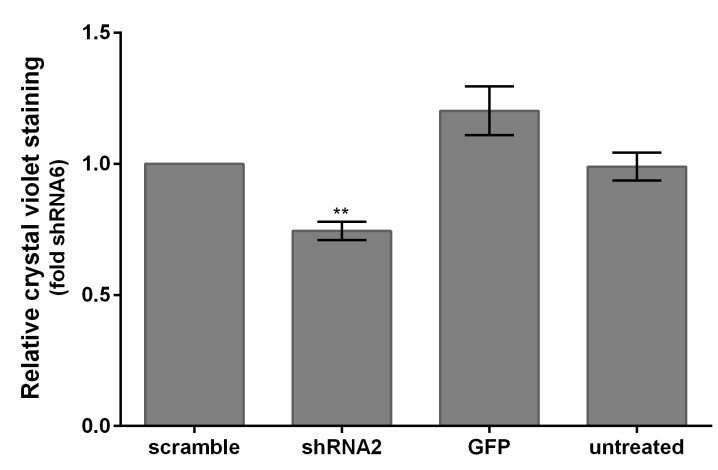

Figure 8 Changes in cell number in WISP3-deficient primary chondrocytes.
Reduction of WISP3 mRNA was performed in primary chondrocytes with shRNA2, whereby scramble served as control. Cells were stained at day 8 after transduction and crystal violet staining was normalised to scramble. Results are displayed as mean ± SEM. (n = 4; ** p =< 0.001)

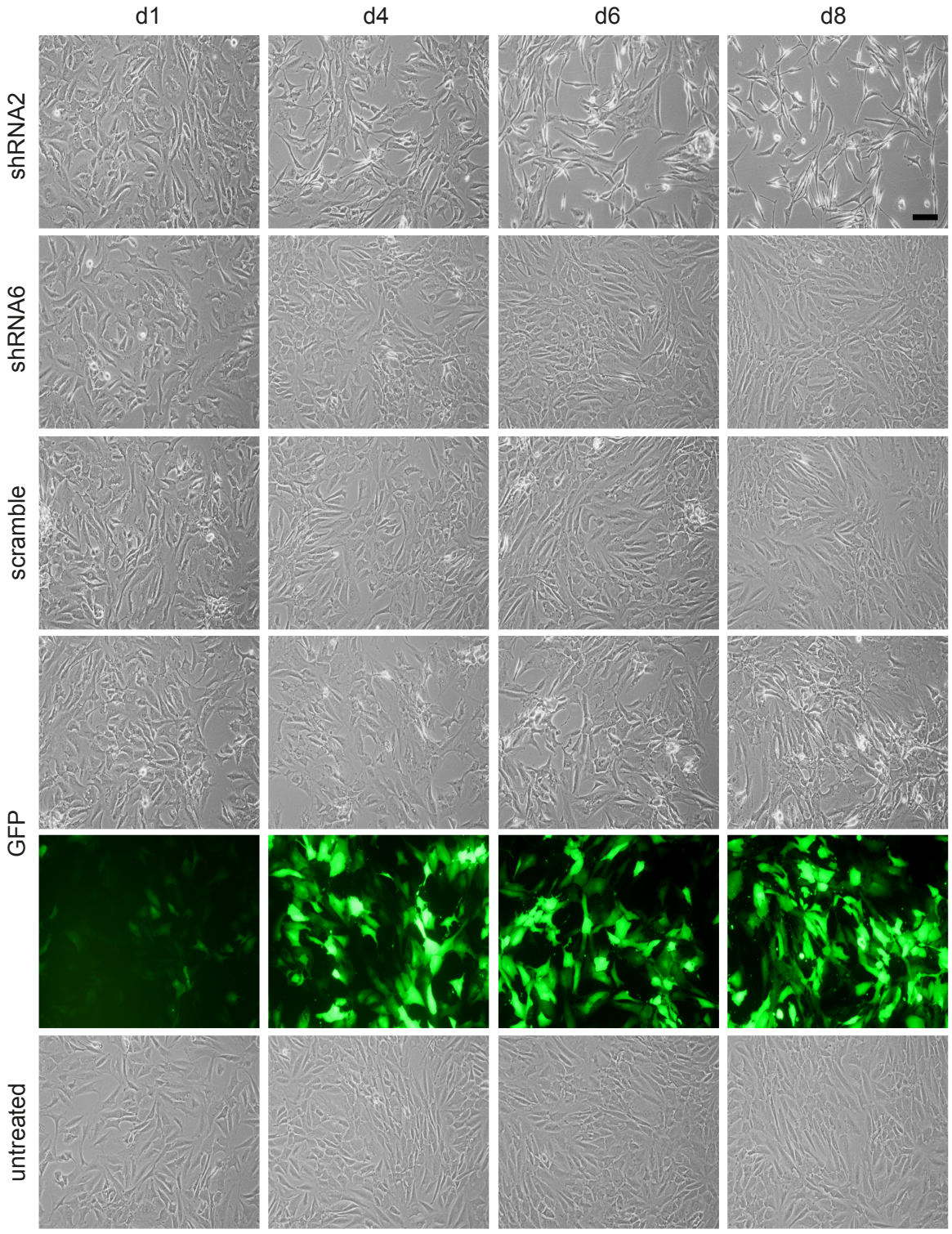

Figure 9 WISP3 knock down in primary chondrocytes on a time series.
WISP3 gene expression was reduced with shRNA2, whereas shRNA6 and scramble served as controls. GFP was used as indicator for transduction efficiency. Scale bar represents 100 µm.

8.4 WISP3 knock down in hMSCs

Another cell type (hMSCs) was investigated for the role of WISP3 over an eight day time period (Figure 12). First GFP positive cells were detected the day after transduction, reaching a maximum at day four with approximately 80 %. The reduction of WISP3 mRNA levels led to morphologic changes and a decreasing cell number over a time series. First changes appeared around day four, displaying elongated cells if transduced with shRNA2 or holes in the cell layer in case of shRNA4 transduction. Cells transduced with shRNA2 became smaller with a more spindle-shaped morphology over time. Transduction with shRNA4 led to the formation of holes in the cell layer which enlarged over the investigated time period. The mRNA analyses showed a loss of WISP3 mRNA in cells transduced with shRNA2 or shRNA4 as early as day four, whereas there were no differences in the controls (Figure 10). The time serie proves that most cells were WISP3-deficient since untransduced cells did not overgrow them. In Figure 11 the cell number of three donors at day six are displayed as a correlation of crystal violet staining normalised to shRNA6. In both WISP3-deficient hMSC samples (shRNA2 and shRNA4) the crystal violet staining was decreased compared to shRNA6, with shRNA2 showing the lowest crystal violet staining. No differences were detected between the controls.

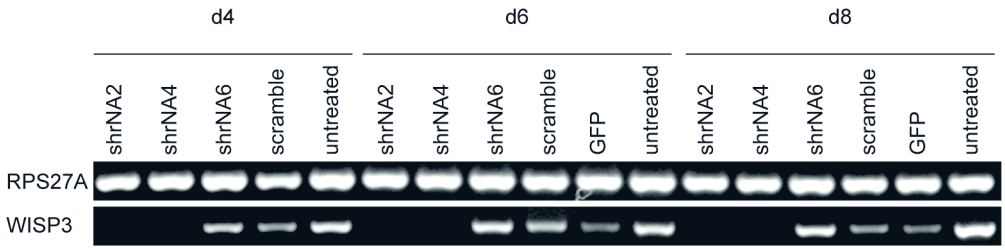

Figure 10 WISP3 mRNA expression in WISP3-deficient hMSCs in a time series.
WISP3 mRNA was reduced by shRNA2 and shRNA4 while shRNA6 and scramble served as controls. RPS27A served as housekeeping gene.

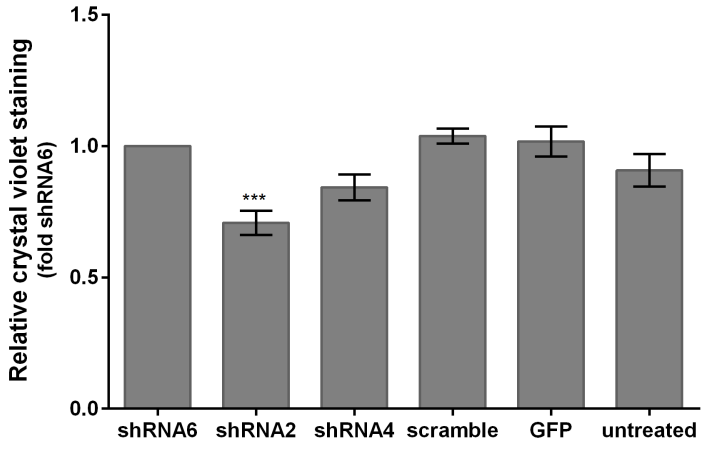

Figure 11 Changes in cell number in WISP3-deficient hMSCs.
Reduction of WISP3 mRNA expression was performed with shRNA2 and shRNA4, while shRNA6 and scramble served as controls. Cells were stained six days after transduction with crystal violet. The staining was normalised to shRNA6. Results are displayed as mean ± SEM. ($n = 5$; *** $p < 0.001$)

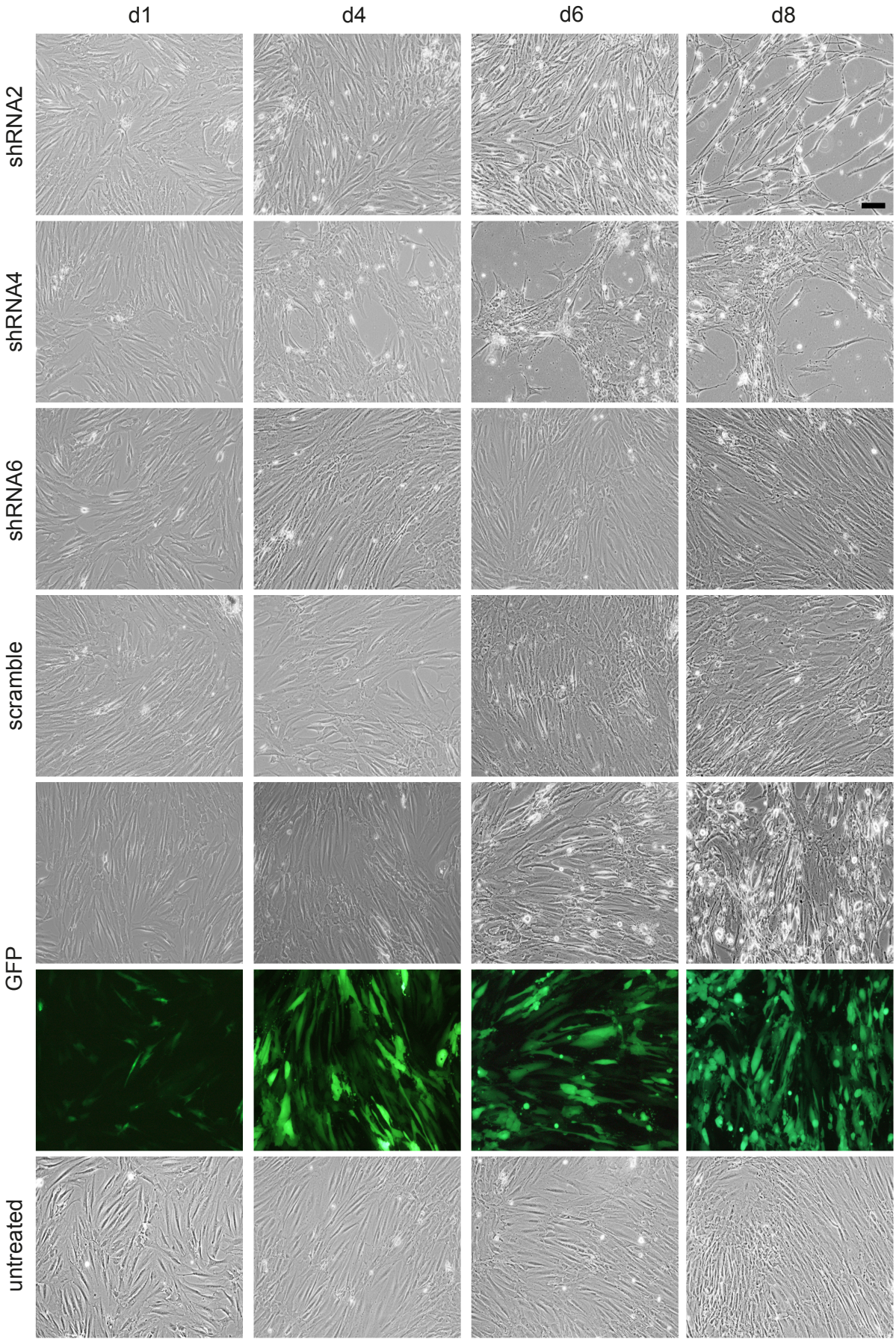

Figure 12 Reduction of WISP3 expression in hMSCs in an eight day time period.
WISP3 mRNA expression was reduced with two shRNAs. Scramble and GFP transduced cells served as controls. Scale bar represents 100 µm.

8.5 No effect of recombinant WISP3 during simultanous knock down

To investigate the rescue of the phenotypic changes seen during WISP3 mRNA reduction, hMSCs transduced with shRNA were immediately treated with 500 ng/mL WISP3-Fc (purity of recombinant proteins checked on silver gel, Section 5.3.3) or 198.6 ng/mL Fc-Tag as control (Figures 14, 15, 16). Treatment with WISP3-Fc did not rescue the phenotypic changes seen before. After four days, WISP3-deficient hMSCs displayed a more elongated shape compared to the controls independent of the treatment. At day six, cells became more spindle-shaped and the cell number decreased in WISP3-deficient hMSCs. Treatment with Fc-Tag displayed the same phenotypic and molecular changes seen without any treatment. No morphological differences were observed in the controls. Gene expression analyses revealed a successful reduction of WISP3 mRNA in shRNA2 and shRNA4 treated hMSCs compared to shRNA6 (Figure 13). No differences in WISP3 mRNA levels were detectable between WISP3-Fc, Fc-Tag or the no treatment control in the single groups.

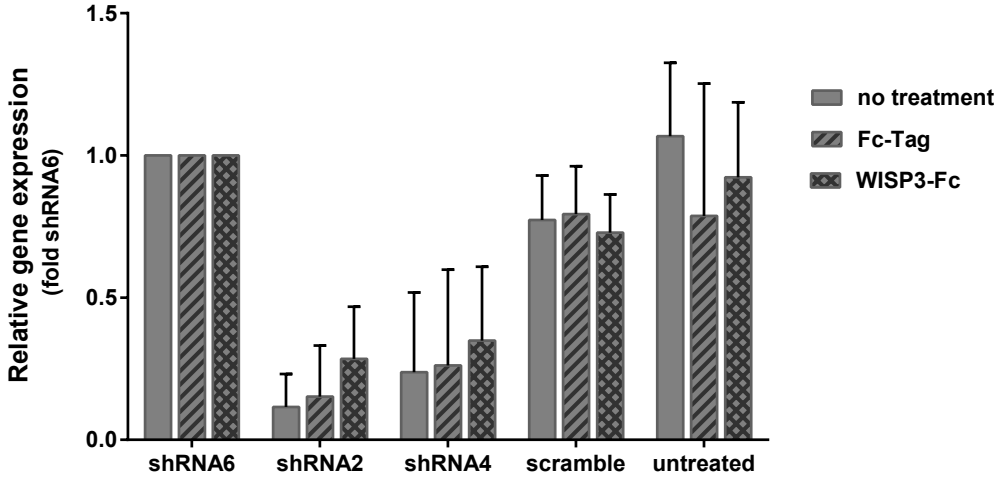

Figure 13 WISP3 gene expression in WISP3-deficient hMSCs treated with recombinant WISP3-Fc. Immediately after transduction cells were either treated with 500 ng/mL WISP3-Fc, 198.6 ng/mL Fc-Tag or left untreated. RNA was harvested 6 days after transduction, reverse transcribed and analysed by qPCR. Gene expression was normalised to the housekeeping genes TBP and OAZ1 as well as its corresponding control of shRNA6. Bar chart represents five independent experiments as mean ± SEM.

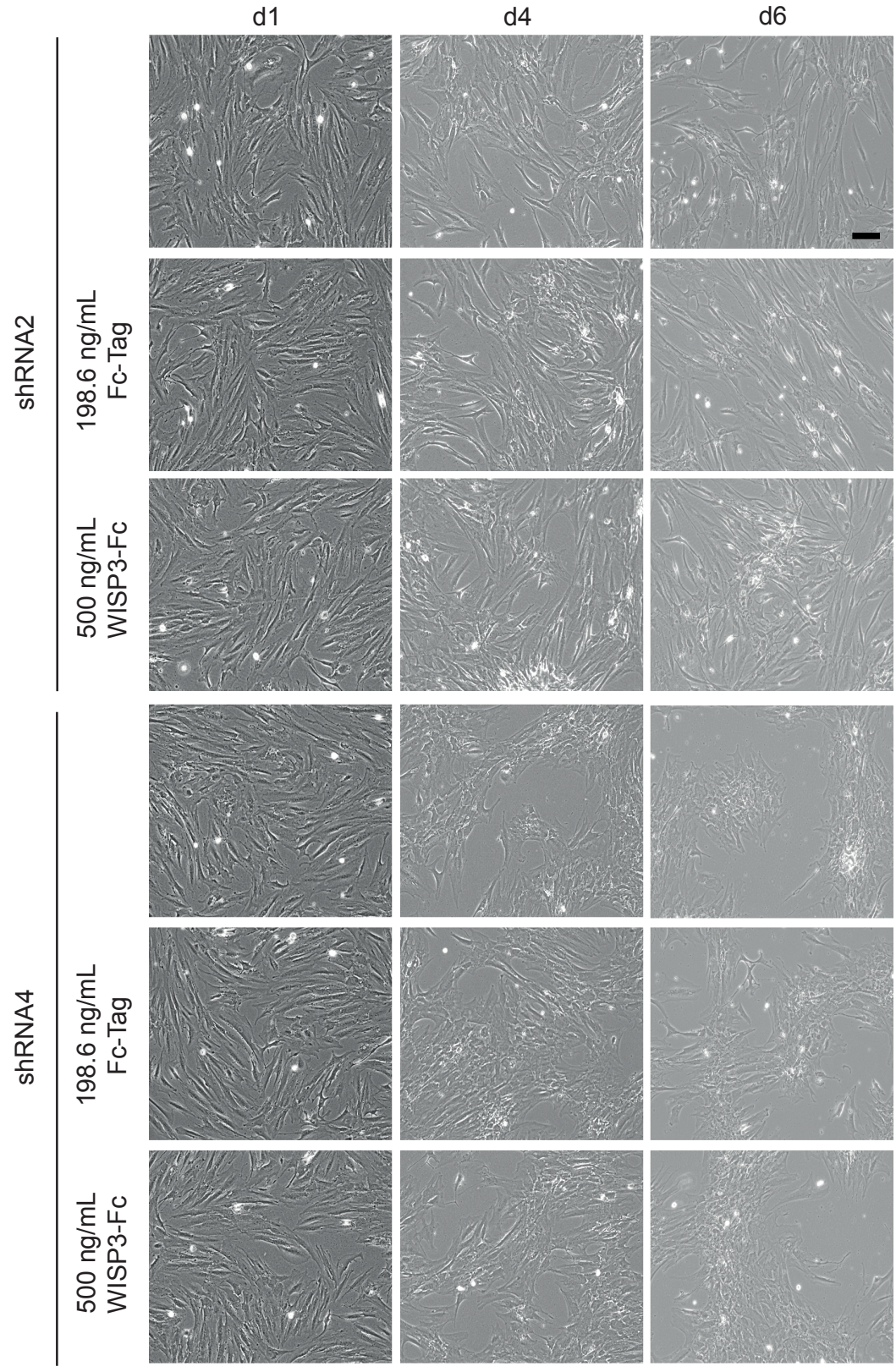

Figure 14 WISP3 knock down in hMSCs treated with recombinant WISP3-Fc. Scale bar represents 100 µm.

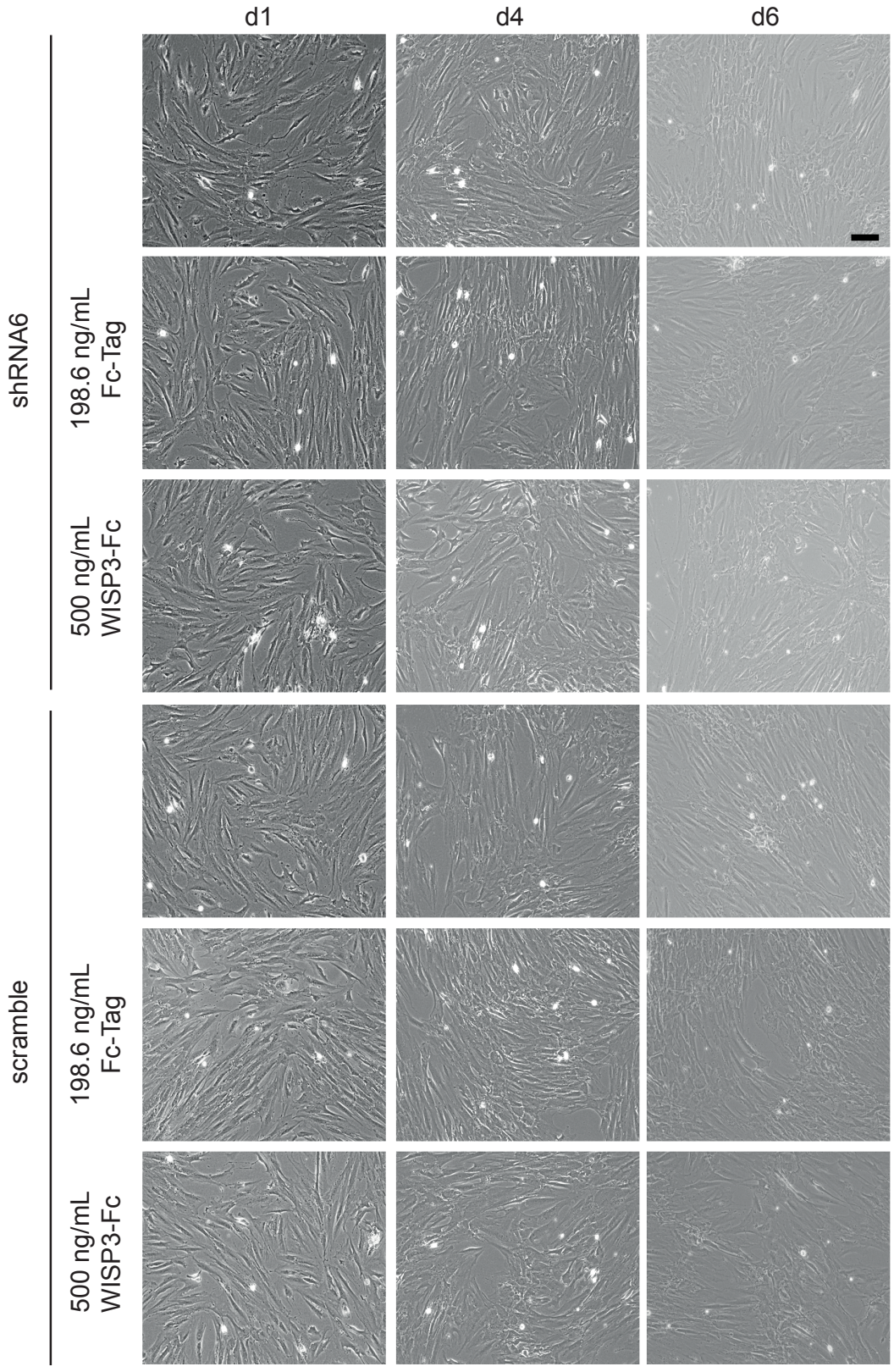

Figure 15 WISP3 knock down controls of hMSCs treated with recombinant WISP3-Fc. Scale bar represent 100 µm.

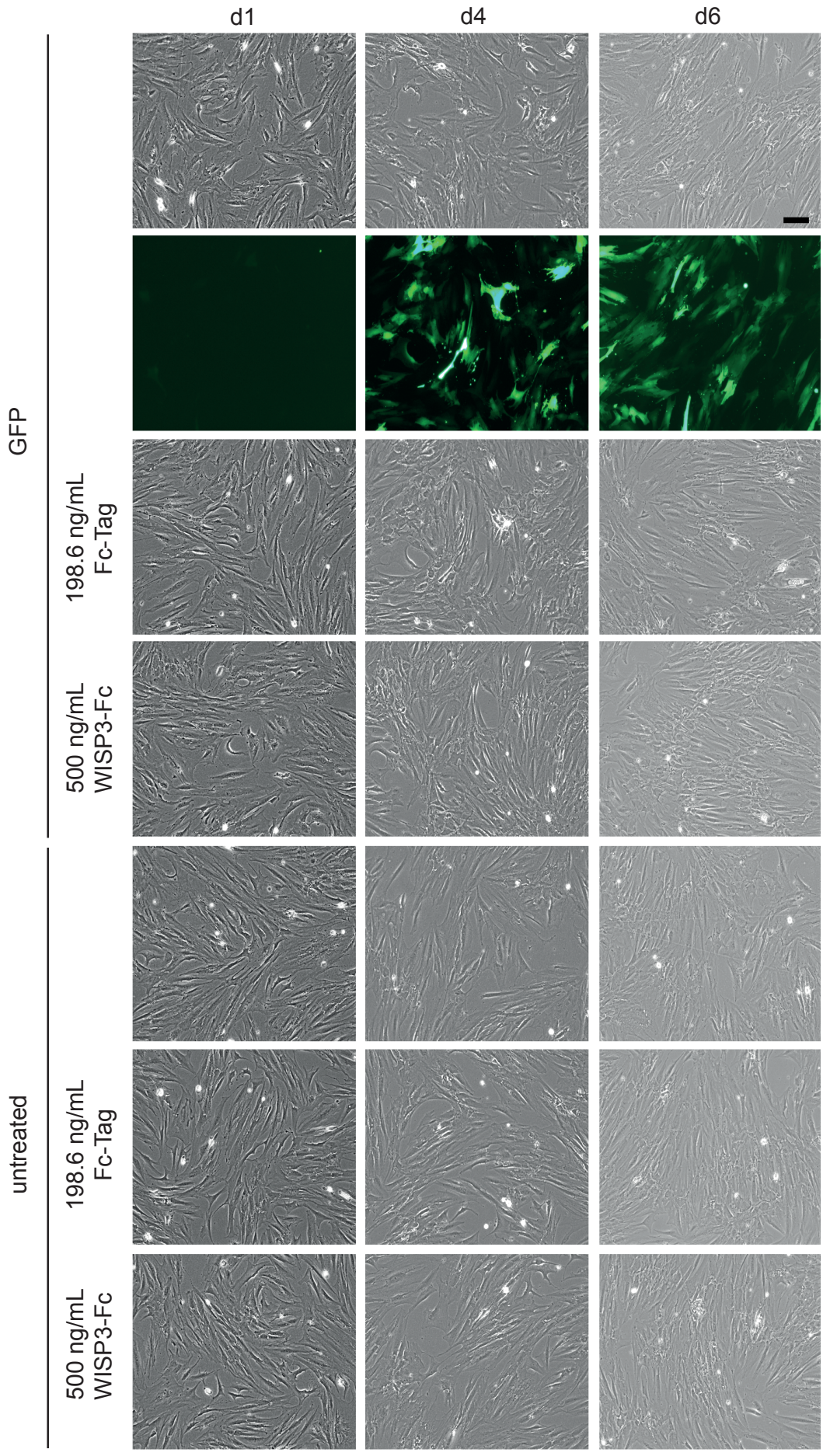

Figure 16 Non- and GFP-transduced hMSCs treated with recombinant WISP3. Scale bar represents 100 µm.

Chapter 9

Detection of cell death markers

9.1 Inactive caspases in WISP3-deficient primary chondrocytes and hMSCs

The observed reduction in cell number during WISP3 knock down was investigated by analysing the activation of caspase 3 12 days (chondrocytes) and 11 days (hMSCs) after transduction (Figure 17). Caspase 3 is an effector caspase that is always activated, independent of the type of apoptosis (intrinsic or extrinsic). Primary chondrocytes and hMSCs were transduced with shRNA2 to reduce WISP3 mRNA, whereas scramble served as control of the shRNA system. A lysate of Jurkat cells served as negative control while Jurkat cells treated with cytochrome C represent a positive control (controls bought from Cell Signaling Technology - #9663) for active caspases. The Western blot showed the uncleaved caspase 3 at 30 kDa and a cleaved protein band at 19 kDa in the positive control. Protein analyses revealed no active caspase 3 in primary chondrocytes or hMSCs. GAPDH was used as a loading control and displayed the expected band at approximately 38 kDa. Activation of all caspases was further analysed in hMSCs eight days after transduction (Figure 18). Cells were transduced with shRNA2 or shRNA4 to reduce WISP3 mRNA and scramble served as control of the shRNA system. Activation of caspases was induced by the incubation with hydrogen peroxide to generate a positive control. Hydrogen peroxide activated cells displayed a bright red fluorescence signal throughout the whole cell. Cells transduced with shRNA2 or shRNA4 mostly revealed dotted staining surrounding the nucleus. Scramble and untreated controls exhibited only slight staining of single cells.

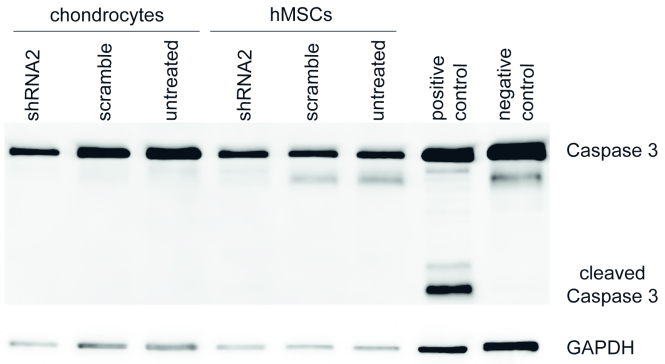

Figure 17 Detection of active caspase 3 in WISP3-deficient primary chondrocytes and hMSCs.
Western blot was performed with cells harvested 12 days (primary chondrocytes) and 11 days (hMSCs) after transduction. WISP3 mRNA expression was reduced by shRNA2 while scramble served as control. Jurkats cells untreated and treated with cytochrome C served as antibody specific controls. GAPDH was used as loading control.

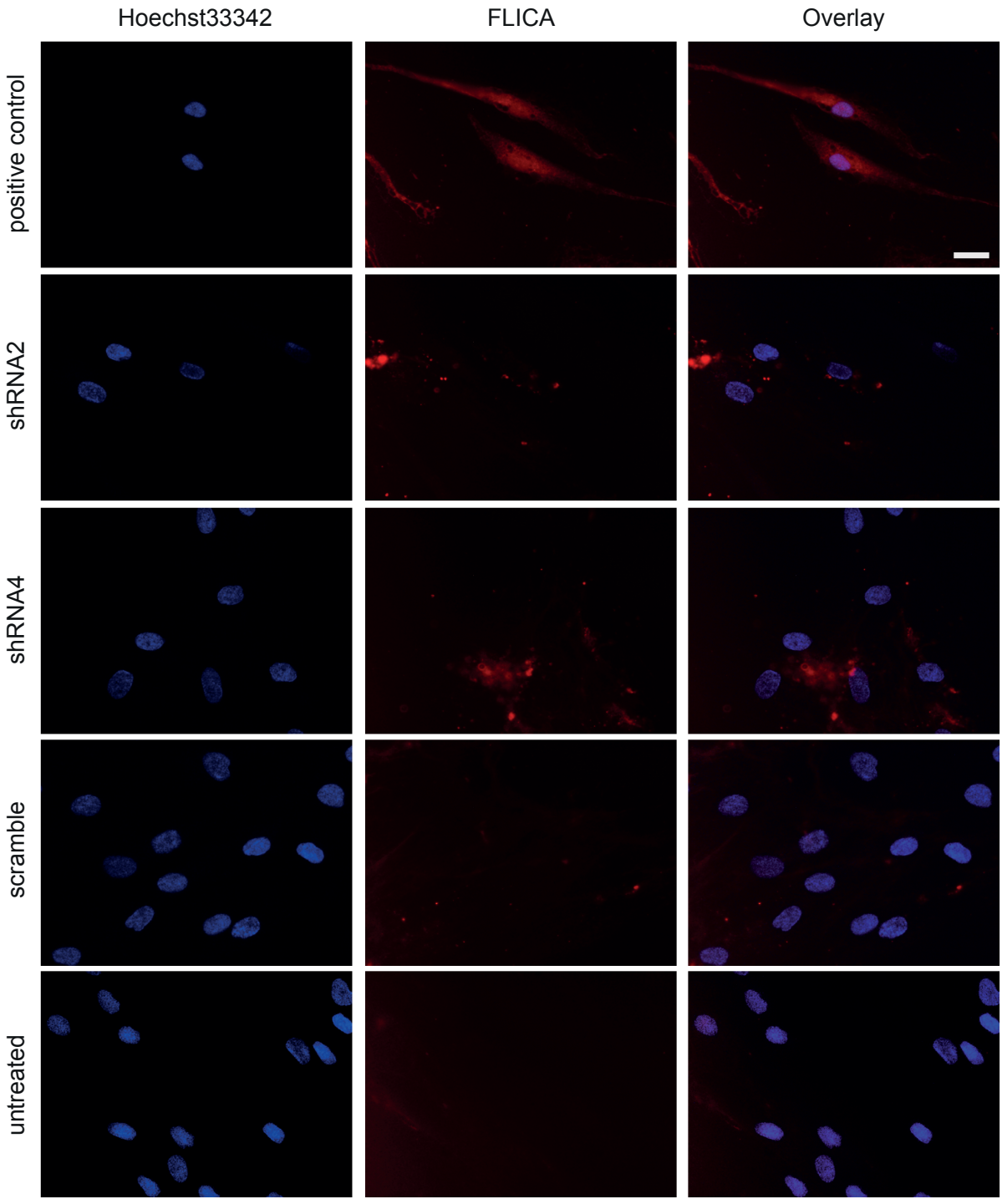

Figure 18 Detection of active caspases in WISP3-deficient hMSCs at day 8.
WISP3 was knocked down with shRNA2 and -4, while scramble served as control. At day 8 cells were stained with the fluorochrome coupled caspase inhibitor (FLICA) whereas cells treated with 6 µL 30 % hydroxide peroxide served as staining control. Scale bar represents 50 µm

9.2 Loss of membrane integrity in WISP3-deficient hMSCs

Loss of cell number during WISP3 knock down was further investigated by the localisation of phosphatidylserine, which translocates from the inner to the outer plasma membrane in response to apoptosis induction. Annexin V binds phosphatidylserine and is used as a detector molecule when coupled to a fluorochrome. WISP3-deficient hMSCs were stained eight days after transduction (Figure 19), when phenotypic changes were clearly visible. Cells incubated with 30 % hydrogen peroxide for approximately 30-45 minutes served as positive control. WISP3 mRNA expression was reduced by shRNA2 and shRNA4. Scramble and vector only were used as controls for the shRNA system. Treatment with hydrogen peroxide revealed a bright red fluorescence signal in the cytoplasma in nearly all cells. Most shRNA2-hMSCs exhibited a positive staining, while cells transduced with shRNA4 show only few positive cells. In contrast, controls (shRNA6 and scramble) displayed only sporadically some stained cells that were expected. Intensity of the staining display minor changes due to variations in transduction efficiency.

9.3 Steady death receptor expression

Extrinsic apoptosis is triggered by the activation of death receptors on the cell surface. TRAILR1 (also called TNFRSF10A or DR4) and TRAILR2 (also TNFRSF10B or DR5) together with CD95 are the most prominent apoptosis inducing death receptors. Furthermore, additional work in our lab demonstrated a activation of TRAILR1 and -2 in WISP1-deficient hMSCs. Since the CCN family members share high amino acid homologies the expression of two of the afore mentioned death receptors was examined to clarify the mechanism of cell death seen in our model. In contrast to WISP1-deficient hMSCs, no induction of the mRNA expression of neither TRAILR1 nor TRAILR2 was determined in cells transduced with shRNA2 or -4 compared to their controls (Figure 20).

9.4 Exclusion of autophagy as cause of cell death

Another form of cell death is autophagy which normally supports cell survival by degradation of accumulated unprocessed proteins. Therefore, autophagy was investigated as a possible mechanism for the observed cell death in hMSCs. Protein lysates of WISP3-deficient hMSCs were tested for the presence of processed light chain 3, a subunit of microtubule-associated protein 1A and 1B (LC3 A/B). LC3 A/B interacts with autophagosomes and is cleaved during autophagy, thus serving as a specific marker. A lysate of HeLa cells served as negative control, while HeLa cells treated with 50 µM chloroquine for 24 h were used as positive control (bought from Cell Signaling Technology - #11972). In Figure 21 a weak band at approximately 16 kDa for the unprocessed LC3 A/B protein was detected. No further bands were found in shRNA2 or shRNA4 transduced cells as well as the shRNA6 control. Only the positive control displayed the expected processed LC3 A/B band at approximately 14 kDa. GAPDH was used as loading control and revealed a band at approximately 38 kDa.

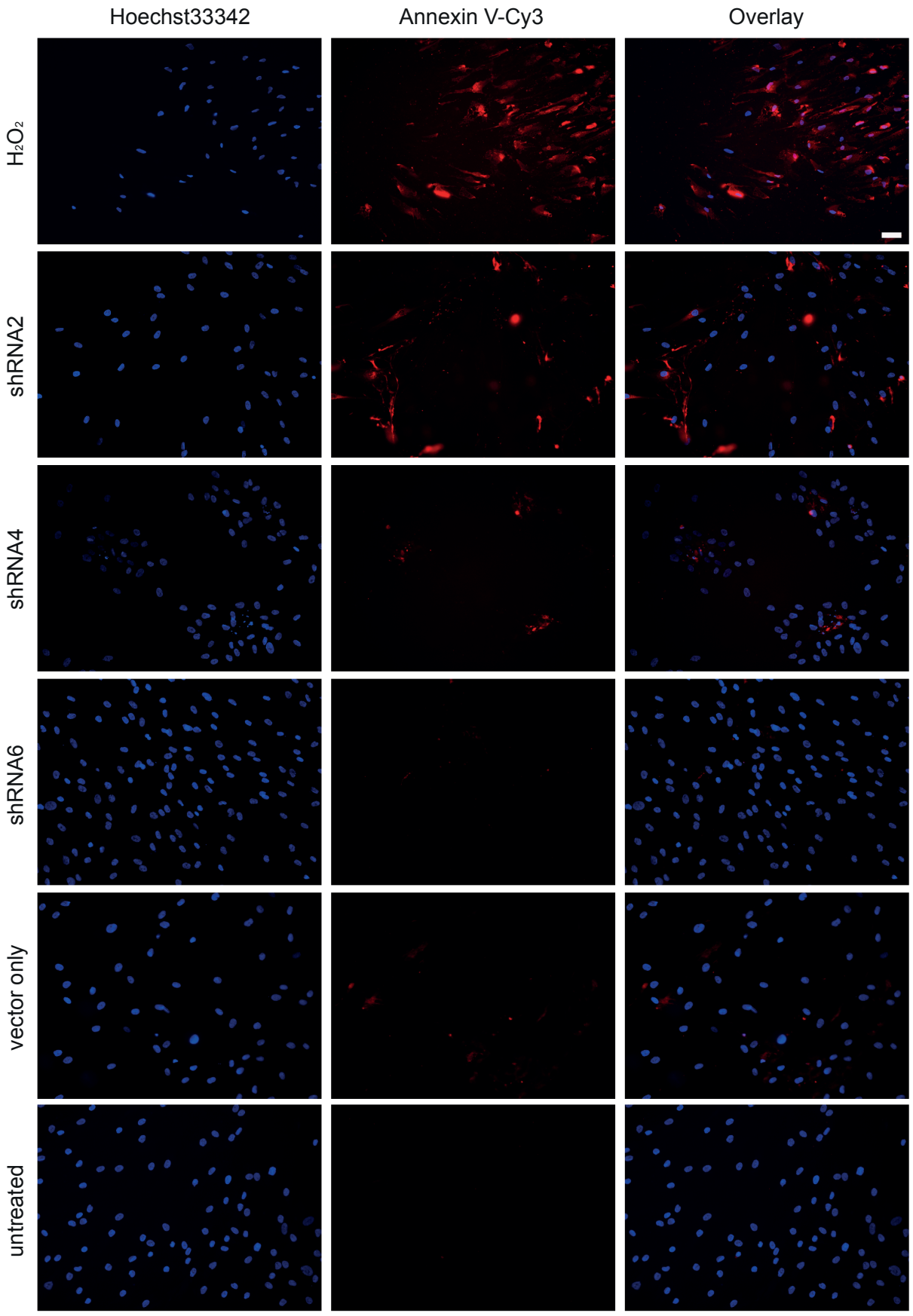

Figure 19 Annexin V-Cy3 staining of WISP3-deficient hMSCs at day 8 after transduction.
At day 8 cells were stained with Annexin V-Cy3, whereas cells treated with 6 µL 30 % hydroxide peroxide served as staining control. Scale bar represents 50 µm.

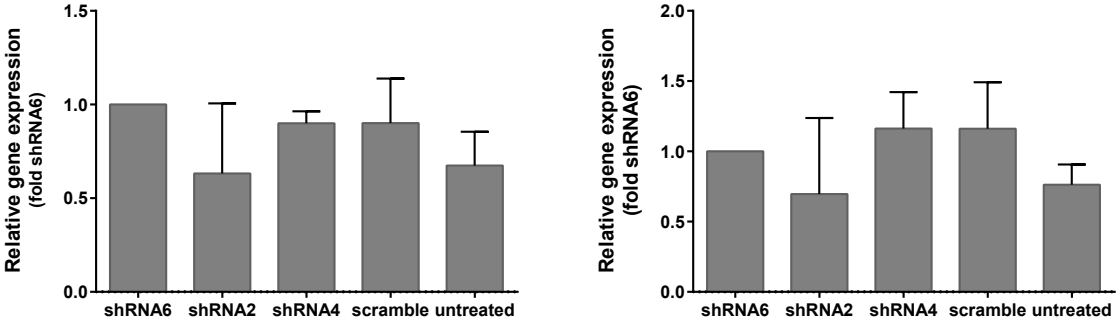

(a) TRAILR1 mRNA expression.

(b) TRAILR2 mRNA expression.

Figure 20 TRAILR1 (a) and TRAILR2 (b) mRNA expression in WISP3-deficient hMSCs 6 days after transduction.
Reduction of WISP3 was performed with shRNA2 and -4 while shRNA6 and scramble served as control. mRNA expression was analysed by RT-PCR and normalised to RPS27A. Results of three independent experiments are displayed as mean ± SEM.

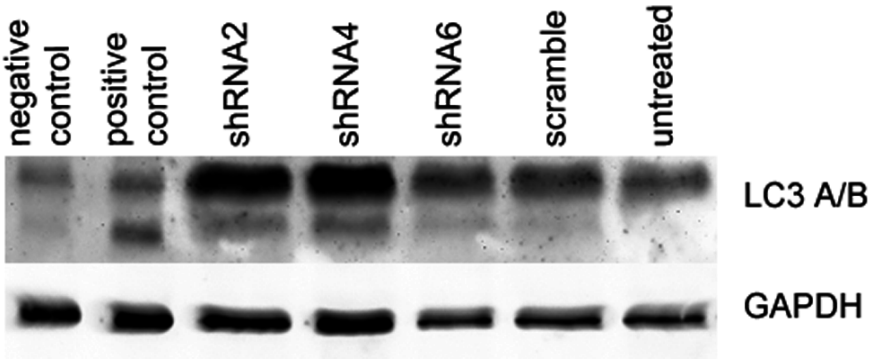

Figure 21 Detection of the autophagic marker LC3 A/B in WISP3-deficient hMSCs.
Western blot was performed with cells harvested at day 7 after transduction. WISP3 mRNA expression was reduced by the effective shRNAs (shRNA2 and -4) while shRNA6 and scramble served as controls. HeLa cells untreated or treated with 50 µM chloroquine for 24 h served as antibody specific controls. GAPDH was used as loading control.

Chapter 10

Microarray analyses

10.1 Overall regulation in the microarray analyses

Knock down of WISP3 resulted in changed phenotype where the responsible signalling pathway was unknown. For that reason, microarray analyses were performed to uncover the role of WISP3 as survival factor. The analyses comprised shRNA5 transduced WISP3-deficient hMSCs compared to scramble of three independent experiments at day six.
The analyses revealed a total of 679 regulated probe sets, whereby 323 probe sets were upregulated and 374 probe sets were downregulated. The top 25 regulated genes, up- and downregulated, are presented in Table 10 and in Table 11. The microarray analyses did not reveal clusters of genes specific for apoptosis or autophagy. The Kyoto Encyclopedia of Genes and Genomes (KEGG) is a database on interactions of signalling pathways based on molecular informatics of the involved genes. This database was included in the analyses to get an overview of overexpressed signalling pathways. The results display the counted regulated genes of a specific signalling pathway. The following signalling pathways were found under the top ten: the cell cytoskeleton and cell cycle as well as focal adhesion and MAPK signal pathway (Figure 22).

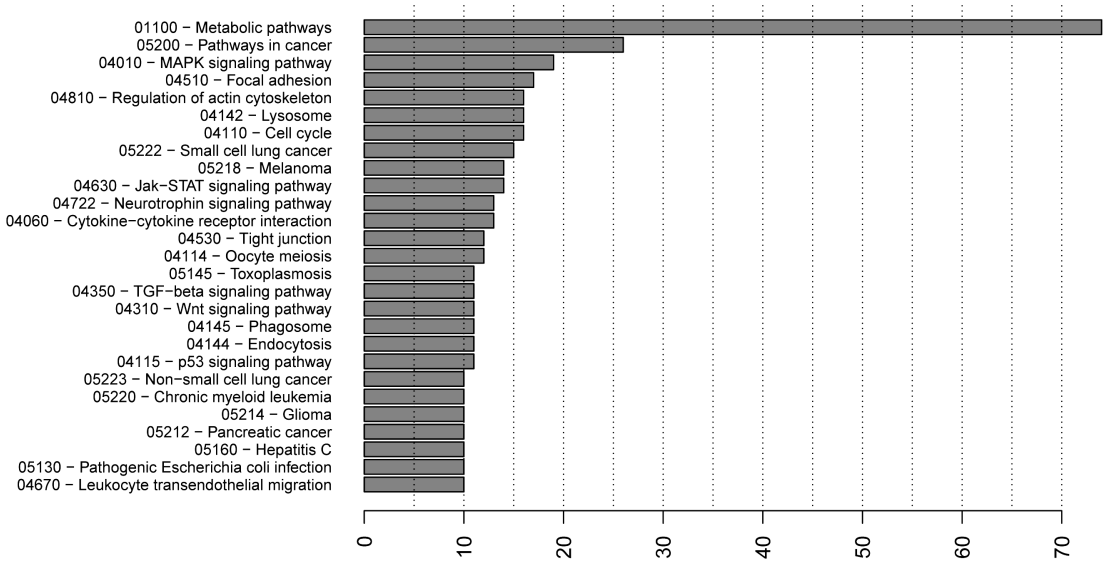

Figure 22 KEGG overexpression pathways of the hMSCs microarray.
Bar chart represents the amount of regulated genes counted for a specific signalling pathway (pathways are numbered according to KEGG database).

Table 10 Excerpt of the 25 most upregulated genes of the hMSCs microarray analyses. The logFc is displayed for the highest regulated probe sets.

Probe set ID	Symbol	Gene name	logFc	adj. p-value
213782_s_at	MYOZ2	myozenin 2	1.75	0.0082
213222_at	PLCB1	phospholipase C, beta 1 (phosphoinositide-specific)	1.70	0.0082
244360_at	FBXL17	F-box and leucine-rich repeat protein 17	1.69	0.0568
205113_at	NEFM	neurofilament, medium polypeptide	1.67	0.0116
224680_at	TMED4	transmembrane emp24 protein transport domain containing 4	1.65	0.0180
232000_at	TTC39B	tetratricopeptide repeat domain 39B	1.57	0.0139
232914_s_at	SYTL2	synaptotagmin-like 2	1.53	0.0118
212636_at	QKI	quaking homolog, KH domain RNA binding (mouse)	1.48	0.0162
235004_at	RBM24	RNA binding motif protein 24	1.44	0.0180
205475_at	SCRG1	stimulator of chondrogenesis 1	1.42	0.0387
1554997_a_at	PTGS2	prostaglandin-endoperoxide synthase 2 (prostaglandin G/H synthase and cyclooxygenase)	1.41	0.0149
228817_at	ALG9	asparagine-linked glycosylation 9, alpha-1,2-mannosyltransferase homolog (S. cerevisiae)	1.40	0.0118
208096_s_at	COL21A1	collagen, type XXI, alpha 1	1.39	0.0421
239835_at	KBTBD8	kelch repeat and BTB (POZ) domain containing 8	1.38	0.0118
210755_at	HGF	hepatocyte growth factor (hepapoietin A; scatter factor)	1.35	0.0291
228186_s_at	RSPO3	R-spondin 3 homolog (Xenopus laevis)	1.32	0.0278
209197_at	SYT11	synaptotagmin XI	1.32	0.0118
222379_at	KCNE4	potassium voltage-gated channel, Isk-related family, member 4	1.31	0.0548
202498_s_at	SLC2A3	solute carrier family 2 (facilitated glucose transporter), member 3	1.28	0.0568
217738_at	NAMPT	nicotinamide phosphoribosyltransferase	1.27	0.0145
205608_s_at	ANGPT1	angiopoietin 1	1.26	0.0118

...continuous on the next page

Table 10 Excerpt of the 25 most upregulated genes of the hMSCs microarray analyses. The logFc is displayed for the highest regulated probe sets.

Probe set ID	Symbol	Gene name	logFc	adj. p-value
1561615_s_at	SLC8A1	solute carrier family 8 (sodium/calcium exchanger), member 1	1.24	0.0244
226189_at	ITGB8	integrin, beta 8	1.22	0.0118
217428_s_at	COL10A1	collagen, type X, alpha 1	1.21	0.0278
203989_x_at	F2R	coagulation factor II (thrombin) receptor	1.20	0.0266

Table 11 Excerpt of the 25 most downregulated genes of the hMSCs microarray analyses. The logFc is displayed for the highest regulated probe sets.

Probe set ID	Symbol	Gene name	logFc	adj. p-value
210861_s_at	WISP3	WNT1 inducible signalling pathway protein 3	-3.58	0.0082
205302_at	IGFBP1	insulin-like growth factor binding protein 1	-2.38	0.0162
209351_at	KRT14	keratin 14	-2.03	0.0162
219529_at	CLIC3	chloride intracellular channel 3	-1.90	0.0149
208754_s_at	NAP1L1	nucleosome assembly protein 1-like 1	-1.88	0.0082
224436_s_at	NIPSNAP3A	nipsnap homolog 3A (C. elegans)	-1.81	0.0118
201005_at	CD9	CD9 molecule	-1.74	0.0371
228748_at	CD59	CD59 molecule, complement regulatory protein	-1.66	0.0232
208051_s_at	PAIP1	poly(A) binding protein interacting protein 1	-1.65	0.0323
226869_at	MEGF6	multiple EGF-like-domains 6	-1.58	0.0144
203186_s_at	S100A4	S100 calcium binding protein A4	-1.57	0.0180
205498_at	GHR	growth hormone receptor	-1.55	0.0139
201596_x_at	KRT18	keratin 18	-1.54	0.0470
234304_s_at	IPO11	importin 11	-1.54	0.0118
200641_s_at	YWHAZ	tyrosine 3-monooxygenase/tryptophan 5-monooxygenase activation protein, zeta polypeptide	-1.53	0.0118

...continuous on the next page

Table 11 Excerpt of the 25 most downregulated genes of the hMSCs microarray analyses. The logFc is displayed for the highest regulated probe sets.

Probe set ID	Symbol	Gene name	logFc	adj. p-value
224779_s_at	FAM96A	family with sequence similarity 96, member A	-1.53	0.0082
212912_at	RPS6KA2	ribosomal protein S6 kinase, 90kDa, polypeptide 2	-1.53	0.0118
209064_x_at	PAIP1	poly(A) binding protein interacting protein 1	-1.52	0.0265
223519_at	ZAK	sterile alpha motif and leucine zipper containing kinase AZK	-1.49	0.0102
212977_at	CXCR7	chemokine (C-X-C motif) receptor 7	-1.48	0.0179
217814_at	CCDC47	coiled-coil domain containing 47	-1.47	0.0082
236313_at	CDKN2B	cyclin-dependent kinase inhibitor 2B (p15, inhibits CDK4)	-1.46	0.0134
224415_s_at	HINT2	histidine triad nucleotide binding protein 2	-1.46	0.0139
223059_s_at	FAM107B	family with sequence similarity 107, member B	-1.45	0.0118
201189_s_at	ITPR3	inositol 1,4,5-triphosphate receptor, type 3	-1.44	0.0118

10.2 Validation of the microarray analyses of hMSCs

The reliability of the microarray data was verified by gene expression analyses of selected genes with the RNA used for the array as well as additional RNA and a time series. Genes were selected according to their possible role during cell death and high logFc values (Table 12). Figure 23 displays the regulation of a selected set of genes with their respective probe sets over all samples used in the microarray analyses. The colour scheme shows the strength of regulation either during up- or downregulation. In case of more than one probe set, the expression strength in between the sets was nearly the same. Afterwards, data obtained from the microarray analyses were verified by RT-PCR (Figure 24). The expected regulations were found in all three microarray sets as well as in the time series, whereby the expression strength was highest in donors three and four. Moreover, the time series revealed a decreasing expression strength from day four to day eight independent of the sample (Figure 24).

Table 12 Set of genes selected for validation of the microarray analyses.
The logFc is displayed for the highest regulated probe set, while N displays the amount of probe sets regulated in the microarray.

Probe set ID	Symbol	Gene name	logFc	adj. p-value	N
210861_s_at	WISP3	WNT1 inducible signalling pathway protein 3	-3.58	0.0082	1
200641_s_at	YWHAZ	tyrosine 3-monooxygenase/tryptophan 5-monooxygenase activation protein, zeta polypeptide	-1.53	0.0117	4
205302_at	IGFBP1	insulin-like growth factor binding protein 1	-2.37	0.0161	1
218698_at	APIP	APAF1 interacting protein	-1.14	0.0117	1
201656_at	ITGA6	integrin, alpha 6	-1.06	0.0616	1
200606_at	DSP	desmoplakin	-0.91	0.0180	1
205608_s_at	ANGPT1	angiopoietin 1	1.26	0.0117	2
1554997_a_at	PTGS2	prostaglandin-endoperoxide synthase 2 (prostaglandin G/H synthase and cyclooxygenase)	1.40	0.0149	2
224415_s_at	HINT2	histidine triad nucleotide binding protein 2	-1.45	0.0138	1
202551_s_at	CRIM1	cysteine rich transmembrane BMP regulator 1 (chordin-like)	-0.91	0.0138	3
214981_at	POSTN	periostin, osteoblast specific factor	1.08	0.0201	1
206118_at	STAT4	signal transducer and activator of transcription 4	1.05	0.0174	1

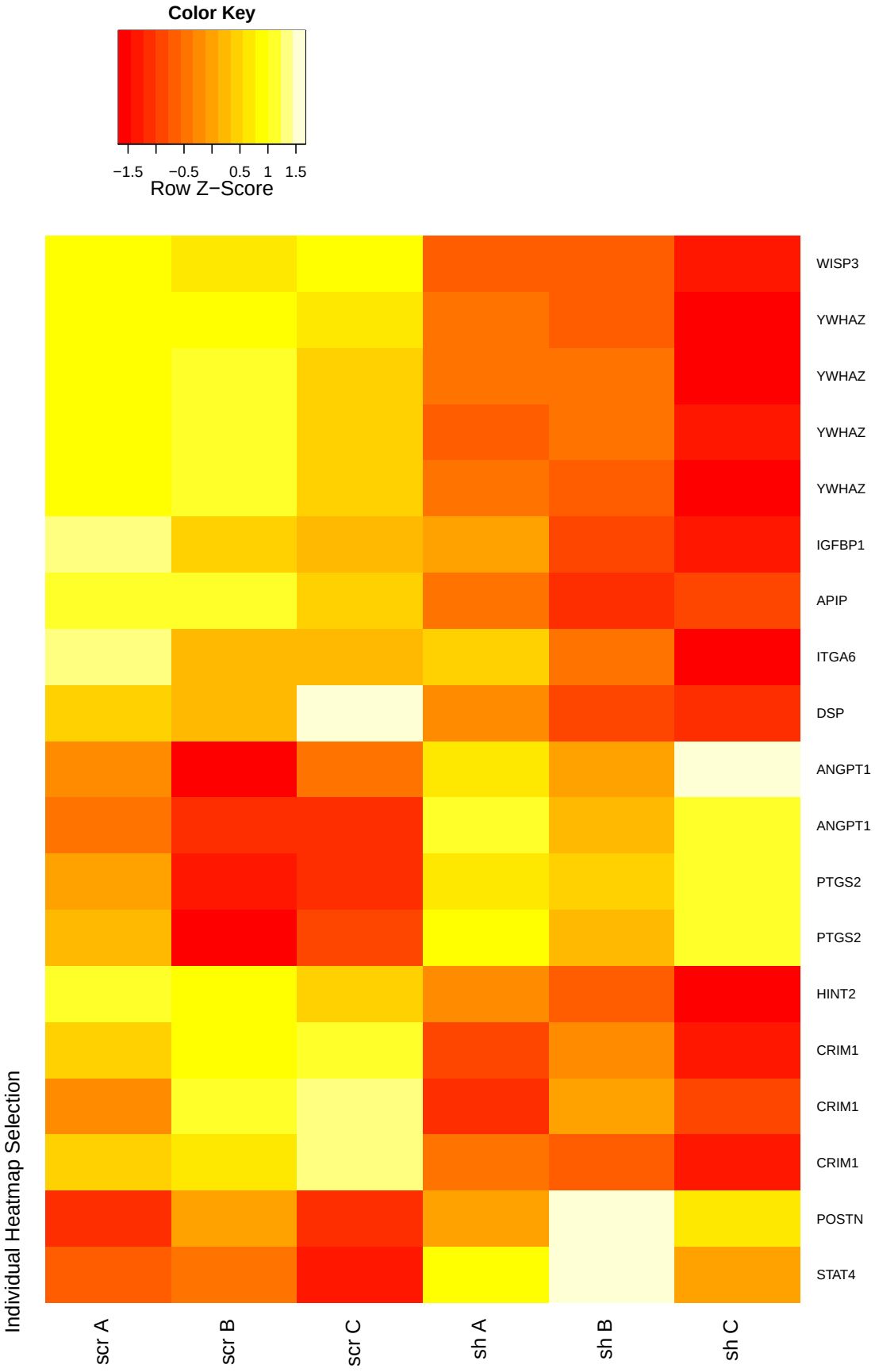

Figure 23 Heat map of validated genes selected from the hMSCs microarray analyses.
The graphic displays the regulation of the validated genes for all probe sets available on the microarray chip via a colour scheme. The sets of samples for all three microarray analyses (A-C) are presented with the shRNA5 transduced WISP3-deficient hMSCs (sh A-C) versus the scramble (scr A-C) controls.

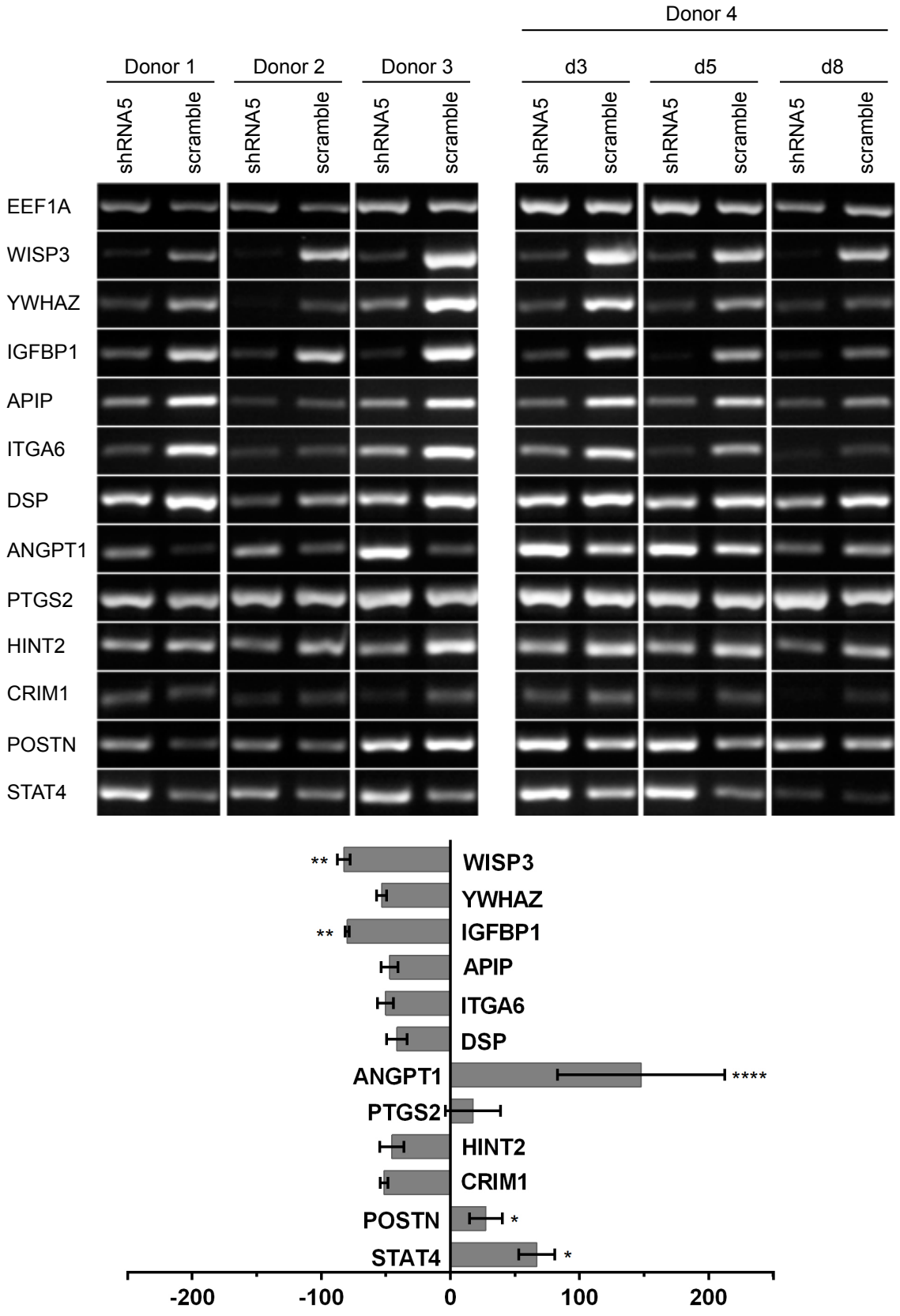

Figure 24 hMSCs microarray validation by selected genes.
RT-PCR gene expression analyses were performed with RNA run in the microarray analyses and additional RNA. Gene expression was normalised to the housekeeping gene EEF1A and scramble. Bar chart represents gene expression as percentage fold change of scramble ± SEM. Scramble is displayed as 0. (n = 3; **** $p < 0.0001$, ** $p < 0.01$, * $p < 0.05$)

Part IV

Discussion

Chapter 11

Effect of WISP3 on musculoskeletal cells

The CCN family belongs to the non-structural matricellular proteins that influence adhesion, migration, proliferation, differentiation and apoptosis [1]. WISP3 is one of its latest members, found in 1998 by Pennica *et al.* [7] and thought to be involved in the autosomal recessive disease Progressive Pseudorheumatoid Dysplasia (PPD). Hurvitz *et al.* performed sequence analyses of WISP3 from different PPD patients, leading to the discovery of varying mutations in this gene, mostly causing frame shifts resulting in protein truncation or no protein production at all [40]. Moreover, the expression of WISP3 mRNA in PPD patients was reduced in comparison to age-related healthy donors [45]. It is well established that cartilage develops from the mesenchymal lineage [116]. In case of PPD, cartilage development is unaffected since disease symptoms first appear around age three to eight [117]. That leaves the question as to how the reduction or loss of WISP3 influences mesenchymal stem cells (MSCs) in their function and how it might influence the MSC-derived chondrocytes. In the present study, the function of WISP3 was investigated in primary chondrocytes and primary human mesenchymal stem cells (hMSCs) to further elicit its role in the musculoskeletal system.

The constant expression of WISP3 in hMSCs and primary chondrocytes was verified in different donors, establishing these cells as reliable cell source with closer connection to the *in vivo* situation than available cell lines. Various CCN members have been shown to exert proliferative effects on different cell types e.g. CTGF induces the proliferation of osteoblasts [118]. Thus, we investigated the proliferative effect of WISP3 on hMSCs by addition of varying concentrations of recombinant WISP3. After 48 hours no proliferative effect on hMSCs was detectable as was previously demonstrated for WISP1 in the same cell type [119]. On the other hand, only reduction of WISP3 seemed to induce a proliferative effect as detected by Kleer *et al.* in human mammary epithelial (HME) cells [120]. Biological functionality of the recombinant CCN proteins produced in Sf21 cells was confirmed in experiments where rCYR61 induced its own splicing in the human myeloma cell line INA6 [121].

Chapter 12

Cell death via WISP3 knock down

The reduction of WISP3 was carried out using different short hairpin RNAs (shRNA), which allow stable knock down of target mRNA, in primary chondrocytes and hMSCs. Successful downregulation of WISP3 mRNA was achieved for three different shRNAs (shRNA2, -4 and -5) in both investigated cell types. Unexpectedly, cells displayed a change of morphology and a reduction in cell number during the investigated time period. This observation was in contrast to the results reported by Zhou *et al.* where an increased proliferation rate in addition to a decreased apoptosis rate was detected. To date it is the only study published about articular chondrocytes isolated from a PPD patient [45].
Nevertheless, it can be argued that the overall concentration of WISP3 protein, freely available, might differ in the analysed systems and that low concentrations of WISP3 are sufficient to maintain the signalling. Whereas the WISP3 loss in our system led to the severe phenotype observed. To date no specific antibody for WISP3 is commercially available to test this hypothesis. The CCN proteins share a 40-60 % amino acid sequence homology [9], explaining the cross reactivity of the available antibodies with other CCN family members. The tested set of WISP3 antibodies exhibited positive staining for all CCN members (data not shown).
The transduction with shRNA2 or shRNA4 displayed two different phenotypes in hMSCs as well as in primary chondrocytes. Cells transduced with shRNA2 exhibited an elongated phenotype, while shRNA4 WISP3-deficient cells appeared to start cell clustering with enlarging space in between the clusters over the investigated time period. An off-target effect was largely excluded since all used shRNAs (shRNA2, -4, -5) led to reduced WISP3 mRNA expressions, changes in morphology and decreased cell numbers. Echeverri *et al.* recommended the application of at least two shRNAs or siRNAs as well as a rescue experiment to exclude off-target effects [122]. To that end, WISP3-deficient hMSCs were treated immediately with recombinant WISP3-Fc to rescue the decreased mRNA expression as well as the cell death. Unfortunately, the phenotype could not be rescued and no elevation of WISP3 mRNA was detectable. We assume that loss of WISP3 triggers a cell death programme due to a change in cell cycle control, where crossed control points cannot be reversed.

12.1 Changes in cell cycle control

The cell cycle is controlled by cyclins and cyclin-dependent kinases, which regulate down-stream signalling of genes orchestrating apoptosis related genes like the apoptotic peptidase activating factor 1 (APAF1) amongst others [49]. Our hypothesis is supported by experiments performed by Huang *et al.* who demonstrated that loss of WISP3 in HME cells resulted in cell cycle progression even under serum-deprived conditions, displaying an increase in cyclin-dependent kinase 1 (CDK1, formerly known as cell cycle division 2 ,CDC2), CDC25A and -C as well as cyclin D1 [47]. Moreover, the re-expression of WISP3 in breast cancer cells resulted in an increased level of $p27^{kip1}$ and $p21^{waf}$, two cell cycle inhibitors, as well as a decrease in cyclin E, which inhibits the entry into the S phase [23]. Microarray analyses of WISP3-deficient versus control hMSCs led to reliable *in silico* data giving hints to an indirect cell cycle regulatory role for WISP3 due to an observed increase of the hepatocyte growth factor (HGF; logFc 1.35). Forte *et al.* supported that by their findings of the cell cycle regulating abilities of HGF in mouse MSCs where HGF arrested the cells in G0-G1 phase followed by the activation of $p27^{kip1}$ and $p21^{waf}$ [123].
Other cell cycle relevant genes revealed in the microarray analyses were CDC14b (logFc -1.05) and cyclin D1 (CCND1, logFc -1.2). The former displays increased entry into DNA replication phase in CDC14B-

deficient MEF cells [124] and is needed for efficient DNA repair [125]. Cyclin D1 is an interaction partner for the cyclin-dependent kinases 4 and 6 (CDK4, CDK6), together promoting the transition of the cell from the quiescence state to the entry of the S phase [48]. Tane *et al.* showed that an induction of CCND1 led cardiomyocytes to re-enter the cell cycle although they normally stop before the M-phase [126]. CDK6 was upregulated (logFc 1.06), which led to an increased proliferation rate in rat fibroblasts with simultaneous cyclin D3 overexpression [127]. Additionally, we found a downregulated adaptor protein, tyrosine 3-monooxygenase/tryptophan 5-monooxygenase activation protein, zeta (YWHAZ also known as 14-3-3 zeta), under the top 20 regulated genes in WISP3-deficient hMSCs with a logFc of -1.5. The 14-3-3 family is known for their role in cell cycle control, extracellular matrix (ECM) organization and apoptosis. 14-3-3 proteins bind with different affinities to CDC25C thereby blocking the translocation of CDC25C into the nucleus, where it adds the cyclin B-CDK1 complex to progress to M phase in the cell cycle [54]. It can be assumed that the loss of cell cycle control leads to a delayed or stopped proliferation of WISP3-deficient hMSCs. Taken together, the data indicate the influence of WISP3 on cell survival by interacting with proteins that affect cell cycle control, cytoskeleton organisation as well as cell-matrix contact. Loss of WISP3 deregulates cell cycle control, resulting in loss of proliferation and making cells prone to programmed cell death.

12.2 Anoikis as special form of apoptosis

Since we observed reduced cell numbers over cultivation period cell death seemed a likely explanation. The most dominant form of cell death is apoptosis, a form of controlled cell death, characterised by the activation of a class of cysteine proteases called caspases [128]. Moreover, anoikis, a special form of apoptosis, is induced by the loss of cell-matrix contact due to missing stimuli. Microarray analyses of WISP3-deficient versus control hMSCs hints to molecules involved in down-stream signalling e.g. integrin α6 (logFc -1.06) and integrin β8 (logFc 1.22). These data were supported by Pal *et al.* who reported that integrin α6 is lost in WISP3-deficient HME cells [129]. Moreover, the morphological changes seen in WISP3-deficient hMSCs and primary chondrocytes were also reported for the human breast cancer cell line SUM149, which endogenously expresses low levels of WISP3. Kleer *et al.* showed a switch from tightly packed cuboidal shaped cells to a round, flat morphology with ill-defined borders in SUM149 cells transfected with WISP3 [23]. Our data together with the changes seen in SUM149 cells might indicate a role for WISP3 in cytoskeleton organisation. This hypothesis is supported by findings that WISP3 is correlated with the phosphorylation of the focal adhesion kinase (FAK) by integrin αvβ3 and αvβ5 [35]. Moreover, Bialkowska *et al.* have reported that 14-3-3 zeta (logFc -1.5) mediates the cytoskeleton reorganisation in the hamster ovarien cell line CHO by the activation of CDC42 and Rac [130]. Knock down of 14-3-3 zeta in the cells of the keratinocyte cell line HaCaT exhibited stronger cell-cell contact displayed by cell clusters, while the extracellular-signal regulated kinases (ERK) were not effected [131]. The authors concluded that 14-3-3 zeta plays an important role in cell adhesion. This was supported by findings of a variety of integrin interactions e.g. binding to integrin α3, α4, β1, β2, β3 and β7 [132, 133, 134].
Additionally, two members of the ezrin-radixin-moesin (ERM) protein family were downregulated in hMSCs: ezrin with logFc -1.02 and moesin with logFc -1.07. The ERM family is known for their interaction linking F-actin to the apical membrane [135], thereby also affecting the cell morphology. Ezrin is able to directly bind the intercellular adhesion molecule (ICAM) and CD44 [135] with its N-terminus [136]. An overexpression in osteosarcoma cells increases the expression of N-cadherin and ERK signalling supporting migration and invasion of these tumour cells [137]. Through its phosphorylation by Src it can indirectly regulate the activation of FAK, which was demonstrated by an ezrin mutation in the phosphorylation site Y145, where cells displayed a failure of cell spreading on fibronectin [138]. These results reveal another direct link between the observed phenotype and the molecular changes induced by WISP3 reduction in hMSCs. Moreover, ezrin directly interacts with death receptor Fas before ligand binding.

Downregulation of ezrin does not prevent the internalisation of the Fas complex but accelerates the assembly of the death-inducing signalling complex (DISC) triggering caspase 8 activation [139]. Furthermore, the reduced expression of ezrin suppresses the expression of anti-apoptotic proteins e.g. survivin and X-linked inhibitor of apoptosis (XIAP) [140], which might contribute to the observed cell death in WISP3-deficient hMSCs and primary chondrocytes. Moesin (logFc -1.07), on the other hand, is involved in cell shape changes necessary in mitosis, where it increases the rigidity of the cell membrane allowing rounding of the cells [141] before accumulating at the metaphase plane to control cell elongation and cytokinesis [142]. Loss of moesin leads to a disruption of the spindle apparatus, possibly due to incorrect actin organisation [143].
Additionally, the loss of WISP3 in HME and MCF10A cells led to survival under serum-deprived conditions and anchorage-independent growth by a process called epithelial mesenchymal transition (EMT) [47] often seen in tumorigenesis. It can be assumed, that the phenotypic changes in WISP3-deficient hMSCs and primary chondrocytes are caused by interaction loss between the F-actin and membrane receptors like integrin $\alpha 6$ and integrin $\beta 8$, since the adaptor protein ezrin or moesin is missing. The reduced cell number in WISP3-deficient hMSCs and primary chondrocytes might be caused by the loss of cell ECM contact resulting in anoikis, which triggers apoptosis.
Activation of apoptosis can be triggered either by extrinsic or intrinsic pathways. The extrinsic activation is started by the binding of ligands to their specific death receptors inducing the assembly of the DISC [62]. On the other hand, the intrinsic pathway is started by the disruption of the mitochondrial integrity which is protected by the Bcl2 family [61]. The 14-3-3 family, also important in cell cycle control, is able to antagonises intrinsic apoptosis by preventing the activation of BCL2-associated agonist of cell death (Bad), forkhead box O3 (FOXO3), mitogen-activated protein kinase kinase kinase 5 (MAP3K5) and nuclear receptor subfamily 4, group A, member 1 (NR4A1) [144]. The translocation of Bax to the mitochondrion is blocked by its binding to 14-3-3 zeta in a phosphorylation-independent manner [145]. This process prevents the mitochondrial outer membrane permeabilisation (MOMP) which in turn leads to the release of cytochrome C starting the caspase cascade resulting in cell death [61]. MOMP normally occurs ahead of caspase activation and in case of blocked caspase activity might induce cell death due to loss of mitochondrial function e.g. respiratory chain function [146]. This data would indicate an increased apoptosis due to unbound Bax.
The presence of apoptosis was tested by analysing the translocation of phosphatidylserine from the inner to the outer plasma membrane which acts as an early hallmark of apoptosis [147]. The presence of phosphatidylserine on the outer plasma membrane surface was investigated with Annexin V-Cy3 staining, where only minor signals were detected in our experiments. Since membrane permeabilisation is observed in most cell death pathways, caspase 3 was investigated as characteristic marker for apoptosis. Caspase 3, the major effector caspase, is activated by intrinsic as well as extrinsic signalling pathways during apoptosis [81]. Western blot analyses revealed the absence of cleaved and therefore activated caspase 3 in both cell types when transduced with shRNA2. The mRNA of another effector caspase, caspase 7, was downregulated in the microarray analyses (logFc -1.02). Additionally, immunofluorescence staining for all active caspases exhibited little activation in shRNA2 and nearly no signal in shRNA4 transduced hMSCs. The investigation of death receptors showed no changes in their expression although an increased expression could be found in hMSCs deficient of WISP1 [115]. Interestingly, WISP1 blocked p53-induced apoptosis by the phosphorylation of Akt [148]. Moreover, its phosphorylation of Bad delays the formation of the pro-apoptotic BCL2-like 11 (Bim)/Bad complex thereby increasing the anti-apoptotic function of BcL-xL which inhibits BCL2-associated X protein (Bax) [149]. Knock down of WISP3 exhibited minor or no changes in WISP1 expression and the other way around. Even though knock down of either WISP1 or WISP3 resulted in cell death, their signalling pathways have to be different.

12.3 Caspase-independent cell death signalling pathways

12.3.1 Autophagy

Missing caspase activity, necessary for apoptosis signalling, in case of WISP3 knock down leaves the question as to which signalling pathway is responsible for the observed cell death. Bypass of apoptosis is possible if the effector caspases are blocked [65], thereby inducing different forms of caspase-independent cell death processes. Autophagy as a recycling process is able to support cell survival by the degradation of dysfunctional mitochondria thereby reducing oxidative stress [150]. Guo *et al.* showed higher concentration of autophagy marker expression in Ras-active tumour cell lines. A knock down of autophagy related 5 (ATG5) or ATG7, enzymes important for phagosome assembly and target cleavage, decreased their survival rate under starvation [151]. On the other hand, several studies indicated the involvement of autophagy in cell death if apoptosis was impaired [152, 153]. To test whether autophagy is involved in the observed cell loss, the expression of cleaved microtubule-associated protein 1A/1B-light chain 3 (LC3 A/B) protein, a substrate of ATG7, was examined in hMSCs, but was not confirmed. It can be argued that the available signals were below the detection level, since cells displayed different process stages of WISP3 mRNA reduction. The collected data indicate a caspase-independent pathway thereby excluding apoptosis as well as autophagy and suggesting necroptosis.

12.3.2 Necroptosis

The impaired caspase activity hints towards necroptosis, since caspase 8 usually cleaves the receptor-interacting serine/threonine protein kinases 1 and -3 (RIPK1 and -3) as well as CYLD, key components of said pathway [154, 155, 156]. Moreover, the induction of autophagy in the human renal carcinoma cell line RCC led to the degradation of RIPK1 and -3 thus impairing necroptosis [157]. If the substrates necessary for necrosis are not cleaved and the death receptor activation is blocked, RIPK1 phosphorylation is triggered which in turn induces the assembly of the necrosome composed of RIPK3 and the mixed lineage kinase domain-like (MLKL) [158]. Cai *et al.* recently found that activated MLKL forms homooligomers that translocate to the plasma membrane inducing an influx of Ca^{2+} and Na^{+} disturbing the homoeostasis of the cell [95]. Necroptosis could possibly be regulated by WISP3 via bone morphogenetic protein (BMP) signalling. Nakamura *et al.* demonstrated a direct interaction of BMP4 with WISP3 by co-immunoprecipitation and pull-down experiments [44]. Furthermore, they detected that ALP activity induced by BMP2 in the mouse embryonic cell line C3H/10T1/2 was reduced by the administration of conditioned medium from WISP3 overexpressing kidney cells [43]. Pal *et al.* reported the phosphorylation of the TGFβ activated kinase 1 (TAK1) due to the upregulation of BMP4 during WISP3 knock down in HME cells. Additionally, Smad4 and -5, molecules downstream of BMP, were downregulated while Smad6, an inhibitor of BMP signalling, was upregulated [129]. Nevertheless, TAK1 was shown to phosphorylate Smad1, -5 and -8 without interfering in the BMP induced phosphorylation of Smads [159]. Additionally, TAK1 inhibited RIPK1-dependent caspase activation, which is recruited into the DISC together with TNF receptor-associated factor 2 (TRAF2), FADD and caspase 8 [160]. Impaired caspase activation induces the phosphorylation of RIPK3 by RIPK1 which together with MLKL forms the necrosome [160, 158]. The knock out of TAK1 displayed an increased TRAIL sensitivity resulting in apoptosis [161], supporting the idea of necroptosis as a possible mechanism. To sum up, inhibition of WISP3 allows BMP4 to activate Smad2 and -3 followed by TAK1 phosphorylation. The activation of TAK1 inhibits RIPK1-induced caspase activation triggering the formation of the necrosome resulting in cell death (Figure 25).

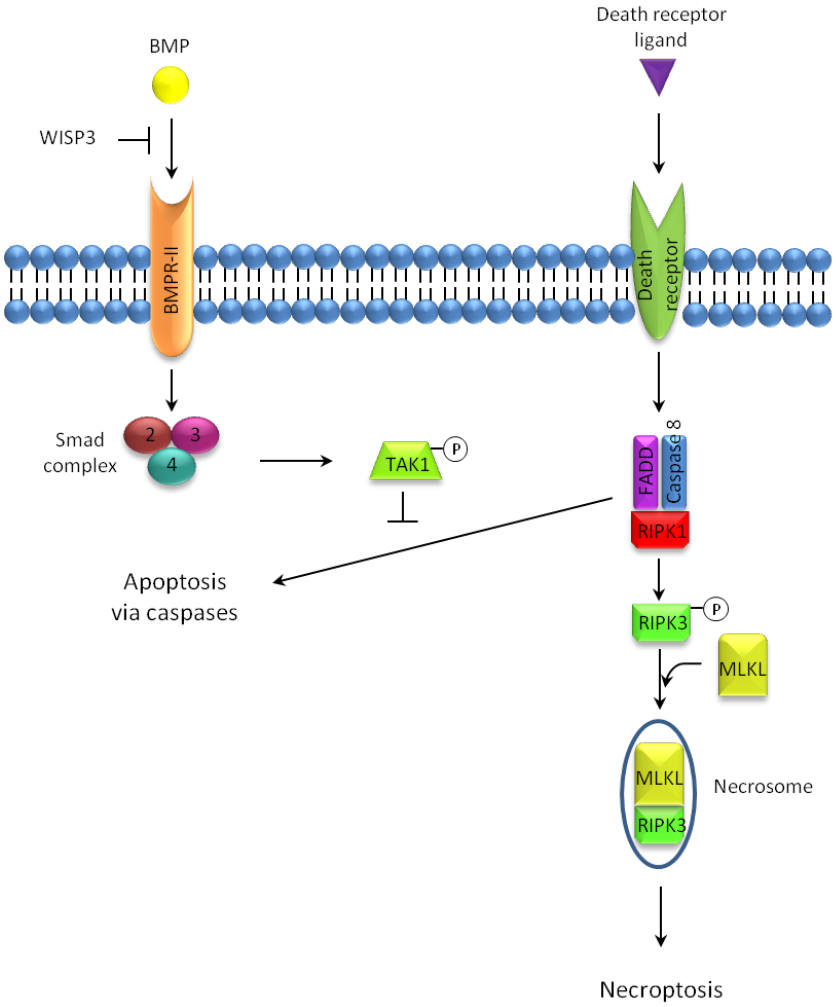

Figure 25 WISP3 signalling induces necroptosis via BMP signalling.
The death inducing signalling complex (DISC) triggers apoptosis by the activation of caspases and can be blocked by the interaction of TAK1 with RIKP1, a component of DISC. In case of WISP3 loss, BMP4 is able to activate the Smad2/3/4 complex following TAK1 phosphorylation. Impaired apoptosis triggers the formation of the necrosome through RIPK1 activated RIPK3 and MLKL aggregation resulting in necroptosis.

Chapter 13

WISP3 signalling correlated to PPD

Until now it is not clear as to how the *in vitro* results can be correlated to PPD, the disease characterised by different mutations in the WISP3 gene. That WISP3 is an important regulator in cell signalling was revealed in various *in vitro* studies in a broad spectrum of cell types. The group around Dr. Celina G. Kleer has focused their interest on the role of WISP3 in breast cancer since they found that 80 % of inflammatory breast cancer exhibited decreased WISP3 expression [24]. WISP3 knock down in HME cells was reported to induce EMT [162] thereby increasing proliferation and colony formation [120]. Loss of WISP3 in HME cells led to the downregulation of integrin α6 and E-cadherin dissolving the anchorage to the ECM [163, 162]. E-cadherin vanished from the HME cell surface because the upregulated zinc finger E-box binding homeobox 1 (ZEB1) induced snail family zinc finger 1 (SNAI1) that accumulated in the nucleus triggering E-cadherin depression [162]. Ras homolog family member C (Rho C), a protein needed for protrusion formation during migration [164], was upregulated during WISP3 knock down in HME cells [120], further revealing the mechanisms of metastasis of breast cancer cells. Taken together these data support the role of WISP3 as tumour suppressor.

Another observation was the loss of cell polarity in WISP-deficient HME cells independent of the investigated 2D or 3D system. Cells displayed an upregulation of the TGFβ receptor 3 (TGFBR3) while the other TGFβ receptors were unchanged [165]. The effect was restored by a double knock down of WISP3 and TGFBR3 exhibiting an increased E-cadherin expression [165]. Moreover, they demonstrated that the overexpression of WISP3 in SUM149 cells reduced the invasiveness and growth of these cells *in vitro* and *in vivo* [23]. In addition, the phosphorylation of the insulin-like growth factor 1 receptor (IGFR1), the insulin receptor substrate 1 (IRS1) and ERK1/2 is decreased in WISP3 transfected SUM149 cells [24]. Taken together these data indicate that WISP3 is able to regulate IGF1 binding to its receptor which controls the expression of adhesion molecules. The conclusion is supported by results from Cui *et al.* who demonstrated that the reduced phosphorylation of IGFR1, IRS1 and ERK1/2 could also be found in different immortalised chondrocyte cell lines (TC28a2 and C28I2) [166]. In C28I2 cells a direct interaction between IGF1 and WISP3 was revealed by Repudi *et al.*, where WISP3 inhibits the IGF1 secretion by approximately 50 %. The effect is nearly reversed in a WISP3 knock down, where 40 % of IGF1 secretion is restored [37]. IGF1 induced collagen type X expression and alkaline phosphatase activity, mechanisms necessary in chondrocyte hypertrophy [38], were suppressed by WISP3 signalling [37]. Furthermore, IGF1 induces reactive oxygen species (ROS) [37], possibly by the redox enzyme $p66^{Shc}$, which produces ROS from cytochrome C that may lead to the loss of mitochondrial function [167]. A feedback loop was created by the upregulation of WISP3 in response to rising ROS levels [37] and inducing the expression of superoxide dismutase (SOD) as demonstrated for C28I2 cells treated with recombinant WISP3 [168]. ROS are correlated to ECM degeneration in cartilage as well as inhibition of proteoglycan synthesis [169]. These facts are supported by the progressive cartilage degeneration observed in PPD patients. Thus, WISP3 might act as fine regulator for cartilage homoeostasis.

Overexpression of WISP3 in TC28a2 and C28I2 cells was found to induce the mRNA and protein expression of collagen type II, aggrecan and SOX9, key molecules in chondrocyte differentiation and ECM synthesis [33]. Aggrecan is a major component of the cartilage needed for hydration [170] and is commonly degraded by a disintegrin and metalloproteinase with thrombospondin motifs 4 (ADAMTS4) and -5 [171]. In WISP3 overexpressing C28I2 cells ADAMTS4 and -5 were decreased while matrix metallopeptidase 1 (MMP1) and -10 were elevated [34]. Since PPD is characterised by cartilage matrix degradation several studies were carried out with truncated WISP3 reflecting mutations found in PPD. Based on the

work of Zhou *et al.* who isolated chondrocytes from a PPD patient [45] another group introduced WISP3 with two different mutations (1000T/C and 840delT) found in the patient into the chondrocyte cell line C20A4 [46]. Wang *et al.* confirmed the observations received from the patient's chondrocytes: increased proliferation and reduced apoptosis rate. Additionally, they noticed that wild type WISP3 distributed evenly throughout the cell while the mutant forms showed a dot-like appearance and exhibited delayed collagen type II secretion [46]. The results were supported by the finding that the mutation of a conserved cysteine (Cys78Arg) in WISP3 inhibited the collagen type II mRNA as well as protein expression [33]. Thus, WISP3 regulates key cartilage molecules needed for ECM synthesis and remodelling.

13.1 WISP3 animal studies

To further unroll the systemic function of WISP3 different animal models were developed in mice and zebrafish. The results were quite unexpected since no differences were seen between knock out and wild type mice although the amino acid sequence homology compared to human is about 78 %. The created mice displayed a truncated WISP3 form since the insulin-like growth factor binding protein (IGFBP) domain was fused to β-galactosidase resulting in a loss of the other domains. The authors were only able to detect WISP3 mRNA by RT-PCR, while detection of endogenous WISP3 by *in situ* hybridisation or on protein level failed [42]. Nakamura *et al.* investigated the overexpression of WISP3 in mice once more showing that there were no differences towards their wild type controls [43]. On the contrary, WISP3 knock out in zebrafish exhibited reduced size of mandibular cartilage and altered pharyngeal cartilage although the amino acid sequence homology compared to human is about 54 % [44]. Moreover, the WISP3 overexpression in zebrafish revealed a disrupted dorsal-ventral patterning where dorsal cells expanded while ventral cells decreased. The symptoms were diminished if WISP3-RNA, displaying missense mutations seen in Progressive Pseudorheumatoid Dysplasia (PPD, C78R, C145Y and Q338L), were injected [44]. All studies showed an interaction of WISP3 with BMP and Wnt signalling by binding to BMP4 as well as the low density lipoprotein receptor-related protein 6 (LPR6) and to a lesser extent to the frizzled class receptor 8 [42, 44, 43].
Kutz *et al.* hypothesised that due to the short life span of mice and the occurrence of PPD around the age of three to eight, WISP3 plays an inferior role in that animal model [42]. A more reasonable explanation came from Nakamura *et al.* who observed that zebrafish WISP3 was expressed as full length protein in the human embryonic kidney cell line HEK293T while mouse and human WISP3 were mostly detected as cleaved proteins. They also demonstrated that the cleaved WISP3 proteins were unable to bind to BMP4 and LRP6 thus impairing WISP3 signalling [44]. These observations might explain the lack of differences between WISP3 knock outs as well as overexpression compared to wild type controls in mice. That raises the question in which way WISP3 differs among the species and whether the zebrafish is missing the enzyme(s) necessary for the cleavage of WISP3. Moreover, since in mice a truncated form of WISP3 was created the protein may lack proper conformational folding needed for its association with binding partners. That the proper folding of WISP3 might play an important role was supported by the finding that conserved cysteines were often affected by mutations in PPD patients [40]. Cysteines are known for their ability to direct the folding of a protein by the formation of disulfide bonds.

13.2 WISP3 mutations and their consequences in PPD patients

Until now approximately 50 different mutations in the WISP3 gene of PPD patients were found in all exons and some introns resulting in similar diagnostic findings [40, 172, 41]. Delague *et al.* compared 16 PPD patients from nine families displaying only slight differing symptoms [172] while in another study different mutations in exons 1, 2 and 5 exhibited identical clinical phenotypes [40]. Overall, mutations were predominantly found in exon 2 and 5 causing frameshift mutations or induce cysteine exchange [173]. The increased proliferation and diminished apoptosis rate observed in chondrocytes isolated from a PPD patient might be due to the presence of a truncated WISP3 protein. The patient showed mutations (840delT and 1000T/C) which by bioinformatics were assumed to result in a truncated protein with an additional amino acid exchange of Ser334Pro [45]. Since both mutations were located on the fifth exon only the CT domain of WISP3 was affected thus still allowing the binding to IGF-1. Repudi *et al.* elegantly demonstrated that the IGFBP domain together with the von Willebrand type C (VWC) domain and the thrombospondin type 1 repeat (TSP-1) domain were enough to bind IGF1 with the same effectiveness as full length WISP3 [37]. Additionally, the existing mutations did not inhibit the phosphorylation of IGFR1 and IRS as well as ERK1/2 in C20A4 cells treated with recombinant WISP3 [166]. Therefore, active ERK is able to provide a survival signal and induce cell growth [174].
To sum up, distinct mutations in the WISP3 gene resulting in either the full loss of the protein or a truncated form give rise to different initial situations for signalling pathways. If the mutations result in a truncated WISP3 the correct confirmation of the protein might be impaired followed by loss of function or only partial activity. Thus, cells are unable to induce chondrogenic markers e.g. collagen type II and aggrecan while remodelling enzymes like ADAMTS are upregulated degrading the cartilage matrix. The loss of ECM receptors e.g. integrin $\alpha 6$ might further accelerate the degradation process. On the other hand IGF1 signalling might still be intact supporting cells with survival signals. Moreover, cell cycle control can become deregulated followed by cell death.

Chapter 14

Conclusion

Less is known about WISP3 signalling and most *in vitro* data was reported for human mammery epithelial cells or chondrocyte cell lines. The exisiting data on WISP3 indicates a role as tumour suppressor and regulator of cartilage homoeostasis due to its deregulated signalling in PPD as well as inflammatory breast cancer. The presented study reinforces the importance of WISP3 as survival factor in the musculoskeletal system since loss resulted in cell death of hMSCs and primary chondrocytes. Apoptosis as cause of death seems unlikely since no activation of caspases or death receptors were detected. Thus, cell death is triggered by a caspase-independent pathway emphasising necroptosis as likely mechanism. Additionally, changes in cell-matrix contact molecules e.g. integrin α6, highlighted by microarray analyses, might further accelerate cell death due to missing survival signals. Microarray analyses revealed a set of genes involved in cytoskeleton organisation, cell cycle control and cell death.
Based on this study, the role of WISP3 as survial factor in the musculoskeletal system can be further investigated. This way, revealing new interactions partners allowing the development of therapeutics for PPD patients or diagnostic tools for cancer with deregulated WISP gene expression.

Chapter 15

Perspectives

The reduction of WISP3 mRNA induces cell death in primary human mesenchymal stem cells (hMSCs) as well as primary chondrocytes as demonstrated in this study. Though positive signals for active caspases and phoshpatidylserine on the outer plasma membrane are missing apoptosis cannot finally be excluded. There is still the chance, that the signalling was too low for detection due to different WISP3 reduction conditions in the cells. Further experiment should comprise the state of the DNA, clearly speaking: Is there evidence for DNA fragmentation? The fact could be tested by the terminal deoxynucleotidyl transferase-mediated dUTP nick end labelling (TUNEL) assay [175] detecting DNA strand breaks. Absence of DNA fragmentation would reinforce a caspase-independent cell death excluding apoptosis.
Additionally, knock down experiments in the presence of caspase inhibitors e.g. benzyloxycarbonyl-val-ala-asp (OMe) fluoromethylketone (z-VAD-FMK) or the tetramer form z-YVAD-FMK, can clarify the involvement of the necroptotic or apoptotic pathway. Cell death would still be observed if it is regulated by necroptosis. A different approach is the detection of the activated receptor-interacting serine-threonine kinase 3 (RIPK3) and the mixed lineage kinase domain-like (MLKL), which together form the necrosome [158]. Therefore, necroptosis-induced cell death can be detected by the inhibition of necroptosis blocking the signalling of RIPK1 and -3 as well as MLKL. Necrostatins (necrostatin 1, -3 and -5) were found to be potent inhibitors of RIPK1 as tested in the FADD-deficient human T lymphocyte cell line Jurkat [176]. Two inhibitors of RIPK3 were successfully evaluated in the toll like receptor (TLR)-induced necrosis in caspase-deficient macrophages [177]. For MLKL, (E)-N-(4-(N-(3-methoxypyrazin-2-yl)sulfamoyl)phenyl)-3-(5-nitrothiophene-2-yl)acrylamide (trivial name: necrosulfonamide) is a potent inhibitor resulting in single spots appearance of RIPK3 throughout the cell [178]. These experiments would further clarify in which way WISP3 is involved in a survival mechanism in hMSCs and primary chondrocytes.
Another approach, would be the overexpression of WISP3 in the investigated cells and the treatment with cell death inducers e.g. TNFα, Fas. In comparison to control cells it would be possible to support the survival function. Moreover, proteomic analyses of WISP3-deficient cells versus its corresponding controls by 2D electrophoresis followed by mass spectrometry could reveal new interaction partners and signalling pathways.

Bibliography

[1] A. H. Morris and T. R. Kyriakides, "Matricellular proteins and biomaterials." *Matrix biology : journal of the International Society for Matrix Biology*, Mar. 2014.

[2] K.-i. Katsube, K. Sakamoto, Y. Tamamura, and A. Yamaguchi, "Role of CCN, a vertebrate specific gene family, in development." *Development, growth & differentiation*, vol. 51, no. 1, pp. 55–67, Jan. 2009.

[3] D. R. Brigstock, R. Goldschmeding, K.-i. Katsube, S. C.-T. Lam, L. F. Lau, K. Lyons, C. Naus, B. Perbal, B. Riser, M. Takigawa, and H. Yeger, "Proposal for a unified CCN nomenclature." *Molecular pathology : MP*, vol. 56, no. 2, pp. 127–8, Apr. 2003.

[4] T. P. O'Brien, G. P. Yang, L. Sanders, and L. F. Lau, "Expression of cyr61, a growth factor-inducible immediate-early gene." *Molecular and cellular biology*, vol. 10, no. 7, pp. 3569–77, Jul. 1990.

[5] D. M. Bradham, A. Igarashi, R. L. Potter, and G. R. Grotendorst, "Connective tissue growth factor: a cysteine-rich mitogen secreted by human vascular endothelial cells is related to the SRC-induced immediate early gene product CEF-10." *The Journal of cell biology*, vol. 114, no. 6, pp. 1285–94, Sep. 1991.

[6] V. Joliot, C. Martinerie, G. Dambrine, G. Plassiart, M. Brisac, J. Crochet, and B. Perbal, "Proviral rearrangements and overexpression of a new cellular gene (nov) in myeloblastosis-associated virus type 1-induced nephroblastomas." *Molecular and cellular biology*, vol. 12, no. 1, pp. 10–21, Jan. 1992.

[7] D. Pennica, T. A. Swanson, J. W. Welsh, M. A. Roy, D. A. Lawrence, J. Lee, J. Brush, L. A. Taneyhill, B. Deuel, M. Lew, C. Watanabe, R. L. Cohen, M. F. Melhem, G. G. Finley, P. Quirke, A. D. Goddard, K. J. Hillan, A. L. Gurney, D. Botstein, and A. J. Levine, "WISP genes are members of the connective tissue growth factor family that are up-regulated in wnt-1-transformed cells and aberrantly expressed in human colon tumors." *Proceedings of the National Academy of Sciences of the United States of America*, vol. 95, no. 25, pp. 14 717–22, Dec. 1998.

[8] G.-w. Zuo, C. D. Kohls, B.-C. He, L. Chen, W. Zhang, Q. Shi, B.-Q. Zhang, Q. Kang, J. Luo, X. Luo, E. R. Wagner, S. H. Kim, F. Restegar, R. C. Haydon, Z.-L. Deng, H. H. Luu, T.-C. He, and Q. Luo, "The CCN proteins: important signaling mediators in stem cell differentiation and tumorigenesis." *Histology and histopathology*, vol. 25, no. 6, pp. 795–806, Jun. 2010.

[9] K. P. Holbourn, K. R. Acharya, and B. Perbal, "The CCN family of proteins: structure-function relationships." *Trends in biochemical sciences*, vol. 33, no. 10, pp. 461–73, Oct. 2008.

[10] P.-C. Chen, H.-C. Cheng, S.-F. Yang, C.-W. Lin, and C.-H. Tang, "The CCN Family Proteins: Modulators of Bone Development and Novel Targets in Bone-Associated Tumors." *BioMed research international*, vol. 2014, p. 437096, Jan. 2014.

[11] D. R. Brigstock, "The CCN family: a new stimulus package." *The Journal of endocrinology*, vol. 178, no. 2, pp. 169–75, Aug. 2003.

[12] A. Leask and D. J. Abraham, "All in the CCN family: essential matricellular signaling modulators emerge from the bunker." *Journal of cell science*, vol. 119, no. Pt 23, pp. 4803–10, Dec. 2006.

[13] C.-C. Chen and L. F. Lau, "Functions and mechanisms of action of CCN matricellular proteins." *The international journal of biochemistry & cell biology*, vol. 41, no. 4, pp. 771–83, Apr. 2009.

[14] J.-I. I. Jun and L. F. Lau, "Taking aim at the extracellular matrix : CCN proteins as emerging therapeutic targets," *Nature Reviews Drug Discovery*, vol. 10, no. 12, pp. 945–963, Dec. 2011.

[15] M.-T. Lin, C.-C. Chang, S.-T. Chen, H.-L. Chang, J.-L. Su, Y.-P. Chau, and M.-L. Kuo, "Cyr61 expression confers resistance to apoptosis in breast cancer MCF-7 cells by a mechanism of NF-kappaB-dependent XIAP up-regulation." *The Journal of biological chemistry*, vol. 279, no. 23, pp. 24 015–23, Jun. 2004.

[16] X. Tong, D. Xie, J. O'Kelly, C. W. Miller, C. Muller-Tidow, and H. P. Koeffler, "Cyr61, a member of CCN family, is a tumor suppressor in non-small cell lung cancer." *The Journal of biological chemistry*, vol. 276, no. 50, pp. 47 709–14, Dec. 2001.

[17] S. K. Johnson, J. P. Stewart, R. Bam, P. Qu, B. Barlogie, F. van Rhee, J. D. Shaughnessy, J. Epstein, and S. Yaccoby, "Overexpression of CYR61/CCN1 in the multiple myeloma microenvironment is associated with superior survival and prevention of bone disease." *Blood*, Jul. 2014.

[18] J. E. Wells, M. Howlett, C. H. Cole, and U. R. Kees, "Deregulated expression of connective tissue growth factor (CTGF/CCN2) is linked to poor outcome in human cancer." *International journal of cancer. Journal international du cancer*, May 2014.

[19] L. Pi, A. K. Shenoy, J. Liu, S. Kim, N. Nelson, H. Xia, W. W. Hauswirth, B. E. Petersen, G. S. Schultz, and E. W. Scott, "CCN2/CTGF regulates neovessel formation via targeting structurally conserved cystine knot motifs in multiple angiogenic regulators." *FASEB journal : official publication of the Federation of American Societies for Experimental Biology*, vol. 26, no. 8, pp. 3365–79, Aug. 2012.

[20] T. Nishida, S. Kubota, T. Fukunaga, S. Kondo, G. Yosimichi, T. Nakanishi, T. Takano-Yamamoto, and M. Takigawa, "CTGF/Hcs24, hypertrophic chondrocyte-specific gene product, interacts with perlecan in regulating the proliferation and differentiation of chondrocytes." *Journal of cellular physiology*, vol. 196, no. 2, pp. 265–75, Aug. 2003.

[21] P.-C. Chen, H.-C. Cheng, and C.-H. Tang, "CCN3 promotes prostate cancer bone metastasis by modulating the tumor-bone microenvironment through RANKL-dependent pathway." *Carcinogenesis*, vol. 34, no. 7, pp. 1669–79, Jul. 2013.

[22] S. K. Banerjee and S. Banerjee, "CCN5/WISP-2: A micromanager of breast cancer progression." *Journal of cell communication and signaling*, vol. 6, no. 2, pp. 63–71, Jun. 2012.

[23] C. G. Kleer, Y. Zhang, Q. Pan, K. L. van Golen, Z.-f. Wu, D. Livant, and S. D. Merajver, "WISP3 is a novel tumor suppressor gene of inflammatory breast cancer." *Oncogene*, vol. 21, no. 20, pp. 3172–80, May 2002.

[24] C. G. Kleer, Y. Zhang, Q. Pan, and S. D. Merajver, "WISP3 (CCN6) Is a Secreted Tumor-Suppressor Protein that Modulates IGF Signaling in Inflammatory Breast Cancer 1," *Neoplasia*, vol. 6, no. 2, pp. 179–185, 2004.

[25] J.-L. Su, J. Chiou, C.-H. Tang, M. Zhao, C.-H. Tsai, P.-S. Chen, Y.-W. Chang, M.-H. Chien, C.-Y. Peng, M. Hsiao, M.-L. Kuo, and M.-L. Yen, "CYR61 regulates BMP-2-dependent osteoblast differentiation through the {alpha}v{beta}3 integrin/integrin-linked kinase/ERK pathway." *The Journal of biological chemistry*, vol. 285, no. 41, pp. 31 325–36, Oct. 2010.

[26] M. Wong, M. L. Kireeva, T. V. Kolesnikova, and L. F. Lau, "Cyr61, product of a growth factor-inducible immediate-early gene, regulates chondrogenesis in mouse limb bud mesenchymal cells." *Developmental biology*, vol. 192, no. 2, pp. 492–508, Dec. 1997.

[27] C. Mundy, M. Gannon, and S. N. Popoff, "Connective tissue growth factor (CTGF/CCN2) negatively regulates BMP-2 induced osteoblast differentiation and signaling." *Journal of cellular physiology*, vol. 229, no. 5, pp. 672–81, May 2014.

[28] E. Heath, D. Tahri, E. Andermarcher, P. Schofield, S. Fleming, and C. A. Boulter, "Abnormal skeletal and cardiac development, cardiomyopathy, muscle atrophy and cataracts in mice with a targeted disruption of the Nov (Ccn3) gene." *BMC developmental biology*, vol. 8, p. 18, Jan. 2008.

[29] Y. Katsuki, K. Sakamoto, T. Minamizato, H. Makino, A. Umezawa, M.-A. Ikeda, B. Perbal, T. Amagasa, A. Yamaguchi, and K.-I. Katsube, "Inhibitory effect of CT domain of CCN3/NOV on proliferation and differentiation of osteogenic mesenchymal stem cells, Kusa-A1." *Biochemical and biophysical research communications*, vol. 368, no. 3, pp. 808–14, Apr. 2008.

[30] M. Hoshijima, T. Hattori, E. Aoyama, T. Nishida, T. Yamashiro, and M. Takigawa, "Roles of heterotypic CCN2/CTGF-CCN3/NOV and homotypic CCN2-CCN2 interactions in expression of the differentiated phenotype of chondrocytes." *The FEBS journal*, vol. 279, no. 19, pp. 3584–97, Oct. 2012.

[31] M. Ono, C. A. Inkson, T. M. Kilts, and M. F. Young, "WISP-1/CCN4 regulates osteogenesis by enhancing BMP-2 activity." *Journal of bone and mineral research : the official journal of the American Society for Bone and Mineral Research*, vol. 26, no. 1, pp. 193–208, Jan. 2011.

[32] N. Schutze, U. Noth, J. Schneidereit, C. Hendrich, and F. Jakob, "Differential expression of CCN-family members in primary human bone marrow-derived mesenchymal stem cells during osteogenic, chondrogenic and adipogenic differentiation." *Cell communication and signaling : CCS*, vol. 3, no. 1, p. 5, Mar. 2005.

[33] M. Sen, Y.-h. Cheng, M. B. Goldring, M. K. Lotz, and D. A. Carson, "WISP3-dependent regulation of type II collagen and aggrecan production in chondrocytes." *Arthritis and rheumatism*, vol. 50, no. 2, pp. 488–97, Feb. 2004.

[34] N. Baker, P. Sharpe, K. Culley, M. Otero, D. Bevan, P. Newham, W. Barker, K. M. Clements, C. J. Langham, M. B. Goldring, and J. Gavrilović, "Dual regulation of metalloproteinase expression in chondrocytes by Wnt-1-inducible signaling pathway protein 3/CCN6." *Arthritis and rheumatism*, vol. 64, no. 7, pp. 2289–99, Jul. 2012.

[35] Y.-c. Fong, C.-y. Lin, Y.-c. Su, W.-C. Chen, F.-j. Tsai, C.-h. Tsai, C.-Y. Huang, and C.-h. Tang, "CCN6 Enhances ICAM-1 Expression and Cell Motility in Human Chondrosarcoma Cells," *Journal of Cellular Physiology*, vol. 227, no. 91, pp. 223–232, Jan. 2011.

[36] L. Longobardi, F. Granero-Moltó, L. O'Rear, T. J. Myers, T. Li, P. J. Kregor, and A. Spagnoli, "Subcellular localization of IRS-1 in IGF-I-mediated chondrogenic proliferation, differentiation and hypertrophy of bone marrow mesenchymal stem cells." *Growth factors (Chur, Switzerland)*, vol. 27, no. 5, pp. 309–20, Oct. 2009.

[37] S. R. Repudi, M. Patra, and M. Sen, "WISP3-IGF1 interaction regulates chondrocyte hypertrophy." *Journal of cell science*, vol. 126, no. Pt 7, pp. 1650–8, Apr. 2013.

[38] P. Lu Valle, M. Iwamoto, P. Fanning, M. Pacifici, and B. R. Olsen, "Multiple negative elements in a gene that codes for an extracellular matrix protein, collagen X, restrict expression to hypertrophic chondrocytes." *The Journal of cell biology*, vol. 121, no. 5, pp. 1173–9, Jun. 1993.

[39] R. Wynne-Davies, C. Hall, and B. M. Ansell, “Spondylo-epiphysial dysplasia tarda with progressive arthropathy. A "new" disorder of autosomal recessive inheritance.” *The Journal of bone and joint surgery. British volume*, vol. 64, no. 4, pp. 442–5, Jan. 1982.

[40] J. R. Hurvitz, W. M. Suwairi, W. Van Hul, H. El-Shanti, A. Superti-Furga, J. Roudier, D. Holderbaum, R. M. Pauli, J. K. Herd, E. V. Van Hul, H. Rezai-Delui, E. Legius, M. Le Merrer, J. Al-Alami, S. A. Bahabri, and M. L. Warman, “Mutations in the CCN gene family member WISP3 cause progressive pseudorheumatoid dysplasia.” *Nature genetics*, vol. 23, no. 1, pp. 94–8, Sep. 1999. [Online]. Available: http://www.ncbi.nlm.nih.gov/pubmed/10471507

[41] N. Garcia Segarra, L. Mittaz, A. B. Campos-Xavier, C. F. Bartels, B. Tuysuz, Y. Alanay, R. Cimaz, V. Cormier-Daire, M. Di Rocco, H.-C. Duba, N. H. Elcioglu, F. Forzano, T. Hospach, E. Kilic, J. B. Kuemmerle-Deschner, G. Mortier, S. Mrusek, S. Nampoothiri, E. Obersztyn, R. M. Pauli, A. Selicorni, R. Tenconi, S. Unger, G. E. Utine, M. Wright, B. Zabel, M. L. Warman, A. Superti-Furga, and L. Bonafé, “The diagnostic challenge of progressive pseudorheumatoid dysplasia (PPRD): a review of clinical features, radiographic features, and WISP3 mutations in 63 affected individuals.” *American journal of medical genetics. Part C, Seminars in medical genetics*, vol. 160C, no. 3, pp. 217–29, Aug. 2012.

[42] W. E. Kutz, Y. Gong, and M. L. Warman, “WISP3, the gene responsible for the human skeletal disease progressive pseudorheumatoid dysplasia, is not essential for skeletal function in mice.” *Molecular and cellular biology*, vol. 25, no. 1, pp. 414–21, Jan. 2005.

[43] Y. Nakamura, Y. Cui, C. Fernando, W. E. Kutz, and M. L. Warman, “Normal growth and development in mice over-expressing the CCN family member WISP3.” *Journal of cell communication and signaling*, vol. 3, no. 2, pp. 105–13, Jul. 2009.

[44] Y. Nakamura, G. Weidinger, J. O. Liang, A. Aquilina-Beck, K. Tamai, R. T. Moon, and M. L. Warman, “The CCN family member Wisp3, mutant in progressive pseudorheumatoid dysplasia, modulates BMP and Wnt signaling.” *The Journal of clinical investigation*, vol. 117, no. 10, pp. 3075–86, Oct. 2007.

[45] H.-D. Zhou, Y.-H. Bu, Y.-Q. Peng, H. Xie, M. Wang, L.-Q. Yuan, Y. Jiang, D. Li, Q.-Y. Wei, Y.-L. He, T. Xiao, J.-D. Ni, and E.-Y. Liao, “Cellular and molecular responses in progressive pseudorheumatoid dysplasia articular cartilage associated with compound heterozygous WISP3 gene mutation.” *Journal of molecular medicine (Berlin, Germany)*, vol. 85, no. 9, pp. 985–96, Sep. 2007.

[46] M. Wang, X.-F. Man, Y.-Q. Liu, E.-Y. Liao, Z.-F. Shen, X.-H. Luo, L.-J. Guo, X.-P. Wu, and H.-D. Zhou, “Dysfunction of collagen synthesis and secretion in chondrocytes induced by wisp3 mutation.” *International journal of endocrinology*, vol. 2013, p. 679763, Jan. 2013. [Online]. Available: http://www.pubmedcentral.nih.gov/articlerender.fcgi?artid=3614060&tool=pmcentrez&rendertype=abstract

[47] W. Huang, M. E. Gonzalez, K. a. Toy, M. Banerjee, and C. G. Kleer, “Blockade of CCN6 (WISP3) activates growth factor-independent survival and resistance to anoikis in human mammary epithelial cells.” *Cancer research*, vol. 70, no. 8, pp. 3340–50, Apr. 2010.

[48] H. Harashima, N. Dissmeyer, and A. Schnittger, “Cell cycle control across the eukaryotic kingdom.” *Trends in cell biology*, vol. 23, no. 7, pp. 345–56, Jul. 2013.

[49] H. Okayama, “Cell cycle control by anchorage signaling.” *Cellular signalling*, vol. 24, no. 8, pp. 1599–609, Aug. 2012.

[50] D. Schwartz and V. Rotter, "p53-dependent cell cycle control: response to genotoxic stress." *Seminars in cancer biology*, vol. 8, no. 5, pp. 325–36, Jan. 1998.

[51] F. Bunz, P. M. Hwang, C. Torrance, T. Waldman, Y. Zhang, L. Dillehay, J. Williams, C. Lengauer, K. W. Kinzler, and B. Vogelstein, "Disruption of p53 in human cancer cells alters the responses to therapeutic agents." *The Journal of clinical investigation*, vol. 104, no. 3, pp. 263–9, Aug. 1999.

[52] P. M. Flatt, K. Polyak, L. J. Tang, C. D. Scatena, M. D. Westfall, L. A. Rubinstein, J. Yu, K. W. Kinzler, B. Vogelstein, D. E. Hill, and J. A. Pietenpol, "p53-dependent expression of PIG3 during proliferation, genotoxic stress, and reversible growth arrest." *Cancer letters*, vol. 156, no. 1, pp. 63–72, Aug. 2000.

[53] J. A. Pietenpol and Z. A. Stewart, "Cell cycle checkpoint signaling: cell cycle arrest versus apoptosis." *Toxicology*, vol. 181-182, pp. 475–81, Dec. 2002. [Online]. Available: http://www.ncbi.nlm.nih.gov/pubmed/12505356

[54] A. K. Gardino and M. B. Yaffe, "14-3-3 Proteins As Signaling Integration Points for Cell Cycle Control and Apoptosis," *Seminars in Cell & Developmental Biology*, vol. 22, no. 7, pp. 695–688, Sep. 2011.

[55] M. Suzanne and H. Steller, "Shaping organisms with apoptosis." *Cell death and differentiation*, vol. 20, no. 5, pp. 669–75, May 2013.

[56] D. R. Green and G. I. Evan, "A matter of life and death." *Cancer cell*, vol. 1, no. 1, pp. 19–30, Feb. 2002.

[57] A. Smerdel-Ramoya, S. Zanotti, L. Stadmeyer, D. Durant, and E. Canalis, "Skeletal overexpression of connective tissue growth factor impairs bone formation and causes osteopenia." *Endocrinology*, vol. 149, no. 9, pp. 4374–81, Sep. 2008.

[58] V. Juric, C.-C. Chen, and L. F. Lau, "Fas-mediated apoptosis is regulated by the extracellular matrix protein CCN1 (CYR61) in vitro and in vivo." *Molecular and cellular biology*, vol. 29, no. 12, pp. 3266–79, Jun. 2009.

[59] S. Wang, Z. Z. Chong, Y. C. Shang, and K. Maiese, "Wnt1 inducible signaling pathway protein 1 (WISP1) blocks neurodegeneration through phosphoinositide 3 kinase/Akt1 and apoptotic mitochondrial signaling involving Bad, Bax, Bim, and Bcl-xL." *Current neurovascular research*, vol. 9, no. 1, pp. 20–31, Feb. 2012.

[60] J. F. Kerr, A. H. Wyllie, and A. R. Currie, "Apoptosis: a basic biological phenomenon with wide-ranging implications in tissue kinetics." *British journal of cancer*, vol. 26, no. 4, pp. 239–57, Aug. 1972.

[61] E. Ulukaya, C. Acilan, and Y. Yilmaz, "Apoptosis: why and how does it occur in biology?" *Cell biochemistry and function*, vol. 29, no. 6, pp. 468–80, Jul. 2011.

[62] E.-W. Lee, J. Seo, M. Jeong, S. Lee, and J. Song, "The roles of FADD in extrinsic apoptosis and necroptosis." *BMB reports*, vol. 45, no. 9, pp. 496–508, Sep. 2012.

[63] V. Vilmont, L. Tourneur, and G. Chiocchia, "Fas-associated death domain protein and adenosine partnership: fad in RA." *Rheumatology (Oxford, England)*, vol. 51, no. 6, pp. 964–75, Jun. 2012.

[64] E. A. Slee, C. Adrain, and S. J. Martin, "Executioner caspase-3, -6, and -7 perform distinct, non-redundant roles during the demolition phase of apoptosis." *The Journal of biological chemistry*, vol. 276, no. 10, pp. 7320–6, Mar. 2001.

[65] G. Kroemer and S. J. Martin, "Caspase-independent cell death." *Nature medicine*, vol. 11, no. 7, pp. 725–30, Jul. 2005.

[66] P. Wang, J. Lindsay, T. W. Owens, E. J. Mularczyk, S. Warwood, F. Foster, C. H. Streuli, K. Brennan, and A. P. Gilmore, "Phosphorylation of the proapoptotic BH3-only protein bid primes mitochondria for apoptosis during mitotic arrest." *Cell reports*, vol. 7, no. 3, pp. 661–71, May 2014.

[67] M. P. Thomas and J. Lieberman, "Live or let die: posttranscriptional gene regulation in cell stress and cell death." *Immunological reviews*, vol. 253, no. 1, pp. 237–52, May 2013.

[68] L. E. Bröker, F. a. E. Kruyt, and G. Giaccone, "Cell death independent of caspases: a review." *Clinical cancer research : an official journal of the American Association for Cancer Research*, vol. 11, no. 9, pp. 3155–62, May 2005.

[69] H. Dai, Y.-P. Pang, M. Ramirez-Alvarado, and S. H. Kaufmann, "Evaluation of the BH3-only protein Puma as a direct Bak activator." *The Journal of biological chemistry*, vol. 289, no. 1, pp. 89–99, Jan. 2014.

[70] S. Ma, C. Hockings, K. Anwari, T. Kratina, S. Fennell, M. Lazarou, M. T. Ryan, R. M. Kluck, and G. Dewson, "Assembly of the Bak apoptotic pore: a critical role for the Bak protein α6 helix in the multimerization of homodimers during apoptosis." *The Journal of biological chemistry*, vol. 288, no. 36, pp. 26 027–38, Sep. 2013.

[71] L. P. Billen, A. Shamas-Din, and D. W. Andrews, "Bid: a Bax-like BH3 protein." *Oncogene*, vol. 27 Suppl 1, pp. S93–104, Dec. 2008.

[72] B. Antonsson, F. Conti, A. Ciavatta, S. Montessuit, S. Lewis, I. Martinou, L. Bernasconi, A. Bernard, J. J. Mermod, G. Mazzei, K. Maundrell, F. Gambale, R. Sadoul, and J. C. Martinou, "Inhibition of Bax channel-forming activity by Bcl-2." *Science (New York, N.Y.)*, vol. 277, no. 5324, pp. 370–2, Jul. 1997.

[73] A. J. Minn, P. Vélez, S. L. Schendel, H. Liang, S. W. Muchmore, S. W. Fesik, M. Fill, and C. B. Thompson, "Bcl-x(L) forms an ion channel in synthetic lipid membranes." *Nature*, vol. 385, no. 6614, pp. 353–7, Jan. 1997.

[74] S. L. Schendel, R. Azimov, K. Pawlowski, A. Godzik, B. L. Kagan, and J. C. Reed, "Ion channel activity of the BH3 only Bcl-2 family member, BID." *The Journal of biological chemistry*, vol. 274, no. 31, pp. 21 932–6, Jul. 1999.

[75] K. Cosentino and A. J. García-Sáez, "Mitochondrial alterations in apoptosis." *Chemistry and physics of lipids*, vol. 181C, pp. 62–75, Jul. 2014.

[76] S. J. Riedl and G. S. Salvesen, "The apoptosome: signalling platform of cell death." *Nature reviews. Molecular cell biology*, vol. 8, no. 5, pp. 405–13, May 2007.

[77] Y. Hu, M. A. Benedict, L. Ding, and G. Núñez, "Role of cytochrome c and dATP/ATP hydrolysis in Apaf-1-mediated caspase-9 activation and apoptosis." *The EMBO journal*, vol. 18, no. 13, pp. 3586–95, Jul. 1999.

[78] M. Renatus, H. R. Stennicke, F. L. Scott, R. C. Liddington, and G. S. Salvesen, "Dimer formation drives the activation of the cell death protease caspase 9." *Proceedings of the National Academy of Sciences of the United States of America*, vol. 98, no. 25, pp. 14 250–5, Dec. 2001.

[79] K. M. Boatright, M. Renatus, F. L. Scott, S. Sperandio, H. Shin, I. M. Pedersen, J. E. Ricci, W. A. Edris, D. P. Sutherlin, D. R. Green, and G. S. Salvesen, "A unified model for apical caspase activation." *Molecular cell*, vol. 11, no. 2, pp. 529–41, Mar. 2003.

[80] S. Yuan and C. W. Akey, "Apoptosome structure, assembly, and procaspase activation." *Structure (London, England : 1993)*, vol. 21, no. 4, pp. 501–15, Apr. 2013.

[81] E. A. Slee, M. T. Harte, R. M. Kluck, B. B. Wolf, C. A. Casiano, D. D. Newmeyer, H. G. Wang, J. C. Reed, D. W. Nicholson, E. S. Alnemri, D. R. Green, and S. J. Martin, "Ordering the cytochrome c-initiated caspase cascade: hierarchical activation of caspases-2, -3, -6, -7, -8, and -10 in a caspase-9-dependent manner." *The Journal of cell biology*, vol. 144, no. 2, pp. 281–92, Jan. 1999.

[82] I. Kitazumi and M. Tsukahara, "Regulation of DNA fragmentation: the role of caspases and phosphorylation." *The FEBS journal*, vol. 278, no. 3, pp. 427–41, Feb. 2011.

[83] R. W. Oppenheim, R. A. Flavell, S. Vinsant, D. Prevette, C. Y. Kuan, and P. Rakic, "Programmed cell death of developing mammalian neurons after genetic deletion of caspases." *The Journal of neuroscience : the official journal of the Society for Neuroscience*, vol. 21, no. 13, pp. 4752–60, Jul. 2001.

[84] T. Lindsten, A. J. Ross, A. King, W. X. Zong, J. C. Rathmell, H. A. Shiels, E. Ulrich, K. G. Waymire, P. Mahar, K. Frauwirth, Y. Chen, M. Wei, V. M. Eng, D. M. Adelman, M. C. Simon, A. Ma, J. A. Golden, G. Evan, S. J. Korsmeyer, G. R. MacGregor, and C. B. Thompson, "The combined functions of proapoptotic Bcl-2 family members bak and bax are essential for normal development of multiple tissues." *Molecular cell*, vol. 6, no. 6, pp. 1389–99, Dec. 2000.

[85] J. E. Chipuk and D. R. Green, "Do inducers of apoptosis trigger caspase-independent cell death?" *Nature reviews. Molecular cell biology*, vol. 6, no. 3, pp. 268–75, Mar. 2005.

[86] M. Donovan and T. G. Cotter, "Control of mitochondrial integrity by Bcl-2 family members and caspase-independent cell death." *Biochimica et biophysica acta*, vol. 1644, no. 2-3, pp. 133–47, Mar. 2004.

[87] P. G. Ekert, J. Silke, and D. L. Vaux, "Caspase inhibitors." *Cell death and differentiation*, vol. 6, no. 11, pp. 1081–6, Nov. 1999.

[88] P. Golstein and G. Kroemer, "Cell death by necrosis: towards a molecular definition." *Trends in biochemical sciences*, vol. 32, no. 1, pp. 37–43, Jan. 2007.

[89] D. V. Krysko, T. Vanden Berghe, K. D'Herde, and P. Vandenabeele, "Apoptosis and necrosis: detection, discrimination and phagocytosis." *Methods (San Diego, Calif.)*, vol. 44, no. 3, pp. 205–21, Mar. 2008.

[90] D. Moquin and F. K.-M. Chan, "The molecular regulation of programmed necrotic cell injury." *Trends in biochemical sciences*, vol. 35, no. 8, pp. 434–41, Aug. 2010.

[91] L. Galluzzi, O. Kepp, S. Krautwald, G. Kroemer, and A. Linkermann, "Molecular mechanisms of regulated necrosis." *Seminars in cell & developmental biology*, vol. 35, pp. 24–32, Nov. 2014.

[92] A. Linkermann and D. R. Green, "Necroptosis." *The New England journal of medicine*, vol. 370, no. 5, pp. 455–65, Jan. 2014.

[93] S. Challa and F. K.-M. Chan, "Going up in flames: necrotic cell injury and inflammatory diseases." *Cellular and molecular life sciences : CMLS*, vol. 67, no. 19, pp. 3241–53, Oct. 2010.

[94] S. J. Kim and J. Li, "Caspase blockade induces RIP3-mediated programmed necrosis in Toll-like receptor-activated microglia." *Cell death & disease*, vol. 4, p. e716, Jan. 2013.

[95] Z. Cai, S. Jitkaew, J. Zhao, H.-C. Chiang, S. Choksi, J. Liu, Y. Ward, L.-G. Wu, and Z.-G. Liu, "Plasma membrane translocation of trimerized MLKL protein is required for TNF-induced necroptosis." *Nature cell biology*, vol. 16, no. 1, pp. 55–65, Jan. 2014.

[96] J. B. Kirkland, "Poly ADP-ribose polymerase-1 and health." *Experimental biology and medicine (Maywood, N.J.)*, vol. 235, no. 5, pp. 561–8, May 2010.

[97] M. Di Stefano and L. Conforti, "Diversification of NAD biological role: the importance of location." *The FEBS journal*, vol. 280, no. 19, pp. 4711–28, Oct. 2013.

[98] B. C. Woodhouse and G. L. Dianov, "Poly ADP-ribose polymerase-1: an international molecule of mystery." *DNA repair*, vol. 7, no. 7, pp. 1077–86, Jul. 2008.

[99] M. Jin and D. J. Klionsky, "Regulation of autophagy: Modulation of the size and number of autophagosomes." *FEBS letters*, Jun. 2014.

[100] J. Zhang, "Autophagy and Mitophagy in Cellular Damage Control." *Redox biology*, vol. 1, no. 1, pp. 19–23, Jan. 2013.

[101] D. Denton, S. Nicolson, and S. Kumar, "Cell death by autophagy: facts and apparent artefacts." *Cell death and differentiation*, vol. 19, no. 1, pp. 87–95, Jan. 2012.

[102] K. R. Parzych and D. J. Klionsky, "An Overview of Autophagy: Morphology, Mechanism, and Regulation." *Antioxidants & redox signaling*, vol. 00, no. 00, Aug. 2013.

[103] W.-w. Li, J. Li, and J.-k. Bao, "Microautophagy: lesser-known self-eating." *Cellular and molecular life sciences : CMLS*, vol. 69, no. 7, pp. 1125–36, Apr. 2012.

[104] S. Kaushik and A. M. Cuervo, "Chaperone-mediated autophagy: a unique way to enter the lysosome world." *Trends in cell biology*, vol. 22, no. 8, pp. 407–17, Aug. 2012.

[105] Y. Feng, D. He, Z. Yao, and D. J. Klionsky, "The machinery of macroautophagy." *Cell research*, vol. 24, no. 1, pp. 24–41, Jan. 2014.

[106] C. A. Lamb, T. Yoshimori, and S. A. Tooze, "The autophagosome: origins unknown, biogenesis complex." *Nature reviews. Molecular cell biology*, vol. 14, no. 12, pp. 759–74, Dec. 2013.

[107] W. Bursch, A. Ellinger, H. Kienzl, L. Török, S. Pandey, M. Sikorska, R. Walker, and R. S. Hermann, "Active cell death induced by the anti-estrogens tamoxifen and ICI 164 384 in human mammary carcinoma cells (MCF-7) in culture: the role of autophagy." *Carcinogenesis*, vol. 17, no. 8, pp. 1595–607, Aug. 1996.

[108] T. Kanzawa, I. M. Germano, T. Komata, H. Ito, Y. Kondo, and S. Kondo, "Role of autophagy in temozolomide-induced cytotoxicity for malignant glioma cells." *Cell death and differentiation*, vol. 11, no. 4, pp. 448–57, Apr. 2004.

[109] M. Hoeyer-Hansen, L. Bastholm, I. S. Mathiasen, F. Elling, and M. Jäättelä, "Vitamin D analog EB1089 triggers dramatic lysosomal changes and Beclin 1-mediated autophagic cell death." *Cell death and differentiation*, vol. 12, no. 10, pp. 1297–309, Oct. 2005.

[110] V. Nikoletopoulou, M. Markaki, K. Palikaras, and N. Tavernarakis, "Crosstalk between apoptosis, necrosis and autophagy." *Biochimica et biophysica acta*, vol. 1833, no. 12, pp. 3448–59, Dec. 2013.

[111] C. Gordy and Y.-W. He, "The crosstalk between autophagy and apoptosis: where does this lead?" *Protein & cell*, vol. 3, no. 1, pp. 17–27, Jan. 2012.

[112] N. Schütze, R. Schenk, J. Fiedler, T. Mattes, F. Jakob, and R. E. Brenner, "CYR61/CCN1 and WISP3/CCN6 are chemoattractive ligands for human multipotent mesenchymal stroma cells." *BMC cell biology*, vol. 8, p. 45, Jan. 2007.

[113] M. M. Bradford, "A rapid and sensitive method for the quantitation of microgram quantities of protein utilizing the principle of protein-dye binding." *Analytical biochemistry*, vol. 72, pp. 248–54, May 1976.

[114] M. W. Pfaffl, "A new mathematical model for relative quantification in real-time RT-PCR." *Nucleic acids research*, vol. 29, no. 9, p. e45, May 2001.

[115] K. Schlegelmilch, A. Keller, V. Zehe, S. Hondke, T. Schilling, F. Jakob, L. Klein-Hitpass, and N. Schütze, "WISP 1 is an important survival factor in human mesenchymal stromal cells." *Gene*, Sep. 2014.

[116] S. Tanabe, "Role of mesenchymal stem cells in cell life and their signaling." *World journal of stem cells*, vol. 6, no. 1, pp. 24–32, Jan. 2014.

[117] H. Yue, Z.-l. Zhang, and J.-w. He, "Identification of novel mutations in WISP3 gene in two unrelated Chinese families with progressive pseudorheumatoid dysplasia," *Bone*, vol. 44, no. 4, pp. 547–554, 2009.

[118] F. F. Safadi, J. Xu, S. L. Smock, R. A. Kanaan, A.-H. Selim, P. R. Odgren, S. C. Marks, T. A. Owen, and S. N. Popoff, "Expression of connective tissue growth factor in bone: its role in osteoblast proliferation and differentiation in vitro and bone formation in vivo." *Journal of cellular physiology*, vol. 196, no. 1, pp. 51–62, Jul. 2003.

[119] C. A. Inkson, M. Ono, Y. Bi, S. A. Kuznetsov, L. W. Fisher, and M. F. Young, "The potential functional interaction of biglycan and WISP-1 in controlling differentiation and proliferation of osteogenic cells." *Cells, tissues, organs*, vol. 189, no. 1-4, pp. 153–7, Jan. 2009.

[120] C. G. Kleer, Y. Zhang, Q. Pan, S. D. Merajver, G. Gallagher, M. Wu, and Z.-f. Wu, "WISP3 and RhoC guanosine triphosphatase cooperate in the development of inflammatory breast cancer." *Breast cancer research : BCR*, vol. 6, no. 2, pp. 179–185, Jan. 2004.

[121] J. Dotterweich, R. Ebert, S. Kraus, R. J. Tower, F. Jakob, and N. Schütze, "Mesenchymal stem cell contact promotes CCN1 splicing and transcription in myeloma cells." *Cell communication and signaling : CCS*, vol. 12, p. 36, Jan. 2014.

[122] C. J. Echeverri, P. A. Beachy, B. Baum, M. Boutros, F. Buchholz, S. K. Chanda, J. Downward, J. Ellenberg, A. G. Fraser, N. Hacohen, W. C. Hahn, A. L. Jackson, A. Kiger, P. S. Linsley, L. Lum, Y. Ma, B. Mathey-Prévôt, D. E. Root, D. M. Sabatini, J. Taipale, N. Perrimon, and R. Bernards, "Minimizing the risk of reporting false positives in large-scale RNAi screens." *Nature methods*, vol. 3, no. 10, pp. 777–9, Oct. 2006.

[123] G. Forte, M. Minieri, P. Cossa, D. Antenucci, M. Sala, V. Gnocchi, R. Fiaccavento, F. Carotenuto, P. De Vito, P. M. Baldini, M. Prat, and P. Di Nardo, "Hepatocyte growth factor effects on mesenchymal stem cells: proliferation, migration, and differentiation." *Stem cells (Dayton, Ohio)*, vol. 24, no. 1, pp. 23–33, Jan. 2006.

[124] M. Guillamot, E. Manchado, M. Chiesa, G. Gómez-López, D. G. Pisano, M. P. Sacristán, and M. Malumbres, "Cdc14b regulates mammalian RNA polymerase II and represses cell cycle transcription." *Scientific reports*, vol. 1, p. 189, Jan. 2011.

[125] A. Mocciaro, E. Berdougo, K. Zeng, E. Black, P. Vagnarelli, W. Earnshaw, D. Gillespie, P. Jallepalli, and E. Schiebel, "Vertebrate cells genetically deficient for Cdc14A or Cdc14B retain DNA damage checkpoint proficiency but are impaired in DNA repair." *The Journal of cell biology*, vol. 189, no. 4, pp. 631–9, May 2010.

[126] S. Tane, M. Kubota, H. Okayama, A. Ikenishi, S. Yoshitome, N. Iwamoto, Y. Satoh, A. Kusakabe, S. Ogawa, A. Kanai, J. D. Molkentin, K. Nakamura, T. Ohbayashi, and T. Takeuchi, "Repression of Cyclin D1 Expression is Necessary for the Maintenance of Cell Cycle Exit in Adult Mammalian Cardiomyocytes." *The Journal of biological chemistry*, May 2014.

[127] Q. Chen, J. Lin, S. Jinno, and H. Okayama, "Overexpression of Cdk6-cyclin D3 highly sensitizes cells to physical and chemical transformation." *Oncogene*, vol. 22, no. 7, pp. 992–1001, Feb. 2003.

[128] M. Poreba, A. Strózyk, G. S. Salvesen, and M. Drag, "Caspase substrates and inhibitors." *Cold Spring Harbor perspectives in biology*, vol. 5, no. 8, p. a008680, Aug. 2013.

[129] A. Pal, W. Huang, X. Li, K. a. Toy, Z. Nikolovska-Coleska, and C. G. Kleer, "CCN6 modulates BMP signaling via the Smad-independent TAK1/p38 pathway, acting to suppress metastasis of breast cancer." *Cancer research*, vol. 72, no. 18, pp. 4818–28, Sep. 2012.

[130] K. Bialkowska, Y. Zaffran, S. C. Meyer, and J. E. B. Fox, "14-3-3 zeta mediates integrin-induced activation of Cdc42 and Rac. Platelet glycoprotein Ib-IX regulates integrin-induced signaling by sequestering 14-3-3 zeta." *The Journal of biological chemistry*, vol. 278, no. 35, pp. 33 342–50, Aug. 2003.

[131] M. Niemantsverdriet, K. Wagner, M. Visser, and C. Backendorf, "Cellular functions of 14-3-3 zeta in apoptosis and cell adhesion emphasize its oncogenic character." *Oncogene*, vol. 27, no. 9, pp. 1315–9, Feb. 2008.

[132] J.-E. Oh, D. H. Jang, H. Kim, H. K. Kang, C.-P. Chung, W. H. Park, and B.-M. Min, "alpha3beta1 integrin promotes cell survival via multiple interactions between 14-3-3 isoforms and proapoptotic proteins." *Experimental cell research*, vol. 315, no. 18, pp. 3187–200, Nov. 2009.

[133] N. O. Deakin, M. D. Bass, S. Warwood, J. Schoelermann, Z. Mostafavi-Pour, D. Knight, C. Ballestrem, and M. J. Humphries, "An integrin-alpha4-14-3-3zeta-paxillin ternary complex mediates localised Cdc42 activity and accelerates cell migration." *Journal of cell science*, vol. 122, no. Pt 10, pp. 1654–64, May 2009.

[134] R. Bonet, I. Vakonakis, and I. D. Campbell, "Characterization of 14-3-3-ζ Interactions with integrin tails." *Journal of molecular biology*, vol. 425, no. 17, pp. 3060–72, Sep. 2013.

[135] A. L. Neisch and R. G. Fehon, "Ezrin, Radixin and Moesin: key regulators of membrane-cortex interactions and signaling." *Current opinion in cell biology*, vol. 23, no. 4, pp. 377–82, Aug. 2011.

[136] M. Algrain, O. Turunen, A. Vaheri, D. Louvard, and M. Arpin, "Ezrin contains cytoskeleton and membrane binding domains accounting for its proposed role as a membrane-cytoskeletal linker." *The Journal of cell biology*, vol. 120, no. 1, pp. 129–39, Jan. 1993.

[137] J. Zhang, J. Zuo, M. Lei, S. Wu, X. Zang, and C. Zhang, "Ezrin promotes invasion and migration of the MG63 osteosarcoma cell." *Chinese medical journal*, vol. 127, no. 10, pp. 1954–9, May 2014.

[138] J. Srivastava, B. E. Elliott, D. Louvard, and M. Arpin, "Src-dependent ezrin phosphorylation in adhesion-mediated signaling." *Molecular biology of the cell*, vol. 16, no. 3, pp. 1481–90, Mar. 2005.

[139] W.-C. Kuo, K.-T. Yang, S.-L. Hsieh, and M.-Z. Lai, "Ezrin is a negative regulator of death receptor-induced apoptosis." *Oncogene*, vol. 29, no. 9, pp. 1374–83, Mar. 2010.

[140] P. D. Leiphrakpam, A. Rajput, M. Mathiesen, E. Agarwal, A. J. Lazenby, C. Are, M. G. Brattain, and S. Chowdhury, "Ezrin expression and cell survival regulation in colorectal cancer." *Cellular signalling*, vol. 26, no. 5, pp. 868–79, May 2014.

[141] C. Roubinet, B. Decelle, G. Chicanne, J. F. Dorn, B. Payrastre, F. Payre, and S. Carreno, "Molecular networks linked by Moesin drive remodeling of the cell cortex during mitosis." *The Journal of cell biology*, vol. 195, no. 1, pp. 99–112, Oct. 2011.

[142] P. Kunda, N. T. L. Rodrigues, E. Moeendarbary, T. Liu, A. Ivetic, G. Charras, and B. Baum, "PP1-mediated moesin dephosphorylation couples polar relaxation to mitotic exit." *Current biology : CB*, vol. 22, no. 3, pp. 231–6, Feb. 2012.

[143] M. Théry and M. Bornens, "Get round and stiff for mitosis." *HFSP journal*, vol. 2, no. 2, pp. 65–71, Apr. 2008.

[144] F. Tsuruta, J. Sunayama, Y. Mori, S. Hattori, S. Shimizu, Y. Tsujimoto, K. Yoshioka, N. Masuyama, and Y. Gotoh, "JNK promotes Bax translocation to mitochondria through phosphorylation of 14-3-3 proteins." *The EMBO journal*, vol. 23, no. 8, pp. 1889–99, Apr. 2004.

[145] G. E. Lim, M. Piske, and J. D. Johnson, "14-3-3 proteins are essential signalling hubs for beta cell survival." *Diabetologia*, vol. 56, no. 4, pp. 825–37, Apr. 2013.

[146] L. Lartigue, Y. Kushnareva, Y. Seong, H. Lin, B. Faustin, and D. D. Newmeyer, "Caspase-independent mitochondrial cell death results from loss of respiration, not cytotoxic protein release." *Molecular biology of the cell*, vol. 20, no. 23, pp. 4871–84, Dec. 2009.

[147] M. Mourdjeva, D. Kyurkchiev, A. Mandinova, I. Altankova, I. Kehayov, and S. Kyurkchiev, "Dynamics of membrane translocation of phosphatidylserine during apoptosis detected by a monoclonal antibody." *Apoptosis : an international journal on programmed cell death*, vol. 10, no. 1, pp. 209–17, Jan. 2005.

[148] F. Su, M. Overholtzer, D. Besser, and A. J. Levine, "WISP-1 attenuates p53-mediated apoptosis in response to DNA damage through activation of the Akt kinase." *Genes & development*, vol. 16, no. 1, pp. 46–57, Jan. 2002.

[149] S. Wang, Z. Z. Chong, Y. C. Shang, and K. Maiese, "WISP1 (CCN4) autoregulates its expression and nuclear trafficking of β-catenin during oxidant stress with limited effects upon neuronal autophagy." *Current neurovascular research*, vol. 9, no. 2, pp. 91–101, May 2012.

[150] Y. Matsui, H. Takagi, X. Qu, M. Abdellatif, H. Sakoda, T. Asano, B. Levine, and J. Sadoshima, "Distinct roles of autophagy in the heart during ischemia and reperfusion: roles of AMP-activated protein kinase and Beclin 1 in mediating autophagy." *Circulation research*, vol. 100, no. 6, pp. 914–22, Mar. 2007.

[151] J. Y. Guo, H.-Y. Chen, R. Mathew, J. Fan, A. M. Strohecker, G. Karsli-Uzunbas, J. J. Kamphorst, G. Chen, J. M. S. Lemons, V. Karantza, H. A. Coller, R. S. DiPaola, C. Gelinas, J. D. Rabinowitz, and E. White, "Activated Ras requires autophagy to maintain oxidative metabolism and tumorigenesis," *Genes & Development*, vol. 25, no. 5, pp. 460–470, Feb. 2011.

[152] L. Yu, A. Alva, H. Su, P. Dutt, E. Freundt, S. Welsh, E. H. Baehrecke, and M. J. Lenardo, "Regulation of an ATG7-beclin 1 program of autophagic cell death by caspase-8." *Science (New York, N.Y.)*, vol. 304, no. 5676, pp. 1500–2, Jun. 2004.

[153] S. Shimizu, T. Kanaseki, N. Mizushima, T. Mizuta, S. Arakawa-Kobayashi, C. B. Thompson, and Y. Tsujimoto, "Role of Bcl-2 family proteins in a non-apoptotic programmed cell death dependent on autophagy genes." *Nature cell biology*, vol. 6, no. 12, pp. 1221–8, Dec. 2004.

[154] S. Feng, Y. Yang, Y. Mei, L. Ma, D.-e. Zhu, N. Hoti, M. Castanares, and M. Wu, "Cleavage of RIP3 inactivates its caspase-independent apoptosis pathway by removal of kinase domain." *Cellular signalling*, vol. 19, no. 10, pp. 2056–67, Oct. 2007.

[155] C. Rébé, S. Cathelin, S. Launay, R. Filomenko, L. Prévotat, C. L'Ollivier, E. Gyan, O. Micheau, S. Grant, A. Dubart-Kupperschmitt, M. Fontenay, and E. Solary, "Caspase-8 prevents sustained activation of NF-kappaB in monocytes undergoing macrophagic differentiation." *Blood*, vol. 109, no. 4, pp. 1442–50, Feb. 2007.

[156] M. A. O'Donnell, E. Perez-Jimenez, A. Oberst, A. Ng, R. Massoumi, R. Xavier, D. R. Green, and A. T. Ting, "Caspase 8 inhibits programmed necrosis by processing CYLD." *Nature cell biology*, vol. 13, no. 12, pp. 1437–42, Dec. 2011.

[157] K. Bray, R. Mathew, A. Lau, J. J. Kamphorst, J. Fan, J. Chen, H.-Y. Chen, A. Ghavami, M. Stein, R. S. DiPaola, D. Zhang, J. D. Rabinowitz, and E. White, "Autophagy suppresses RIP kinase-dependent necrosis enabling survival to mTOR inhibition." *PloS one*, vol. 7, no. 7, Jan. 2012.

[158] S. W. G. Tait, G. Ichim, and D. R. Green, "Die another way - non-apoptotic mechanisms of cell death." *Journal of cell science*, vol. 127, no. Pt 10, pp. 2135–44, May 2014.

[159] M. B. Greenblatt, J.-H. Shim, and L. H. Glimcher, "TAK1 mediates BMP signaling in cartilage." *Annals of the New York Academy of Sciences*, vol. 1192, pp. 385–90, Mar. 2010.

[160] S. Morioka, P. Broglie, E. Omori, Y. Ikeda, G. Takaesu, K. Matsumoto, and J. Ninomiya-Tsuji, "TAK1 kinase switches cell fate from apoptosis to necrosis following TNF stimulation." *The Journal of cell biology*, vol. 204, no. 4, pp. 607–23, Feb. 2014.

[161] K. Azijli, B. Weyhenmeyer, G. J. Peters, S. de Jong, and F. A. E. Kruyt, "Non-canonical kinase signaling by the death ligand TRAIL in cancer cells: discord in the death receptor family." *Cell death and differentiation*, vol. 20, no. 7, pp. 858–68, Jul. 2013.

[162] W. Huang, Y. Zhang, S. Varambally, A. M. Chinnaiyan, M. Banerjee, S. D. Merajver, and C. G. Kleer, "Inhibition of CCN6 (Wnt-1-induced signaling protein 3) down-regulates E-cadherin in the breast epithelium through induction of snail and ZEB1." *The American journal of pathology*, vol. 172, no. 4, pp. 893–904, Apr. 2008.

[163] A. Pal, W. Huang, X. Li, K. A. Toy, Z. Nikolovska-Coleska, and C. G. Kleer, "Supplement - CCN6 modulates BMP signaling via the Smad-independent TAK1/p38 pathway, acting to suppress metastasis of breast cancer," *Cancer research*, vol. 72, no. 18, pp. 4818–28, Sep. 2012.

[164] J. J. Bravo-Cordero, V. P. Sharma, M. Roh-Johnson, X. Chen, R. Eddy, J. Condeelis, and L. Hodgson, "Spatial regulation of RhoC activity defines protrusion formation in migrating cells." *Journal of cell science*, vol. 126, no. Pt 15, pp. 3356–69, Aug. 2013.

[165] A. Pal, W. Huang, K. A. Toy, and C. G. Kleer, "CCN6 knockdown disrupts acinar organization of breast cells in three-dimensional cultures through up-regulation of type III TGF-β receptor." *Neoplasia (New York, N.Y.)*, vol. 14, no. 11, pp. 1067–74, Nov. 2012.

[166] R.-R. Cui, J. Huang, L. Yi, H. Xie, H.-D. Zhou, L.-Q. Yuan, M. Wang, Y.-Q. Peng, X.-H. Luo, and E.-Y. Liao, "WISP3 suppresses insulin-like growth factor signaling in human chondrocytes." *Molecular and cellular endocrinology*, vol. 279, no. 1-2, pp. 1–8, Dec. 2007.

[167] M. Giorgio, E. Migliaccio, F. Orsini, D. Paolucci, M. Moroni, C. Contursi, G. Pelliccia, L. Luzi, S. Minucci, M. Marcaccio, P. Pinton, R. Rizzuto, P. Bernardi, F. Paolucci, and P. G. Pelicci, "Electron transfer between cytochrome c and p66Shc generates reactive oxygen species that trigger mitochondrial apoptosis." *Cell*, vol. 122, no. 2, pp. 221–33, Jul. 2005.

[168] L. Davis, Y. Chen, and M. Sen, "WISP-3 functions as a ligand and promotes superoxide dismutase activity." *Biochemical and biophysical research communications*, vol. 342, no. 1, pp. 259–65, Mar. 2006.

[169] N. Jallali, H. Ridha, C. Thrasivoulou, C. Underwood, P. E. M. Butler, and T. Cowen, "Vulnerability to ROS-induced cell death in ageing articular cartilage: the role of antioxidant enzyme activity." *Osteoarthritis and cartilage / OARS, Osteoarthritis Research Society*, vol. 13, no. 7, pp. 614–22, Jul. 2005.

[170] J. Dudhia, "Aggrecan, aging and assembly in articular cartilage." *Cellular and molecular life sciences : CMLS*, vol. 62, no. 19-20, pp. 2241–56, Oct. 2005.

[171] P. Verma and K. Dalal, "ADAMTS-4 and ADAMTS-5: key enzymes in osteoarthritis." *Journal of cellular biochemistry*, vol. 112, no. 12, pp. 3507–14, Dec. 2011.

[172] V. Delague, E. Chouery, S. Corbani, I. Ghanem, S. Aamar, J. Fischer, E. Levy-Lahad, J. A. Urtizberea, and A. Mégarbané, "Molecular study of WISP3 in nine families originating from the Middle-East and presenting with progressive pseudorheumatoid dysplasia: identification of two novel mutations, and description of a founder effect." *American journal of medical genetics. Part A*, vol. 138A, no. 2, pp. 118–26, Oct. 2005.

[173] A. Dalal, S. L. Bhavani G, P. P. Togarrati, T. Bierhals, M. R. Nandineni, S. Danda, D. Danda, H. Shah, S. Vijayan, K. Gowrishankar, S. R. Phadke, A. M. Bidchol, A. P. Rao, S. Nampoothiri, K. Kutsche, and K. M. Girisha, "Analysis of the WISP3 gene in Indian families with progressive pseudorheumatoid dysplasia." *American journal of medical genetics. Part A*, vol. 158A, no. 11, pp. 2820–8, Nov. 2012.

[174] J.-I. Park, "Growth arrest signaling of the Raf/MEK/ERK pathway in cancer." *Frontiers in biology*, vol. 9, no. 2, pp. 95–103, Feb. 2014.

[175] J. Zhang and M. Xu, "Apoptotic DNA fragmentation and tissue homeostasis." *Trends in cell biology*, vol. 12, no. 2, pp. 84–9, Feb. 2002.

[176] A. Degterev, J. Hitomi, M. Germscheid, I. L. Ch'en, O. Korkina, X. Teng, D. Abbott, G. D. Cuny, C. Yuan, G. Wagner, S. M. Hedrick, S. A. Gerber, A. Lugovskoy, and J. Yuan, "Identification of RIP1 kinase as a specific cellular target of necrostatins." *Nature chemical biology*, vol. 4, no. 5, pp. 313–21, May 2008.

[177] W. J. Kaiser, H. Sridharan, C. Huang, P. Mandal, J. W. Upton, P. J. Gough, C. A. Sehon, R. W. Marquis, J. Bertin, and E. S. Mocarski, "Toll-like receptor 3-mediated necrosis via TRIF, RIP3, and MLKL." *The Journal of biological chemistry*, vol. 288, no. 43, pp. 31 268–79, Oct. 2013.

[178] L. Sun, H. Wang, Z. Wang, S. He, S. Chen, D. Liao, L. Wang, J. Yan, W. Liu, X. Lei, and X. Wang, "Mixed lineage kinase domain-like protein mediates necrosis signaling downstream of RIP3 kinase." *Cell*, vol. 148, no. 1-2, pp. 213–27, Jan. 2012.

Part V

Appendix

Microarray data

Probe set ID	Gene symbol	Gene name	logFc	adj. p-value
210861_s_at	WISP3	WNT1 inducible signalling pathway protein 3	-3.58	8.22E-03
205302_at	IGFBP1	insulin-like growth factor binding protein 1	-2.38	1.62E-02
209351_at	KRT14	keratin 14	-2.03	1.62E-02
219529_at	CLIC3	chloride intracellular channel 3	-1.90	1.49E-02
208754_s_at	NAP1L1	nucleosome assembly protein 1-like 1	-1.88	8.22E-03
224436_s_at	NIPSNAP3A	nipsnap homolog 3A (C. elegans)	-1.81	1.18E-02
201005_at	CD9	CD9 molecule	-1.74	3.71E-02
228748_at	CD59	CD59 molecule, complement regulatory protein	-1.66	2.32E-02
208051_s_at	PAIP1	poly(A) binding protein interacting protein 1	-1.65	3.23E-02
226869_at	MEGF6	multiple EGF-like-domains 6	-1.58	1.44E-02
203186_s_at	S100A4	S100 calcium binding protein A4	-1.57	1.80E-02
205498_at	GHR	growth hormone receptor	-1.55	1.39E-02
201596_x_at	KRT18	keratin 18	-1.54	4.70E-02
234304_s_at	IPO11	importin 11	-1.54	1.18E-02
200641_s_at	YWHAZ	tyrosine 3-monooxygenase/tryptophan 5-monooxygenase activation protein, zeta polypeptide	-1.53	1.18E-02
224779_s_at	FAM96A	family with sequence similarity 96, member A	-1.53	8.22E-03
212912_at	RPS6KA2	ribosomal protein S6 kinase, 90kDa, polypeptide 2	-1.53	1.18E-02
227051_at	NA	NA	-1.52	1.18E-02
209064_x_at	PAIP1	poly(A) binding protein interacting protein 1	-1.52	2.65E-02
223519_at	ZAK	sterile alpha motif and leucine zipper containing kinase AZK	-1.49	1.02E-02
212977_at	CXCR7	chemokine (C-X-C motif) receptor 7	-1.48	1.79E-02

...continuous on the next page

Probe set ID	Gene symbol	Gene name	logFc	adj. p-value
217814_at	CCDC47	coiled-coil domain containing 47	-1.47	8.22E-03
236313_at	CDKN2B	cyclin-dependent kinase inhibitor 2B (p15, inhibits CDK4)	-1.46	1.34E-02
224415_s_at	HINT2	histidine triad nucleotide binding protein 2	-1.46	1.39E-02
223059_s_at	FAM107B	family with sequence similarity 107, member B	-1.45	1.18E-02
212463_at	CD59	CD59 molecule, complement regulatory protein	-1.45	1.39E-02
201189_s_at	ITPR3	inositol 1,4,5-triphosphate receptor, type 3	-1.44	1.18E-02
204863_s_at	IL6ST	interleukin 6 signal transducer (gp130, oncostatin M receptor)	-1.44	1.85E-02
212195_at	IL6ST	interleukin 6 signal transducer (gp130, oncostatin M receptor)	-1.42	1.39E-02
218957_s_at	PAAF1	proteasomal ATPase-associated factor 1	-1.42	1.18E-02
1556121_at	NAP1L1	nucleosome assembly protein 1-like 1	-1.42	1.18E-02
209016_s_at	KRT7	keratin 7	-1.42	1.44E-02
204735_at	PDE4A	phosphodiesterase 4A, cAMP-specific	-1.41	1.80E-02
225665_at	ZAK	sterile alpha motif and leucine zipper containing kinase AZK	-1.40	1.39E-02
202852_s_at	AAGAB	alpha- and gamma-adaptin binding protein	-1.40	1.18E-02
203359_s_at	MYCBP	c-myc binding protein	-1.38	8.22E-03
225411_at	TMEM87B	transmembrane protein 87B	-1.36	8.22E-03
218011_at	UBL5	ubiquitin-like 5	-1.36	8.22E-03
202205_at	VASP	vasodilator-stimulated phosphoprotein	-1.36	1.18E-02
211000_s_at	IL6ST	interleukin 6 signal transducer (gp130, oncostatin M receptor)	-1.35	1.85E-02
223058_at	FAM107B	family with sequence similarity 107, member B	-1.34	1.18E-02
225055_at	LOC100499466	hypothetical LOC100499466	-1.31	1.18E-02
226865_at	NA	NA	-1.31	1.34E-02
40189_at	SET	SET nuclear oncogene	-1.31	1.18E-02
201943_s_at	CPD	carboxypeptidase D	-1.30	1.18E-02

...continuous on the next page

Probe set ID	Gene symbol	Gene name	logFc	adj. p-value
212198_s_at	TM9SF4	transmembrane 9 superfamily protein member 4	-1.27	1.18E-02
226582_at	LOC400043	hypothetical LOC400043	-1.27	1.36E-02
212196_at	IL6ST	interleukin 6 signal transducer (gp130, oncostatin M receptor)	-1.27	1.56E-02
218210_at	FN3KRP	fructosamine 3 kinase related protein	-1.26	1.39E-02
202270_at	GBP1	guanylate binding protein 1, interferon-inducible	-1.21	1.85E-02
201312_s_at	SH3BGRL	SH3 domain binding glutamic acid-rich protein like	-1.21	1.77E-02
208711_s_at	CCND1	cyclin D1	-1.21	3.35E-02
200640_at	YWHAZ	tyrosine 3-monooxygenase/tryptophan 5-monooxygenase activation protein, zeta polypeptide	-1.20	1.18E-02
200638_s_at	YWHAZ	tyrosine 3-monooxygenase/tryptophan 5-monooxygenase activation protein, zeta polypeptide	-1.20	1.18E-02
200631_s_at	SET	SET nuclear oncogene	-1.20	1.18E-02
212228_s_at	COQ9	coenzyme Q9 homolog (S. cerevisiae)	-1.19	1.77E-02
217970_s_at	CNOT6	CCR4-NOT transcription complex, subunit 6	-1.19	8.22E-03
208131_s_at	PTGIS	prostaglandin I2 (prostacyclin) synthase	-1.18	2.73E-02
225867_at	VASN	vasorin	-1.18	1.20E-02
213047_x_at	SET	SET nuclear oncogene	-1.18	1.18E-02
225662_at	ZAK	sterile alpha motif and leucine zipper containing kinase AZK	-1.18	1.36E-02
1553960_at	SNX21	sorting nexin family member 21	-1.17	1.18E-02
200878_at	EPAS1	endothelial PAS domain protein 1	-1.17	1.80E-02
225944_at	NLN	neurolysin (metallopeptidase M3 family)	-1.17	1.32E-02
203323_at	CAV2	caveolin 2	-1.17	1.18E-02
226671_at	LAMP2	lysosomal-associated membrane protein 2	-1.17	1.39E-02
218953_s_at	PCYOX1L	prenylcysteine oxidase 1 like	-1.16	1.44E-02
208712_at	CCND1	cyclin D1	-1.16	2.32E-02
231577_s_at	GBP1	guanylate binding protein 1, interferon-inducible	-1.16	1.85E-02

...continuous on the next page

Probe set ID	Gene symbol	Gene name	logFc	adj. p-value
206969_at	KRT34	keratin 34	-1.15	2.83E-02
228618_at	PEAR1	platelet endothelial aggregation receptor 1	-1.15	4.58E-02
201941_at	CPD	carboxypeptidase D	-1.15	1.18E-02
218698_at	APIP	APAF1 interacting protein	-1.15	1.18E-02
200639_s_at	YWHAZ	tyrosine 3-monooxygenase/tryptophan 5-monooxygenase activation protein, zeta polypeptide	-1.14	1.22E-02
52164_at	C11orf24	chromosome 11 open reading frame 24	-1.14	1.77E-02
200743_s_at	TPP1	tripeptidyl peptidase I	-1.14	1.18E-02
232130_at	NA	NA	-1.14	1.62E-02
222659_at	IPO11	importin 11	-1.14	1.34E-02
238613_at	ZAK	sterile alpha motif and leucine zipper containing kinase AZK	-1.14	1.39E-02
203360_s_at	MYCBP	c-myc binding protein	-1.13	8.22E-03
200742_s_at	TPP1	tripeptidyl peptidase I	-1.13	1.57E-02
225716_at	NA	NA	-1.12	1.82E-02
209884_s_at	SLC4A7	solute carrier family 4, sodium bicarbonate cotransporter, member 7	-1.12	1.85E-02
212813_at	JAM3	junctional adhesion molecule 3	-1.11	1.18E-02
214110_s_at	NA	NA	-1.11	1.68E-02
225049_at	BLOC1S2	biogenesis of lysosomal organelles complex-1, subunit 2	-1.10	8.39E-03
231808_at	LOC729082	hypothetical LOC729082	-1.10	1.18E-02
219563_at	C14orf139	chromosome 14 open reading frame 139	-1.10	1.79E-02
226608_at	C16orf87	chromosome 16 open reading frame 87	-1.10	1.18E-02
210276_s_at	NA	NA	-1.10	1.45E-02
209800_at	KRT16	keratin 16	-1.10	2.33E-02
209073_s_at	NUMB	numb homolog (Drosophila)	-1.08	1.56E-02
217877_s_at	GPBP1L1	GC-rich promoter binding protein 1-like 1	-1.08	1.18E-02
202269_x_at	GBP1	guanylate binding protein 1, interferon-inducible	-1.08	1.85E-02
200600_at	MSN	moesin	-1.07	1.80E-02
227961_at	CTSB	cathepsin B	-1.07	1.80E-02

...continuous on the next page

Probe set ID	Gene symbol	Gene name	logFc	adj. p-value
212992_at	AHNAK2	AHNAK nucleoprotein 2	-1.07	2.42E-02
218299_at	C11orf24	chromosome 11 open reading frame 24	-1.07	1.77E-02
233571_x_at	PPDPF	pancreatic progenitor cell differentiation and proliferation factor homolog (zebrafish)	-1.07	1.80E-02
227095_at	LEPROT	leptin receptor overlapping transcript	-1.07	1.08E-02
201656_at	ITGA6	integrin, alpha 6	-1.06	6.16E-02
211979_at	GPR107	G protein-coupled receptor 107	-1.06	1.18E-02
224564_s_at	RTN3	reticulon 3	-1.06	1.34E-02
1552263_at	MAPK1	mitogen-activated protein kinase 1	-1.06	1.18E-02
221556_at	CDC14B	CDC14 cell division cycle 14 homolog B (S. cerevisiae)	-1.06	1.34E-02
225002_s_at	SUMF2	sulfatase modifying factor 2	-1.06	1.77E-02
209609_s_at	MRPL9	mitochondrial ribosomal protein L9	-1.05	1.80E-02
213405_at	RAB22A	RAB22A, member RAS oncogene family	-1.05	1.18E-02
207545_s_at	NUMB	numb homolog (Drosophila)	-1.04	1.49E-02
208753_s_at	NAP1L1	nucleosome assembly protein 1-like 1	-1.04	1.18E-02
214848_at	NA	NA	-1.04	1.18E-02
221571_at	TRAF3	TNF receptor-associated factor 3	-1.04	1.18E-02
227951_s_at	FAM98C	family with sequence similarity 98, member C	-1.04	1.18E-02
222476_at	CNOT6	CCR4-NOT transcription complex, subunit 6	-1.04	1.18E-02
225308_s_at	TANC1	tetratricopeptide repeat, ankyrin repeat and coiled-coil containing 1	-1.04	1.62E-02
200617_at	MLEC	malectin	-1.03	1.18E-02
226625_at	TGFBR3	transforming growth factor, beta receptor III	-1.03	2.45E-02
202013_s_at	EXT2	exostosin 2	-1.03	1.82E-02
201940_at	CPD	carboxypeptidase D	-1.03	1.22E-02
224684_at	SNX12	sorting nexin 12	-1.03	1.85E-02
1559965_at	LOC100192378	hypothetical LOC100192378	-1.03	3.38E-02
202349_at	TOR1A	torsin family 1, member A (torsin A)	-1.02	1.44E-02
208623_s_at	EZR	ezrin	-1.02	2.82E-02

...continuous on the next page

Probe set ID	Gene symbol	Gene name	logFc	adj. p-value
210830_s_at	PON2	paraoxonase 2	-1.02	2.03E-02
208622_s_at	EZR	ezrin	-1.02	2.26E-02
207181_s_at	CASP7	caspase 7, apoptosis-related cysteine peptidase	-1.02	1.18E-02
227994_x_at	PPDPF	pancreatic progenitor cell differentiation and proliferation factor homolog (zebrafish)	-1.02	1.80E-02
200737_at	PGK1	phosphoglycerate kinase 1	-1.02	2.17E-02
213852_at	NA	NA	-1.01	1.57E-02
227110_at	HNRNPC	heterogeneous nuclear ribonucleoprotein C (C1/C2)	-1.01	2.77E-02
201516_at	SRM	spermidine synthase	-1.01	3.96E-02
219032_x_at	OPN3	opsin 3	-1.01	1.18E-02
216210_x_at	TRIOBP	TRIO and F-actin binding protein	-1.01	1.45E-02
211594_s_at	MRPL9	mitochondrial ribosomal protein L9	-1.01	2.01E-02
219258_at	TIPIN	TIMELESS interacting protein	-1.00	1.85E-02
218010_x_at	PPDPF	pancreatic progenitor cell differentiation and proliferation factor homolog (zebrafish)	-1.00	1.80E-02
203040_s_at	HMBS	hydroxymethylbilane synthase	-1.00	3.73E-02
226793_at	NCRNA00294	non-protein coding RNA 294	-1.00	1.45E-02
226660_at	RPS6KB1	ribosomal protein S6 kinase, 70kDa, polypeptide 1	-0.99	1.18E-02
219549_s_at	RTN3	reticulon 3	-0.99	1.61E-02
208621_s_at	EZR	ezrin	-0.99	6.18E-02
232235_at	DSEL	dermatan sulfate epimerase-like	-0.98	3.60E-02
225447_at	GPD2	glycerol-3-phosphate dehydrogenase 2 (mitochondrial)	-0.98	1.39E-02
201850_at	CAPG	capping protein (actin filament), gelsolin-like	-0.98	2.01E-02
201188_s_at	ITPR3	inositol 1,4,5-triphosphate receptor, type 3	-0.98	1.18E-02
210759_s_at	PSMA1	proteasome (prosome, macropain) subunit, alpha type, 1	-0.98	1.45E-02
201876_at	PON2	paraoxonase 2	-0.97	1.90E-02

...continuous on the next page

Probe set ID	Gene symbol	Gene name	logFc	adj. p-value
201142_at	EIF2S1	eukaryotic translation initiation factor 2, subunit 1 alpha, 35kDa	-0.97	1.18E-02
202068_s_at	LDLR	low density lipoprotein receptor	-0.97	1.62E-02
215780_s_at	NA	NA	-0.97	1.79E-02
227407_at	TAPT1	transmembrane anterior posterior transformation 1	-0.97	1.18E-02
238164_at	USP6NL	USP6 N-terminal like	-0.97	1.44E-02
205081_at	CRIP1	cysteine-rich protein 1 (intestinal)	-0.96	2.67E-02
211977_at	GPR107	G protein-coupled receptor 107	-0.96	1.18E-02
213275_x_at	CTSB	cathepsin B	-0.96	1.85E-02
219079_at	CYB5R4	cytochrome b5 reductase 4	-0.96	2.00E-02
227068_at	PGK1	phosphoglycerate kinase 1	-0.96	1.87E-02
242366_at	NA	NA	-0.95	1.18E-02
226041_at	NAPEPLD	N-acyl phosphatidylethanolamine phospholipase D	-0.95	1.18E-02
201311_s_at	SH3BGRL	SH3 domain binding glutamic acid-rich protein like	-0.95	1.62E-02
218628_at	CCDC53	coiled-coil domain containing 53	-0.95	1.62E-02
208908_s_at	CAST	calpastatin	-0.95	1.18E-02
202795_x_at	TRIOBP	TRIO and F-actin binding protein	-0.95	1.79E-02
212355_at	KHNYN	KH and NYN domain containing	-0.95	1.22E-02
225553_at	NA	NA	-0.94	1.80E-02
221024_s_at	SLC2A10	solute carrier family 2 (facilitated glucose transporter), member 10	-0.94	1.39E-02
222231_s_at	LRRC59	leucine rich repeat containing 59	-0.94	1.85E-02
212838_at	DNMBP	dynamin binding protein	-0.94	5.48E-02
226993_at	NA	NA	-0.94	1.80E-02
202169_s_at	AASDHPPT	aminoadipate-semialdehyde dehydrogenase-phosphopantetheinyl transferase	-0.93	1.18E-02
219799_s_at	DHRS9	dehydrogenase/reductase (SDR family) member 9	-0.93	3.38E-02
205122_at	TMEFF1	transmembrane protein with EGF-like and two follistatin-like domains 1	-0.93	1.18E-02

...continuous on the next page

Probe set ID	Gene symbol	Gene name	logFc	adj. p-value
1556186_s_at	KIAA0090	KIAA0090	-0.92	1.18E-02
204731_at	TGFBR3	transforming growth factor, beta receptor III	-0.92	3.71E-02
207467_x_at	CAST	calpastatin	-0.92	1.31E-02
223361_at	C6orf115	chromosome 6 open reading frame 115	-0.92	1.18E-02
209234_at	KIF1B	kinesin family member 1B	-0.92	1.22E-02
200606_at	DSP	desmoplakin	-0.92	1.80E-02
212446_s_at	LASS6	LAG1 homolog, ceramide synthase 6	-0.92	2.02E-02
202551_s_at	CRIM1	cysteine rich transmembrane BMP regulator 1 (chordin-like)	-0.92	1.39E-02
206857_s_at	FKBP1B	FK506 binding protein 1B, 12.6 kDa	-0.91	1.44E-02
230146_s_at	NCS1	neuronal calcium sensor 1	-0.91	4.34E-02
200636_s_at	PTPRF	protein tyrosine phosphatase, receptor type, F	-0.91	1.80E-02
201676_x_at	PSMA1	proteasome (prosome, macropain) subunit, alpha type, 1	-0.91	1.66E-02
217356_s_at	PGK1	phosphoglycerate kinase 1	-0.91	2.10E-02
200670_at	XBP1	X-box binding protein 1	-0.90	1.34E-02
203180_at	ALDH1A3	aldehyde dehydrogenase 1 family, member A3	-0.90	2.06E-02
217911_s_at	BAG3	BCL2-associated athanogene 3	-0.90	1.18E-02
203840_at	BLZF1	basic leucine zipper nuclear factor 1	-0.89	1.34E-02
208898_at	ATP6V1D	ATPase, H+ transporting, lysosomal 34kDa, V1 subunit D	-0.89	1.44E-02
40472_at	LPCAT4	lysophosphatidylcholine acyltransferase 4	-0.89	2.34E-02
225223_at	SMAD5	SMAD family member 5	-0.89	1.18E-02
231175_at	BEND6	BEN domain containing 6	-0.89	1.85E-02
229873_at	KCTD21	potassium channel tetramerisation domain containing 21	-0.88	1.68E-02
211746_x_at	PSMA1	proteasome (prosome, macropain) subunit, alpha type, 1	-0.88	1.56E-02
205436_s_at	H2AFX	H2A histone family, member X	-0.88	2.46E-02
204337_at	RGS4	regulator of G-protein signaling 4	-0.88	5.29E-02

...continuous on the next page

Probe set ID	Gene symbol	Gene name	logFc	adj. p-value
228802_at	RBPMS2	RNA binding protein with multiple splicing 2	-0.88	4.30E-02
216899_s_at	SKAP2	src kinase associated phosphoprotein 2	-0.88	1.18E-02
202796_at	SYNPO	synaptopodin	-0.88	1.77E-02
203537_at	PRPSAP2	phosphoribosyl pyrophosphate synthetase-associated protein 2	-0.87	1.18E-02
213274_s_at	CTSB	cathepsin B	-0.87	2.51E-02
1560208_at	NA	NA	-0.87	5.26E-02
217367_s_at	ZHX3	zinc fingers and homeoboxes 3	-0.87	1.77E-02
202444_s_at	ERLIN1	ER lipid raft associated 1	-0.86	1.85E-02
210337_s_at	ACLY	ATP citrate lyase	-0.86	3.24E-02
236483_at	NA	NA	-0.86	3.20E-02
203245_s_at	NCRNA00094	non-protein coding RNA 94	-0.86	1.82E-02
201887_at	IL13RA1	interleukin 13 receptor, alpha 1	-0.86	1.56E-02
227272_at	C15orf52	chromosome 15 open reading frame 52	-0.86	1.77E-02
225219_at	SMAD5	SMAD family member 5	-0.86	1.18E-02
235747_at	SLC25A16	solute carrier family 25 (mitochondrial carrier; Graves disease autoantigen), member 16	-0.86	1.65E-02
224414_s_at	CARD6	caspase recruitment domain family, member 6	-0.86	4.84E-02
203480_s_at	OTUD4	OTU domain containing 4	-0.85	1.18E-02
55081_at	MICALL1	MICAL-like 1	-0.85	1.85E-02
229501_s_at	USP8	ubiquitin specific peptidase 8	-0.85	1.44E-02
212313_at	CHMP7	CHMP family, member 7	-0.85	1.85E-02
201880_at	ARIH1	ariadne homolog, ubiquitin-conjugating enzyme E2 binding protein, 1 (Drosophila)	-0.85	1.57E-02
213075_at	OLFML2A	olfactomedin-like 2A	-0.85	6.04E-02
202131_s_at	RIOK3	RIO kinase 3 (yeast)	-0.85	1.53E-02
214934_at	ATP9B	ATPase, class II, type 9B	-0.85	1.34E-02
209684_at	RIN2	Ras and Rab interactor 2	-0.85	1.62E-02
219022_at	C12orf43	chromosome 12 open reading frame 43	-0.85	1.99E-02
226395_at	HOOK3	hook homolog 3 (Drosophila)	-0.85	1.45E-02

...continuous on the next page

Probe set ID	Gene symbol	Gene name	logFc	adj. p-value
212586_at	CAST	calpastatin	-0.84	2.97E-02
231810_at	BRI3BP	BRI3 binding protein	-0.84	2.45E-02
213392_at	IQCK	IQ motif containing K	-0.84	2.47E-02
227935_s_at	PCGF5	polycomb group ring finger 5	-0.84	1.99E-02
218592_s_at	CECR5	cat eye syndrome chromosome region, candidate 5	-0.84	1.99E-02
211026_s_at	MGLL	monoglyceride lipase	-0.84	1.39E-02
217383_at	PGK1	phosphoglycerate kinase 1	-0.84	4.32E-02
227804_at	TLCD1	TLC domain containing 1	-0.84	1.85E-02
201536_at	DUSP3	dual specificity phosphatase 3	-0.84	1.49E-02
226485_at	VSIG10	V-set and immunoglobulin domain containing 10	-0.84	1.49E-02
203074_at	NA	NA	-0.84	4.86E-02
219192_at	UBAP2	ubiquitin associated protein 2	-0.83	2.13E-02
202130_at	RIOK3	RIO kinase 3 (yeast)	-0.83	1.81E-02
202012_s_at	EXT2	exostosin 2	-0.83	1.91E-02
41037_at	TEAD4	TEA domain family member 4	-0.83	1.85E-02
209019_s_at	PINK1	PTEN induced putative kinase 1	-0.83	1.76E-02
221988_at	C19orf42	chromosome 19 open reading frame 42	-0.83	2.16E-02
59999_at	HIF1AN	hypoxia inducible factor 1, alpha subunit inhibitor	-0.83	1.80E-02
209147_s_at	PPAP2A	phosphatidic acid phosphatase type 2A	-0.83	1.88E-02
205078_at	PIGF	phosphatidylinositol glycan anchor biosynthesis, class F	-0.83	1.76E-02
213030_s_at	PLXNA2	plexin A2	-0.83	2.87E-02
201074_at	SMARCC1	SWI/SNF related, matrix associated, actin dependent regulator of chromatin, subfamily c, member 1	-0.83	1.44E-02
235141_at	MARVELD2	MARVEL domain containing 2	-0.83	1.81E-02
218684_at	LRRC8D	leucine rich repeat containing 8 family, member D	-0.83	2.10E-02
229173_at	KIAA1715	KIAA1715	-0.83	2.01E-02
213078_x_at	LPCAT4	lysophosphatidylcholine acyltransferase 4	-0.83	1.96E-02
212573_at	ENDOD1	endonuclease domain containing 1	-0.83	1.76E-02

...continuous on the next page

Probe set ID	Gene symbol	Gene name	logFc	adj. p-value
213118_at	UHRF1BP1L	UHRF1 binding protein 1-like	-0.83	1.18E-02
222452_s_at	GPBP1L1	GC-rich promoter binding protein 1-like 1	-0.83	1.18E-02
235463_s_at	LASS6	LAG1 homolog, ceramide synthase 6	-0.83	1.77E-02
223125_s_at	C1orf21	chromosome 1 open reading frame 21	-0.82	2.08E-02
230071_at	SEPT11	septin 11	-0.82	5.29E-02
225639_at	SKAP2	src kinase associated phosphoprotein 2	-0.82	1.39E-02
218266_s_at	NCS1	neuronal calcium sensor 1	-0.82	2.93E-02
203743_s_at	TDG	thymine-DNA glycosylase	-0.82	1.39E-02
226504_at	FAM109B	family with sequence similarity 109, member B	-0.82	1.65E-02
210231_x_at	SET	SET nuclear oncogene	-0.82	1.68E-02
220643_s_at	FAIM	Fas apoptotic inhibitory molecule	-0.82	2.91E-02
201143_s_at	EIF2S1	eukaryotic translation initiation factor 2, subunit 1 alpha, 35kDa	-0.81	1.56E-02
226160_at	H6PD	hexose-6-phosphate dehydrogenase (glucose 1-dehydrogenase)	-0.81	1.85E-02
209691_s_at	DOK4	docking protein 4	-0.81	1.38E-02
217761_at	ADI1	acireductone dioxygenase 1	-0.81	5.31E-02
204108_at	NFYA	nuclear transcription factor Y, alpha	-0.81	1.45E-02
210106_at	RDH5	retinol dehydrogenase 5 (11-cis/9-cis)	-0.81	2.13E-02
228783_at	BVES	blood vessel epicardial substance	-0.81	1.22E-02
228933_at	NHS	Nance-Horan syndrome (congenital cataracts and dental anomalies)	-0.81	2.05E-02
217844_at	CTDSP1	CTD (carboxy-terminal domain, RNA polymerase II, polypeptide A) small phosphatase 1	-0.81	1.39E-02
208783_s_at	CD46	CD46 molecule, complement regulatory protein	-0.80	1.49E-02
226748_at	LYSMD2	LysM, putative peptidoglycan-binding, domain containing 2	-0.80	4.85E-02
225102_at	MGLL	monoglyceride lipase	-0.80	1.49E-02
221689_s_at	PIGP	phosphatidylinositol glycan anchor biosynthesis, class P	-0.80	5.35E-02
206949_s_at	RUSC1	RUN and SH3 domain containing 1	-0.80	2.76E-02

...continuous on the next page

Probe set ID	Gene symbol	Gene name	logFc	adj. p-value
203605_at	SRP54	signal recognition particle 54kDa	-0.79	1.45E-02
222388_s_at	VPS35	vacuolar protein sorting 35 homolog (S. cerevisiae)	-0.79	1.36E-02
228026_at	SIKE1	suppressor of IKBKE 1	-0.79	1.45E-02
202647_s_at	NRAS	neuroblastoma RAS viral (v-ras) oncogene homolog	-0.79	1.39E-02
204362_at	SKAP2	src kinase associated phosphoprotein 2	-0.79	1.18E-02
204401_at	KCNN4	potassium intermediate/small conductance calcium-activated channel, subfamily N, member 4	-0.79	4.61E-02
225752_at	NIPA1	non imprinted in Prader-Willi/Angelman syndrome 1	-0.78	1.92E-02
212442_s_at	LASS6	LAG1 homolog, ceramide synthase 6	-0.78	1.91E-02
202420_s_at	DHX9	DEAH (Asp-Glu-Ala-His) box polypeptide 9	-0.78	3.45E-02
223495_at	CCDC8	coiled-coil domain containing 8	-0.78	2.13E-02
234464_s_at	EME1	essential meiotic endonuclease 1 homolog 1 (S. pombe)	-0.78	1.85E-02
224711_at	YY1	YY1 transcription factor	-0.78	1.82E-02
204906_at	RPS6KA2	ribosomal protein S6 kinase, 90kDa, polypeptide 2	-0.78	2.10E-02
218126_at	FAM82A2	family with sequence similarity 82, member A2	-0.78	1.39E-02
201581_at	TMX4	thioredoxin-related transmembrane protein 4	-0.78	2.18E-02
224989_at	NA	NA	-0.78	1.39E-02
203851_at	IGFBP6	insulin-like growth factor binding protein 6	-0.78	2.10E-02
218001_at	MRPS2	mitochondrial ribosomal protein S2	-0.78	1.90E-02
222400_s_at	ADI1	acireductone dioxygenase 1	-0.78	4.70E-02
32088_at	BLZF1	basic leucine zipper nuclear factor 1	-0.77	1.45E-02
203592_s_at	FSTL3	follistatin-like 3 (secreted glycoprotein)	-0.77	1.53E-02
231921_at	DCAF17	DDB1 and CUL4 associated factor 17	-0.77	1.45E-02
225880_at	NA	NA	-0.77	1.76E-02

...continuous on the next page

Probe set ID	Gene symbol	Gene name	logFc	adj. p-value
218525_s_at	HIF1AN	hypoxia inducible factor 1, alpha subunit inhibitor	-0.77	1.74E-02
221756_at	PIK3IP1	phosphoinositide-3-kinase interacting protein 1	-0.77	1.86E-02
218911_at	YEATS4	YEATS domain containing 4	-0.77	1.56E-02
202709_at	FMOD	fibromodulin	-0.77	2.91E-02
222416_at	ALDH18A1	aldehyde dehydrogenase 18 family, member A1	-0.76	1.49E-02
228496_s_at	CRIM1	cysteine rich transmembrane BMP regulator 1 (chordin-like)	-0.76	2.86E-02
227094_at	DHTKD1	dehydrogenase E1 and transketolase domain containing 1	-0.76	2.26E-02
200630_x_at	SET	SET nuclear oncogene	-0.76	1.68E-02
223342_at	RRM2B	ribonucleotide reductase M2 B (TP53 inducible)	-0.76	1.62E-02
201135_at	ECHS1	enoyl CoA hydratase, short chain, 1, mitochondrial	-0.76	2.86E-02
216958_s_at	IVD	isovaleryl-CoA dehydrogenase	-0.76	1.80E-02
225525_at	KIAA1671	KIAA1671	-0.76	1.44E-02
223734_at	C4orf49	chromosome 4 open reading frame 49	-0.76	3.32E-02
228479_at	SOAT1	sterol O-acyltransferase 1	-0.76	1.85E-02
233540_s_at	CDK5RAP2	CDK5 regulatory subunit associated protein 2	-0.76	4.32E-02
201075_s_at	SMARCC1	SWI/SNF related, matrix associated, actin dependent regulator of chromatin, subfamily c, member 1	-0.76	1.85E-02
201990_s_at	CREBL2	cAMP responsive element binding protein-like 2	-0.76	2.18E-02
224578_at	RCC2	regulator of chromosome condensation 2	-0.76	1.44E-02
225776_at	RBMS2	RNA binding motif, single stranded interacting protein 2	-0.75	1.68E-02
201864_at	GDI1	GDP dissociation inhibitor 1	-0.75	1.45E-02
202441_at	ERLIN1	ER lipid raft associated 1	-0.75	1.56E-02
201195_s_at	SLC7A5	solute carrier family 7 (cationic amino acid transporter, y+ system), member 5	-0.75	1.85E-02

...continuous on the next page

Probe set ID	Gene symbol	Gene name	logFc	adj. p-value
218606_at	ZDHHC7	zinc finger, DHHC-type containing 7	-0.75	1.56E-02
238587_at	UBASH3B	ubiquitin associated and SH3 domain containing B	-0.75	4.36E-02
242317_at	HIGD1A	HIG1 hypoxia inducible domain family, member 1A	-0.75	1.85E-02
203397_s_at	GALNT3	UDP-N-acetyl-alpha-D-galactosamine:polypeptide N-acetylgalactosaminyltransferase 3 (GalNAc-T3)	-0.75	3.18E-02
227713_at	KATNAL1	katanin p60 subunit A-like 1	-0.75	2.01E-02
214736_s_at	ADD1	adducin 1 (alpha)	-0.75	1.85E-02
218247_s_at	MEX3C	mex-3 homolog C (C. elegans)	-0.74	1.39E-02
241344_at	NA	NA	-0.74	1.62E-02
202552_s_at	CRIM1	cysteine rich transmembrane BMP regulator 1 (chordin-like)	-0.74	1.68E-02
202663_at	WIPF1	WAS/WASL interacting protein family, member 1	-0.74	1.76E-02
204761_at	USP6NL	USP6 N-terminal like	-0.74	1.39E-02
202892_at	CDC23	cell division cycle 23 homolog (S. cerevisiae)	-0.74	1.39E-02
208914_at	GGA2	golgi-associated, gamma adaptin ear containing, ARF binding protein 2	-0.74	1.45E-02
231927_at	ATF6	activating transcription factor 6	-0.73	1.79E-02
208899_x_at	ATP6V1D	ATPase, H+ transporting, lysosomal 34kDa, V1 subunit D	-0.73	1.80E-02
208483_x_at	KRT33A	keratin 33A	-0.73	5.82E-02
200738_s_at	PGK1	phosphoglycerate kinase 1	-0.73	3.45E-02
225574_at	RWDD4	RWD domain containing 4	-0.73	1.85E-02
224461_s_at	AIFM2	apoptosis-inducing factor, mitochondrion-associated, 2	-0.73	1.44E-02
209717_at	EVI5	ecotropic viral integration site 5	-0.73	1.56E-02
214198_s_at	DGCR2	DiGeorge syndrome critical region gene 2	-0.72	1.61E-02
1554414_a_at	OSGIN2	oxidative stress induced growth inhibitor family member 2	-0.72	2.31E-02
208030_s_at	ADD1	adducin 1 (alpha)	-0.72	1.81E-02

...continuous on the next page

Probe set ID	Gene symbol	Gene name	logFc	adj. p-value
222745_s_at	C15orf29	chromosome 15 open reading frame 29	-0.72	1.39E-02
220935_s_at	CDK5RAP2	CDK5 regulatory subunit associated protein 2	-0.72	4.93E-02
1554627_a_at	ASCC1	activating signal cointegrator 1 complex subunit 1	-0.72	1.49E-02
201515_s_at	TSN	translin	-0.72	1.58E-02
209476_at	TMX1	thioredoxin-related transmembrane protein 1	-0.71	1.56E-02
210230_at	NA	NA	-0.71	1.81E-02
217954_s_at	PHF3	PHD finger protein 3	-0.71	1.45E-02
212744_at	BBS4	Bardet-Biedl syndrome 4	-0.70	1.71E-02
203339_at	SLC25A12	solute carrier family 25 (mitochondrial carrier, Aralar), member 12	-0.70	6.27E-02
213048_s_at	NA	NA	-0.70	1.44E-02
212394_at	KIAA0090	KIAA0090	-0.70	1.80E-02
227295_at	IKBIP	IKBKB interacting protein	-0.70	1.74E-02
204361_s_at	SKAP2	src kinase associated phosphoprotein 2	-0.70	1.53E-02
204400_at	EFS	embryonal Fyn-associated substrate	-0.70	1.85E-02
203028_s_at	CYBA	cytochrome b-245, alpha polypeptide	-0.70	2.22E-02
212333_at	FAM98A	family with sequence similarity 98, member A	-0.70	1.85E-02
227052_at	NA	NA	-0.70	1.82E-02
210609_s_at	TP53I3	tumor protein p53 inducible protein 3	-0.70	5.65E-02
201988_s_at	CREBL2	cAMP responsive element binding protein-like 2	-0.70	1.82E-02
219384_s_at	ADAT1	adenosine deaminase, tRNA-specific 1	-0.69	1.45E-02
212922_s_at	SMYD2	SET and MYND domain containing 2	-0.69	5.55E-02
200635_s_at	PTPRF	protein tyrosine phosphatase, receptor type, F	-0.69	2.46E-02
217791_s_at	ALDH18A1	aldehyde dehydrogenase 18 family, member A1	-0.69	1.87E-02
228437_at	CNIH4	cornichon homolog 4 (Drosophila)	-0.68	1.59E-02
218823_s_at	KCTD9	potassium channel tetramerisation domain containing 9	-0.68	1.80E-02

...continuous on the next page

Probe set ID	Gene symbol	Gene name	logFc	adj. p-value
231901_at	C19orf52	chromosome 19 open reading frame 52	-0.68	1.85E-02
1553961_s_at	SNX21	sorting nexin family member 21	-0.68	1.77E-02
223692_at	NMNAT1	nicotinamide nucleotide adenylyltransferase 1	-0.68	1.62E-02
221752_at	SSH1	slingshot homolog 1 (Drosophila)	-0.68	2.05E-02
200616_s_at	MLEC	malectin	-0.68	1.62E-02
224777_s_at	PAFAH1B2	platelet-activating factor acetylhydrolase 1b, catalytic subunit 2 (30kDa)	-0.68	1.56E-02
228139_at	RIPK3	receptor-interacting serine-threonine kinase 3	-0.68	2.46E-02
218679_s_at	VPS28	vacuolar protein sorting 28 homolog (S. cerevisiae)	-0.67	3.03E-02
211986_at	AHNAK	AHNAK nucleoprotein	-0.67	2.82E-02
202685_s_at	AXL	AXL receptor tyrosine kinase	-0.67	1.85E-02
212589_at	RRAS2	related RAS viral (r-ras) oncogene homolog 2	-0.67	1.81E-02
203848_at	AKAP8	A kinase (PRKA) anchor protein 8	-0.67	1.85E-02
215537_x_at	DDAH2	dimethylarginine dimethylaminohydrolase 2	-0.67	2.01E-02
209514_s_at	RAB27A	RAB27A, member RAS oncogene family	-0.67	4.44E-02
200731_s_at	PTP4A1	protein tyrosine phosphatase type IVA, member 1	-0.67	1.62E-02
225053_at	CNOT7	CCR4-NOT transcription complex, subunit 7	-0.67	1.58E-02
229980_s_at	SNX5	sorting nexin 5	-0.67	1.77E-02
1569129_s_at	C3orf38	chromosome 3 open reading frame 38	-0.67	2.08E-02
203361_s_at	MYCBP	c-myc binding protein	-0.67	1.45E-02
221593_s_at	RPL31	ribosomal protein L31	-0.67	2.44E-02
226013_at	TRAK1	trafficking protein, kinesin binding 1	-0.66	4.25E-02
221667_s_at	HSPB8	heat shock 22kDa protein 8	-0.66	1.56E-02
223297_at	AMMECR1L	AMME chromosomal region gene 1-like	-0.66	1.65E-02
209018_s_at	PINK1	PTEN induced putative kinase 1	-0.66	1.77E-02
202996_at	POLD4	polymerase (DNA-directed), delta 4	-0.66	1.77E-02

...continuous on the next page

Probe set ID	Gene symbol	Gene name	logFc	adj. p-value
208626_s_at	VAT1	vesicle amine transport protein 1 homolog (T. californica)	-0.66	3.33E-02
208937_s_at	ID1	inhibitor of DNA binding 1, dominant negative helix-loop-helix protein	-0.66	6.64E-02
224443_at	C1orf97	chromosome 1 open reading frame 97	-0.66	1.85E-02
204943_at	ADAM12	ADAM metallopeptidase domain 12	-0.66	2.65E-02
203502_at	BPGM	2,3-bisphosphoglycerate mutase	-0.66	1.62E-02
212745_s_at	BBS4	Bardet-Biedl syndrome 4	-0.66	2.33E-02
202851_at	AAGAB	alpha- and gamma-adaptin binding protein	-0.66	1.74E-02
218047_at	OSBPL9	oxysterol binding protein-like 9	-0.66	3.55E-02
243166_at	SLC30A5	solute carrier family 30 (zinc transporter), member 5	-0.66	4.08E-02
200872_at	S100A10	S100 calcium binding protein A10	-0.66	1.84E-02
203175_at	RHOG	ras homolog gene family, member G (rho G)	-0.65	2.01E-02
1559433_at	LOC149773	hypothetical LOC149773	-0.65	4.13E-02
205077_s_at	PIGF	phosphatidylinositol glycan anchor biosynthesis, class F	-0.65	1.86E-02
233864_s_at	VPS35	vacuolar protein sorting 35 homolog (S. cerevisiae)	-0.65	1.67E-02
227156_at	CASK	calcium/calmodulin-dependent serine protein kinase (MAGUK family)	-0.65	3.38E-02
227826_s_at	NA	NA	-0.65	2.47E-02
231406_at	ORAI2	ORAI calcium release-activated calcium modulator 2	-0.65	2.20E-02
208913_at	GGA2	golgi-associated, gamma adaptin ear containing, ARF binding protein 2	-0.65	1.49E-02
210041_s_at	PGM3	phosphoglucomutase 3	-0.65	1.57E-02
222585_x_at	KRCC1	lysine-rich coiled-coil 1	-0.65	2.18E-02
223155_at	HDHD2	haloacid dehalogenase-like hydrolase domain containing 2	-0.65	1.85E-02
220199_s_at	AIDA	axin interactor, dorsalization associated	-0.65	1.62E-02
226363_at	ABCC5	ATP-binding cassette, sub-family C (CFTR/MRP), member 5	-0.64	1.61E-02

...continuous on the next page

Probe set ID	Gene symbol	Gene name	logFc	adj. p-value
1569631_at	NMNAT1	nicotinamide nucleotide adenylyltransferase 1	-0.64	1.85E-02
219215_s_at	SLC39A4	solute carrier family 39 (zinc transporter), member 4	-0.64	1.89E-02
218477_at	TMEM14A	transmembrane protein 14A	-0.64	4.14E-02
201061_s_at	STOM	stomatin	-0.64	1.80E-02
201275_at	FDPS	farnesyl diphosphate synthase	-0.64	2.38E-02
212098_at	NA	NA	-0.64	2.16E-02
221493_at	TSPYL1	TSPY-like 1	-0.64	1.85E-02
232080_at	HECW2	HECT, C2 and WW domain containing E3 ubiquitin protein ligase 2	-0.64	5.70E-02
223004_s_at	C3orf1	chromosome 3 open reading frame 1	-0.64	1.83E-02
222041_at	NA	NA	-0.64	2.09E-02
224773_at	NAV1	neuron navigator 1	-0.64	4.58E-02
222369_at	NAA40	N(alpha)-acetyltransferase 40, NatD catalytic subunit, homolog (S. cerevisiae)	-0.64	2.25E-02
227766_at	LIG4	ligase IV, DNA, ATP-dependent	-0.64	1.62E-02
225778_at	RBMS2	RNA binding motif, single stranded interacting protein 2	-0.64	1.80E-02
208979_at	NCOA6	nuclear receptor coactivator 6	-0.63	1.80E-02
212300_at	TXLNA	taxilin alpha	-0.63	1.82E-02
202119_s_at	CPNE3	copine III	-0.62	2.10E-02
209152_s_at	TCF3	transcription factor 3 (E2A immunoglobulin enhancer binding factors E12/E47)	-0.62	1.86E-02
225361_x_at	FAM122B	family with sequence similarity 122B	-0.62	2.45E-02
203090_at	SDF2	stromal cell-derived factor 2	-0.62	1.77E-02
226977_at	C5orf53	chromosome 5 open reading frame 53	-0.62	6.35E-02
212526_at	SPG20	spastic paraplegia 20 (Troyer syndrome)	-0.62	2.53E-02
204407_at	TTF2	transcription termination factor, RNA polymerase II	-0.62	2.18E-02
201060_x_at	STOM	stomatin	-0.62	1.79E-02
239891_x_at	RAB12	RAB12, member RAS oncogene family	-0.62	6.50E-02
208190_s_at	LSR	lipolysis stimulated lipoprotein receptor	-0.62	7.63E-02

...continuous on the next page

Probe set ID	Gene symbol	Gene name	logFc	adj. p-value
210951_x_at	RAB27A	RAB27A, member RAS oncogene family	-0.61	5.08E-02
217995_at	SQRDL	sulfide quinone reductase-like (yeast)	-0.61	4.90E-02
218180_s_at	EPS8L2	EPS8-like 2	-0.61	2.13E-02
203925_at	GCLM	glutamate-cysteine ligase, modifier subunit	-0.61	7.44E-02
204928_s_at	SLC10A3	solute carrier family 10 (sodium/bile acid cotransporter family), member 3	-0.61	1.82E-02
242800_at	NHS	Nance-Horan syndrome (congenital cataracts and dental anomalies)	-0.61	1.85E-02
204662_at	CP110	CP110 protein	-0.61	1.76E-02
52169_at	STRADA	STE20-related kinase adaptor alpha	-0.60	1.85E-02
201336_at	VAMP3	vesicle-associated membrane protein 3 (cellubrevin)	-0.60	1.75E-02
212637_s_at	WWP1	WW domain containing E3 ubiquitin protein ligase 1	-0.60	2.01E-02
208103_s_at	ANP32E	acidic (leucine-rich) nuclear phosphoprotein 32 family, member E	-0.60	1.79E-02
224718_at	YY1	YY1 transcription factor	-0.60	2.48E-02
213630_at	NACAD	NAC alpha domain containing	-0.59	1.89E-02
226834_at	NA	NA	-0.59	7.63E-02
212845_at	SAMD4A	sterile alpha motif domain containing 4A	-0.59	7.01E-02
205202_at	PCMT1	protein-L-isoaspartate (D-aspartate) O-methyltransferase	-0.59	2.01E-02
203068_at	KLHL21	kelch-like 21 (Drosophila)	-0.59	2.39E-02
226735_at	TAPT1	transmembrane anterior posterior transformation 1	-0.58	1.84E-02
203066_at	CHST15	carbohydrate (N-acetylgalactosamine 4-sulfate 6-O) sulfotransferase 15	-0.58	4.61E-02
219118_at	FKBP11	FK506 binding protein 11, 19 kDa	-0.58	1.86E-02
222243_s_at	TOB2	transducer of ERBB2, 2	-0.58	1.86E-02
222309_at	NA	NA	-0.58	6.65E-02
1555226_s_at	C1orf43	chromosome 1 open reading frame 43	-0.57	1.96E-02
212143_s_at	IGFBP3	insulin-like growth factor binding protein 3	-0.57	3.75E-02

...continuous on the next page

Probe set ID	Gene symbol	Gene name	logFc	adj. p-value
235037_at	TMEM41A	transmembrane protein 41A	-0.57	1.80E-02
226372_at	CHST11	carbohydrate (chondroitin 4) sulfotransferase 11	-0.57	7.81E-02
202140_s_at	CLK3	CDC-like kinase 3	-0.57	1.99E-02
204225_at	HDAC4	histone deacetylase 4	-0.57	3.45E-02
234973_at	SLC38A5	solute carrier family 38, member 5	-0.57	7.47E-02
217529_at	ORAI2	ORAI calcium release-activated calcium modulator 2	-0.56	2.08E-02
38158_at	ESPL1	extra spindle pole bodies homolog 1 (S. cerevisiae)	-0.56	3.21E-02
210970_s_at	IBTK	inhibitor of Bruton agammaglobulinemia tyrosine kinase	-0.56	1.81E-02
225868_at	TRIM47	tripartite motif containing 47	-0.56	2.77E-02
212800_at	STX6	syntaxin 6	-0.56	5.47E-02
226276_at	TMEM167A	transmembrane protein 167A	-0.56	1.82E-02
206042_x_at	NA	NA	-0.56	2.58E-02
201073_s_at	SMARCC1	SWI/SNF related, matrix associated, actin dependent regulator of chromatin, subfamily c, member 1	-0.56	5.06E-02
221554_at	STRADA	STE20-related kinase adaptor alpha	-0.56	1.85E-02
230930_at	LOC338620	hypothetical protein LOC338620	-0.55	7.27E-02
202318_s_at	SENP6	SUMO1/sentrin specific peptidase 6	-0.55	1.82E-02
200730_s_at	PTP4A1	protein tyrosine phosphatase type IVA, member 1	-0.55	4.93E-02
225604_s_at	GLIPR2	GLI pathogenesis-related 2	-0.54	4.19E-02
224629_at	LMAN1	lectin, mannose-binding, 1	-0.54	2.06E-02
226110_at	PTAR1	protein prenyltransferase alpha subunit repeat containing 1	-0.54	1.85E-02
212621_at	TMEM194A	transmembrane protein 194A	-0.53	2.48E-02
218248_at	FAM111A	family with sequence similarity 111, member A	-0.53	7.25E-02
209041_s_at	UBE2G2	ubiquitin-conjugating enzyme E2G 2 (UBC7 homolog, yeast)	-0.53	6.00E-02
229674_at	SERTAD4	SERTA domain containing 4	-0.52	1.97E-02

...continuous on the next page

Probe set ID	Gene symbol	Gene name	logFc	adj. p-value
219559_at	SLC17A9	solute carrier family 17, member 9	-0.52	2.02E-02
213836_s_at	WIPI1	WD repeat domain, phosphoinositide interacting 1	-0.48	6.15E-02
216484_x_at	HDGF	hepatoma-derived growth factor	-0.48	4.44E-02
212875_s_at	C2CD2	C2 calcium-dependent domain containing 2	-0.48	8.92E-02
219416_at	SCARA3	scavenger receptor class A, member 3	-0.48	8.87E-02
200838_at	CTSB	cathepsin B	-0.48	5.82E-02
215222_x_at	MACF1	microtubule-actin crosslinking factor 1	-0.44	6.82E-02
204823_at	NAV3	neuron navigator 3	-0.37	1.21E-01
238877_at	EYA4	eyes absent homolog 4 (Drosophila)	0.40	1.03E-01
224854_s_at	SLAIN2	SLAIN motif family, member 2	0.43	1.00E-01
224828_at	CPEB4	cytoplasmic polyadenylation element binding protein 4	0.45	8.31E-02
231200_at	LSM14B	LSM14B, SCD6 homolog B (S. cerevisiae)	0.46	7.62E-02
228471_at	ANKRD44	ankyrin repeat domain 44	0.46	9.33E-02
219842_at	ARL15	ADP-ribosylation factor-like 15	0.47	8.42E-02
215775_at	THBS1	thrombospondin 1	0.48	7.44E-02
205088_at	MAMLD1	mastermind-like domain containing 1	0.48	8.30E-02
204069_at	MEIS1	Meis homeobox 1	0.48	2.85E-02
210311_at	FGF5	fibroblast growth factor 5	0.49	2.49E-02
229091_s_at	CCNJ	cyclin J	0.50	7.43E-02
212310_at	MIA3	melanoma inhibitory activity family, member 3	0.50	2.92E-02
219882_at	TTLL7	tubulin tyrosine ligase-like family, member 7	0.50	7.62E-02
213001_at	ANGPTL2	angiopoietin-like 2	0.50	6.89E-02
202179_at	BLMH	bleomycin hydrolase	0.51	4.05E-02
213331_s_at	NEK1	NIMA (never in mitosis gene a)-related kinase 1	0.51	2.17E-02
212915_at	PDZRN3	PDZ domain containing ring finger 3	0.51	6.23E-02
222907_x_at	TMEM50B	transmembrane protein 50B	0.51	2.97E-02
205880_at	PRKD1	protein kinase D1	0.51	7.37E-02

...continuous on the next page

Probe set ID	Gene symbol	Gene name	logFc	adj. p-value
202062_s_at	SEL1L	sel-1 suppressor of lin-12-like (C. elegans)	0.52	7.79E-02
1556613_s_at	DPY19L4	dpy-19-like 4 (C. elegans)	0.52	1.99E-02
226609_at	DCBLD1	discoidin, CUB and LCCL domain containing 1	0.52	5.83E-02
221865_at	C9orf91	chromosome 9 open reading frame 91	0.52	2.28E-02
228370_at	SNRPN	small nuclear ribonucleoprotein polypeptide N	0.52	1.97E-02
222663_at	RIOK2	RIO kinase 2 (yeast)	0.52	3.46E-02
221998_s_at	VRK3	vaccinia related kinase 3	0.53	2.08E-02
219175_s_at	SLC41A3	solute carrier family 41, member 3	0.53	2.02E-02
219506_at	C1orf54	chromosome 1 open reading frame 54	0.53	7.13E-02
213313_at	RABGAP1	RAB GTPase activating protein 1	0.53	2.60E-02
205499_at	SRPX2	sushi-repeat containing protein, X-linked 2	0.54	8.03E-02
204160_s_at	ENPP4	ectonucleotide pyrophosphatase/phosphodiesterase 4 (putative)	0.54	7.88E-02
240402_at	KIRREL3	kin of IRRE like 3 (Drosophila)	0.54	2.91E-02
221575_at	SCLY	selenocysteine lyase	0.54	1.96E-02
228654_at	SPIN4	spindlin family, member 4	0.54	3.22E-02
224180_x_at	WDPCP	WD repeat containing planar cell polarity effector	0.54	1.86E-02
218613_at	PSD3	pleckstrin and Sec7 domain containing 3	0.54	7.44E-02
218317_x_at	NA	NA	0.54	2.33E-02
227080_at	ZNF697	zinc finger protein 697	0.54	7.95E-02
214334_x_at	DAZAP2	DAZ associated protein 2	0.55	1.82E-02
226366_at	SHPRH	SNF2 histone linker PHD RING helicase	0.55	2.01E-02
225176_at	NA	NA	0.55	1.92E-02
224931_at	SLC41A3	solute carrier family 41, member 3	0.55	1.82E-02
209905_at	NA	NA	0.55	2.49E-02
215233_at	JMJD6	jumonji domain containing 6	0.55	3.42E-02
218772_x_at	TMEM38B	transmembrane protein 38B	0.55	5.42E-02
228847_at	NA	NA	0.55	1.96E-02

...continuous on the next page

Probe set ID	Gene symbol	Gene name	logFc	adj. p-value
224659_at	SEPN1	selenoprotein N, 1	0.55	2.35E-02
217807_s_at	GLTSCR2	glioma tumor suppressor candidate region gene 2	0.55	1.85E-02
220761_s_at	TAOK3	TAO kinase 3	0.55	1.96E-02
212321_at	SGPL1	sphingosine-1-phosphate lyase 1	0.55	2.36E-02
228964_at	PRDM1	PR domain containing 1, with ZNF domain	0.55	3.67E-02
228029_at	NA	NA	0.56	1.82E-02
212382_at	TCF4	transcription factor 4	0.56	3.97E-02
236026_at	GPATCH2	G patch domain containing 2	0.56	2.82E-02
230129_at	PSTK	phosphoseryl-tRNA kinase	0.56	2.27E-02
220253_s_at	LRP12	low density lipoprotein receptor-related protein 12	0.56	4.05E-02
231929_at	IKZF2	IKAROS family zinc finger 2 (Helios)	0.56	4.82E-02
203124_s_at	SLC11A2	solute carrier family 11 (proton-coupled divalent metal ion transporters), member 2	0.56	4.83E-02
202975_s_at	RHOBTB3	Rho-related BTB domain containing 3	0.57	1.91E-02
214211_at	FTH1	ferritin, heavy polypeptide 1	0.57	3.45E-02
226855_at	PDP2	pyruvate dehyrogenase phosphatase catalytic subunit 2	0.57	2.50E-02
226773_at	NA	NA	0.57	6.78E-02
226641_at	ANKRD44	ankyrin repeat domain 44	0.57	4.98E-02
205355_at	ACADSB	acyl-CoA dehydrogenase, short/branched chain	0.57	2.19E-02
225537_at	TRAPPC6B	trafficking protein particle complex 6B	0.57	2.16E-02
207624_s_at	RPGR	retinitis pigmentosa GTPase regulator	0.58	1.92E-02
212793_at	DAAM2	dishevelled associated activator of morphogenesis 2	0.58	1.85E-02
208784_s_at	KLHDC3	kelch domain containing 3	0.58	1.82E-02
213286_at	ZFR	zinc finger RNA binding protein	0.58	1.92E-02
225089_at	USP40	ubiquitin specific peptidase 40	0.58	2.18E-02

...continuous on the next page

Probe set ID	Gene symbol	Gene name	logFc	adj. p-value
228501_at	GALNTL2	UDP-N-acetyl-alpha-D-galactosamine:polypeptide N-acetylgalactosaminyltransferase-like 2	0.58	5.05E-02
203217_s_at	ST3GAL5	ST3 beta-galactoside alpha-2,3-sialyltransferase 5	0.58	1.92E-02
213889_at	NA	NA	0.58	4.01E-02
209628_at	NXT2	nuclear transport factor 2-like export factor 2	0.58	1.80E-02
221541_at	CRISPLD2	cysteine-rich secretory protein LCCL domain containing 2	0.58	3.19E-02
204642_at	S1PR1	sphingosine-1-phosphate receptor 1	0.58	1.98E-02
228867_at	TATDN3	TatD DNase domain containing 3	0.59	2.02E-02
209291_at	ID4	inhibitor of DNA binding 4, dominant negative helix-loop-helix protein	0.59	6.68E-02
208883_at	UBR5	ubiquitin protein ligase E3 component n-recognin 5	0.59	1.76E-02
212607_at	AKT3	v-akt murine thymoma viral oncogene homolog 3 (protein kinase B, gamma)	0.59	6.35E-02
227361_at	HS3ST3B1	heparan sulfate (glucosamine) 3-O-sulfotransferase 3B1	0.59	3.02E-02
243042_at	FAM73A	family with sequence similarity 73, member A	0.59	2.35E-02
218313_s_at	GALNT7	UDP-N-acetyl-alpha-D-galactosamine:polypeptide N-acetylgalactosaminyltransferase 7 (GalNAc-T7)	0.59	1.99E-02
225112_at	ABI2	abl-interactor 2	0.59	1.80E-02
225646_at	CTSC	cathepsin C	0.60	5.05E-02
224801_at	NDFIP2	Nedd4 family interacting protein 2	0.60	2.23E-02
213891_s_at	TCF4	transcription factor 4	0.60	1.76E-02
204976_s_at	AMMECR1	Alport syndrome, mental retardation, midface hypoplasia and elliptocytosis chromosomal region gene 1	0.60	1.79E-02
211935_at	ARL6IP1	ADP-ribosylation factor-like 6 interacting protein 1	0.60	1.81E-02
211383_s_at	WDR37	WD repeat domain 37	0.60	1.97E-02

...continuous on the next page

Probe set ID	Gene symbol	Gene name	logFc	adj. p-value
216048_s_at	RHOBTB3	Rho-related BTB domain containing 3	0.61	1.85E-02
225084_at	EXOC5	exocyst complex component 5	0.61	2.18E-02
225927_at	MAP3K1	mitogen-activated protein kinase kinase kinase 1	0.61	2.92E-02
222447_at	METTL9	methyltransferase like 9	0.61	1.80E-02
230174_at	LYPLAL1	lysophospholipase-like 1	0.61	2.05E-02
229504_at	NA	NA	0.62	1.95E-02
212881_at	PIAS4	protein inhibitor of activated STAT, 4	0.62	1.85E-02
229817_at	ZNF608	zinc finger protein 608	0.62	2.45E-02
223089_at	VEZT	vezatin, adherens junctions transmembrane protein	0.62	2.84E-02
221193_s_at	ZCCHC10	zinc finger, CCHC domain containing 10	0.62	2.01E-02
239909_at	ADAMTSL1	ADAMTS-like 1	0.62	2.17E-02
220980_s_at	ADPGK	ADP-dependent glucokinase	0.62	1.74E-02
226886_at	GFPT1	glutamine–fructose-6-phosphate transaminase 1	0.62	4.86E-02
222726_s_at	EXOC5	exocyst complex component 5	0.62	2.16E-02
240592_at	LCORL	ligand dependent nuclear receptor corepressor-like	0.62	1.89E-02
1555154_a_at	QKI	quaking homolog, KH domain RNA binding (mouse)	0.62	2.45E-02
224832_at	DUSP16	dual specificity phosphatase 16	0.63	1.77E-02
223184_s_at	AGPAT3	1-acylglycerol-3-phosphate O-acyltransferase 3	0.63	1.86E-02
222134_at	DDO	D-aspartate oxidase	0.63	4.86E-02
213657_s_at	NA	NA	0.63	3.54E-02
226719_at	NA	NA	0.63	1.81E-02
203123_s_at	SLC11A2	solute carrier family 11 (proton-coupled divalent metal ion transporters), member 2	0.63	2.68E-02
219631_at	LRP12	low density lipoprotein receptor-related protein 12	0.63	1.88E-02
1552309_a_at	NEXN	nexilin (F actin binding protein)	0.63	3.88E-02
220974_x_at	SFXN3	sideroflexin 3	0.63	2.09E-02

...continuous on the next page

Probe set ID	Gene symbol	Gene name	logFc	adj. p-value
33148_at	ZFR	zinc finger RNA binding protein	0.63	1.65E-02
213017_at	ABHD3	abhydrolase domain containing 3	0.63	2.01E-02
240397_x_at	NA	NA	0.63	7.02E-02
235174_s_at	LOC100128822	hypothetical LOC100128822	0.64	5.90E-02
218195_at	C6orf211	chromosome 6 open reading frame 211	0.64	2.13E-02
209539_at	ARHGEF6	Rac/Cdc42 guanine nucleotide exchange factor (GEF) 6	0.64	1.62E-02
212834_at	DDX52	DEAD (Asp-Glu-Ala-Asp) box polypeptide 52	0.64	1.90E-02
203753_at	TCF4	transcription factor 4	0.64	2.01E-02
225494_at	NA	NA	0.64	1.85E-02
204114_at	NID2	nidogen 2 (osteonidogen)	0.64	4.93E-02
222753_s_at	SPCS3	signal peptidase complex subunit 3 homolog (S. cerevisiae)	0.64	4.93E-02
1552301_a_at	CORO6	coronin 6	0.64	1.77E-02
228214_at	SOX6	SRY (sex determining region Y)-box 6	0.64	1.68E-02
239596_at	SLC30A7	solute carrier family 30 (zinc transporter), member 7	0.64	2.45E-02
219649_at	ALG6	asparagine-linked glycosylation 6, alpha-1,3-glucosyltransferase homolog (S. cerevisiae)	0.65	1.82E-02
218177_at	CHMP1B	chromatin modifying protein 1B	0.65	4.69E-02
225606_at	BCL2L11	BCL2-like 11 (apoptosis facilitator)	0.65	5.42E-02
222146_s_at	TCF4	transcription factor 4	0.65	1.85E-02
228087_at	CCDC126	coiled-coil domain containing 126	0.65	1.65E-02
203212_s_at	MTMR2	myotubularin related protein 2	0.65	2.01E-02
213981_at	COMT	catechol-O-methyltransferase	0.65	1.56E-02
224399_at	PDCD1LG2	programmed cell death 1 ligand 2	0.66	2.02E-02
201869_s_at	TBL1X	transducin (beta)-like 1X-linked	0.66	1.76E-02
212179_at	SFRS18	splicing factor, arginine/serine-rich 18	0.66	1.65E-02
224298_s_at	UBAC2	UBA domain containing 2	0.66	1.68E-02
229083_at	NA	NA	0.66	1.96E-02
238621_at	FMN1	formin 1	0.66	2.93E-02

...continuous on the next page

Probe set ID	Gene symbol	Gene name	logFc	adj. p-value
221918_at	CDK17	cyclin-dependent kinase 17	0.66	1.74E-02
212385_at	TCF4	transcription factor 4	0.66	1.92E-02
223595_at	TMEM133	transmembrane protein 133	0.66	1.80E-02
1554863_s_at	DOK5	docking protein 5	0.66	1.97E-02
209409_at	GRB10	growth factor receptor-bound protein 10	0.66	1.76E-02
213400_s_at	TBL1X	transducin (beta)-like 1X-linked	0.66	1.62E-02
214785_at	VPS13A	vacuolar protein sorting 13 homolog A (S. cerevisiae)	0.66	1.50E-02
238568_s_at	NA	NA	0.66	4.98E-02
210078_s_at	KCNAB1	potassium voltage-gated channel, shaker-related subfamily, beta member 1	0.67	4.08E-02
227856_at	C4orf32	chromosome 4 open reading frame 32	0.67	4.32E-02
222587_s_at	GALNT7	UDP-N-acetyl-alpha-D-galactosamine:polypeptide N-acetylgalactosaminyltransferase 7 (GalNAc-T7)	0.67	2.97E-02
226810_at	OGFRL1	opioid growth factor receptor-like 1	0.67	2.91E-02
235045_at	RBM7	RNA binding motif protein 7	0.67	1.85E-02
229845_at	MAPKAP1	mitogen-activated protein kinase associated protein 1	0.67	1.61E-02
46665_at	SEMA4C	sema domain, immunoglobulin domain (Ig), transmembrane domain (TM) and short cytoplasmic domain, (semaphorin) 4C	0.67	2.46E-02
225282_at	SMAP2	small ArfGAP2	0.67	2.68E-02
229145_at	ANAPC16	anaphase promoting complex subunit 16	0.67	7.08E-02
228941_at	ALG10B	asparagine-linked glycosylation 10, alpha-1,2-glucosyltransferase homolog B (yeast)	0.67	1.96E-02
226769_at	FIBIN	fin bud initiation factor homolog (zebrafish)	0.67	2.91E-02
203139_at	DAPK1	death-associated protein kinase 1	0.68	4.94E-02
217127_at	CTH	cystathionase (cystathionine gamma-lyase)	0.68	5.60E-02
220254_at	LRP12	low density lipoprotein receptor-related protein 12	0.68	4.06E-02

...continuous on the next page

Probe set ID	Gene symbol	Gene name	logFc	adj. p-value
238129_s_at	FZD2	frizzled homolog 2 (Drosophila)	0.68	1.63E-02
228710_at	NA	NA	0.68	1.62E-02
206584_at	LY96	lymphocyte antigen 96	0.68	5.11E-02
228569_at	PAPOLA	poly(A) polymerase alpha	0.68	1.62E-02
228785_at	ZNF281	zinc finger protein 281	0.68	4.10E-02
225085_at	USP40	ubiquitin specific peptidase 40	0.68	1.60E-02
223196_s_at	SESN2	sestrin 2	0.68	1.77E-02
226338_at	TMEM55A	transmembrane protein 55A	0.69	1.80E-02
233072_at	NTNG2	netrin G2	0.69	1.87E-02
226309_at	DNAL1	dynein, axonemal, light chain 1	0.69	1.45E-02
239336_at	THBS1	thrombospondin 1	0.69	1.85E-02
208926_at	NEU1	sialidase 1 (lysosomal sialidase)	0.69	2.22E-02
224455_s_at	ADPGK	ADP-dependent glucokinase	0.69	1.85E-02
225871_at	STEAP2	six transmembrane epithelial antigen of the prostate 2	0.69	1.62E-02
224627_at	GBA2	glucosidase, beta (bile acid) 2	0.69	1.62E-02
226756_at	NA	NA	0.69	1.57E-02
218465_at	TMEM33	transmembrane protein 33	0.69	1.56E-02
219636_s_at	ARMC9	armadillo repeat containing 9	0.69	6.84E-02
203355_s_at	PSD3	pleckstrin and Sec7 domain containing 3	0.70	4.73E-02
239201_at	CDK15	cyclin-dependent kinase 15	0.70	1.96E-02
229299_at	C5orf33	chromosome 5 open reading frame 33	0.70	1.85E-02
228080_at	LAYN	layilin	0.70	2.17E-02
212855_at	DCUN1D4	DCN1, defective in cullin neddylation 1, domain containing 4 (S. cerevisiae)	0.71	1.49E-02
228360_at	LYPD6B	LY6/PLAUR domain containing 6B	0.71	1.77E-02
202846_s_at	PIGC	phosphatidylinositol glycan anchor biosynthesis, class C	0.71	1.89E-02
202350_s_at	MATN2	matrilin 2	0.71	1.81E-02
212425_at	SCAMP1	secretory carrier membrane protein 1	0.71	1.74E-02
224748_at	DCAF7	DDB1 and CUL4 associated factor 7	0.71	1.76E-02
206197_at	NME5	non-metastatic cells 5, protein expressed in (nucleoside-diphosphate kinase)	0.71	1.82E-02

...continuous on the next page

Probe set ID	Gene symbol	Gene name	logFc	adj. p-value
201867_s_at	TBL1X	transducin (beta)-like 1X-linked	0.71	1.81E-02
1558142_at	TNRC6B	trinucleotide repeat containing 6B	0.71	1.76E-02
216178_x_at	ITGB1	integrin, beta 1 (fibronectin receptor, beta polypeptide, antigen CD29 includes MDF2, MSK12)	0.71	4.08E-02
222105_s_at	NKIRAS2	NFKB inhibitor interacting Ras-like 2	0.72	1.44E-02
204462_s_at	SLC16A2	solute carrier family 16, member 2 (monocarboxylic acid transporter 8)	0.72	1.79E-02
216870_x_at	DLEU2	deleted in lymphocytic leukemia 2 (non-protein coding)	0.72	5.80E-02
212387_at	TCF4	transcription factor 4	0.72	1.38E-02
225492_at	TMEM33	transmembrane protein 33	0.72	1.60E-02
229611_at	LMLN	leishmanolysin-like (metallopeptidase M8 family)	0.72	1.80E-02
214844_s_at	DOK5	docking protein 5	0.72	2.16E-02
223800_s_at	LIMS3	LIM and senescent cell antigen-like domains 3	0.72	6.58E-02
1554007_at	NA	NA	0.73	2.55E-02
218421_at	CERK	ceramide kinase	0.73	1.65E-02
242828_at	FIGN	fidgetin	0.73	5.64E-02
223182_s_at	AGPAT3	1-acylglycerol-3-phosphate O-acyltransferase 3	0.73	1.56E-02
221744_at	DCAF7	DDB1 and CUL4 associated factor 7	0.73	1.96E-02
235573_at	NA	NA	0.73	3.01E-02
214043_at	PTPRD	protein tyrosine phosphatase, receptor type, D	0.73	5.78E-02
222619_at	ZNF281	zinc finger protein 281	0.73	4.70E-02
218748_s_at	EXOC5	exocyst complex component 5	0.73	4.93E-02
202817_s_at	SS18	synovial sarcoma translocation, chromosome 18	0.74	1.45E-02
212957_s_at	LOC92249	hypothetical LOC92249	0.74	1.39E-02
208916_at	SLC1A5	solute carrier family 1 (neutral amino acid transporter), member 5	0.74	3.38E-02
203921_at	CHST2	carbohydrate (N-acetylglucosamine-6-O) sulfotransferase 2	0.74	1.76E-02

...continuous on the next page

Probe set ID	Gene symbol	Gene name	logFc	adj. p-value
223249_at	CLDN12	claudin 12	0.74	1.61E-02
218589_at	LPAR6	lysophosphatidic acid receptor 6	0.74	2.47E-02
213637_at	DDX52	DEAD (Asp-Glu-Ala-Asp) box polypeptide 52	0.74	1.65E-02
226546_at	NA	NA	0.74	1.56E-02
231862_at	CBX5	chromobox homolog 5	0.74	2.34E-02
218915_at	NF2	neurofibromin 2 (merlin)	0.74	2.15E-02
204201_s_at	PTPN13	protein tyrosine phosphatase, non-receptor type 13 (APO-1/CD95 (Fas)-associated phosphatase)	0.74	1.62E-02
219532_at	ELOVL4	elongation of very long chain fatty acids (FEN1/Elo2, SUR4/Elo3, yeast)-like 4	0.74	1.45E-02
221898_at	PDPN	podoplanin	0.74	1.89E-02
201564_s_at	FSCN1	fascin homolog 1, actin-bundling protein (Strongylocentrotus purpuratus)	0.75	1.80E-02
218258_at	POLR1D	polymerase (RNA) I polypeptide D, 16kDa	0.75	1.85E-02
214383_x_at	KLHDC3	kelch domain containing 3	0.75	1.68E-02
224653_at	EIF4EBP2	eukaryotic translation initiation factor 4E binding protein 2	0.75	1.56E-02
227554_at	LOC100505881	hypothetical LOC100505881	0.76	2.10E-02
202679_at	NPC1	Niemann-Pick disease, type C1	0.76	1.80E-02
201489_at	PPIF	peptidylprolyl isomerase F	0.77	1.62E-02
218559_s_at	MAFB	v-maf musculoaponeurotic fibrosarcoma oncogene homolog B (avian)	0.77	1.45E-02
225426_at	PPP6C	protein phosphatase 6, catalytic subunit	0.77	1.44E-02
215629_s_at	NA	NA	0.77	6.65E-02
212623_at	TMEM41B	transmembrane protein 41B	0.77	2.22E-02
243438_at	PDE7B	phosphodiesterase 7B	0.77	3.32E-02
219572_at	CADPS2	Ca++-dependent secretion activator 2	0.77	1.80E-02
230201_at	NA	NA	0.77	1.68E-02
213372_at	PAQR3	progestin and adipoQ receptor family member III	0.78	1.39E-02

...continuous on the next page

Probe set ID	Gene symbol	Gene name	logFc	adj. p-value
227126_at	PTPRG	protein tyrosine phosphatase, receptor type, G	0.78	1.85E-02
228946_at	INTU	inturned planar cell polarity effector homolog (Drosophila)	0.78	6.27E-02
228605_at	NA	NA	0.78	1.39E-02
242352_at	NIPBL	Nipped-B homolog (Drosophila)	0.78	1.62E-02
206932_at	CH25H	cholesterol 25-hydroxylase	0.78	1.85E-02
227132_at	ZNF706	zinc finger protein 706	0.79	1.52E-02
235384_at	NUDT19	nudix (nucleoside diphosphate linked moiety X)-type motif 19	0.79	1.34E-02
204926_at	INHBA	inhibin, beta A	0.79	1.44E-02
244574_at	PTPRG	protein tyrosine phosphatase, receptor type, G	0.79	2.15E-02
242923_at	ZNF678	zinc finger protein 678	0.79	1.58E-02
210220_at	FZD2	frizzled homolog 2 (Drosophila)	0.79	1.48E-02
239866_at	NA	NA	0.79	1.68E-02
226390_at	STARD4	StAR-related lipid transfer (START) domain containing 4	0.79	1.99E-02
239468_at	MKX	mohawk homeobox	0.79	3.12E-02
203908_at	SLC4A4	solute carrier family 4, sodium bicarbonate cotransporter, member 4	0.80	2.45E-02
208957_at	ERP44	endoplasmic reticulum protein 44	0.80	1.85E-02
236016_at	NA	NA	0.80	1.79E-02
209700_x_at	PDE4DIP	phosphodiesterase 4D interacting protein	0.80	1.82E-02
1554020_at	BICD1	bicaudal D homolog 1 (Drosophila)	0.80	3.41E-02
222820_at	TNRC6C	trinucleotide repeat containing 6C	0.80	1.44E-02
204984_at	GPC4	glypican 4	0.81	5.14E-02
203283_s_at	HS2ST1	heparan sulfate 2-O-sulfotransferase 1	0.81	1.52E-02
1560792_at	NA	NA	0.81	1.68E-02
217918_at	DYNLRB1	dynein, light chain, roadblock-type 1	0.81	1.45E-02
236265_at	SP4	Sp4 transcription factor	0.81	1.84E-02
201009_s_at	TXNIP	thioredoxin interacting protein	0.81	5.11E-02
226868_at	GXYLT1	glucoside xylosyltransferase 1	0.82	2.06E-02

...continuous on the next page

Probe set ID	Gene symbol	Gene name	logFc	adj. p-value
238468_at	TNRC6B	trinucleotide repeat containing 6B	0.82	1.57E-02
220794_at	GREM2	gremlin 2	0.82	1.59E-02
242138_at	DLX1	distal-less homeobox 1	0.82	1.80E-02
224835_at	GPCPD1	glycerophosphocholine phosphodiesterase GDE1 homolog (S. cerevisiae)	0.82	1.22E-02
244503_at	NA	NA	0.82	6.48E-02
223183_at	AGPAT3	1-acylglycerol-3-phosphate O-acyltransferase 3	0.82	1.39E-02
204627_s_at	ITGB3	integrin, beta 3 (platelet glycoprotein IIIa, antigen CD61)	0.82	1.79E-02
204435_at	NUPL1	nucleoporin like 1	0.82	1.77E-02
231944_at	ERO1LB	ERO1-like beta (S. cerevisiae)	0.82	1.22E-02
217917_s_at	DYNLRB1	dynein, light chain, roadblock-type 1	0.82	1.45E-02
229951_x_at	NA	NA	0.82	1.85E-02
230779_at	TNRC6B	trinucleotide repeat containing 6B	0.82	1.56E-02
212609_s_at	AKT3	v-akt murine thymoma viral oncogene homolog 3 (protein kinase B, gamma)	0.83	1.85E-02
223264_at	MESDC1	mesoderm development candidate 1	0.83	1.96E-02
224730_at	DCAF7	DDB1 and CUL4 associated factor 7	0.83	2.37E-02
224676_at	TMED4	transmembrane emp24 protein transport domain containing 4	0.83	1.49E-02
211742_s_at	EVI2B	ecotropic viral integration site 2B	0.83	6.18E-02
228396_at	PRKG1	protein kinase, cGMP-dependent, type I	0.83	4.26E-02
229431_at	RFXAP	regulatory factor X-associated protein	0.83	1.44E-02
205003_at	DOCK4	dedicator of cytokinesis 4	0.83	1.81E-02
225957_at	C5orf41	chromosome 5 open reading frame 41	0.83	2.49E-02
242939_at	TFDP1	transcription factor Dp-1	0.83	1.62E-02
221787_at	C6orf120	chromosome 6 open reading frame 120	0.83	1.34E-02
205159_at	CSF2RB	colony stimulating factor 2 receptor, beta, low-affinity (granulocyte-macrophage)	0.83	1.68E-02
239286_at	CDH11	cadherin 11, type 2, OB-cadherin (osteoblast)	0.84	1.62E-02
221814_at	GPR124	G protein-coupled receptor 124	0.84	5.66E-02

...continuous on the next page

Probe set ID	Gene symbol	Gene name	logFc	adj. p-value
207057_at	SLC16A7	solute carrier family 16, member 7 (monocarboxylic acid transporter 2)	0.84	6.18E-02
206117_at	TPM1	tropomyosin 1 (alpha)	0.84	2.69E-02
231726_at	PCDHB14	protocadherin beta 14	0.84	4.26E-02
239082_at	FZD3	frizzled homolog 3 (Drosophila)	0.84	4.55E-02
208370_s_at	RCAN1	regulator of calcineurin 1	0.84	1.65E-02
226745_at	CYP4V2	cytochrome P450, family 4, subfamily V, polypeptide 2	0.84	2.57E-02
209031_at	CADM1	cell adhesion molecule 1	0.84	5.34E-02
211965_at	ZFP36L1	zinc finger protein 36, C3H type-like 1	0.85	4.86E-02
235556_at	C5orf41	chromosome 5 open reading frame 41	0.85	2.77E-02
217851_s_at	SLMO2	slowmo homolog 2 (Drosophila)	0.85	1.43E-02
219155_at	PITPNC1	phosphatidylinositol transfer protein, cytoplasmic 1	0.85	4.34E-02
215711_s_at	WEE1	WEE1 homolog (S. pombe)	0.85	5.17E-02
227692_at	GNAI1	guanine nucleotide binding protein (G protein), alpha inhibiting activity polypeptide 1	0.85	1.48E-02
228971_at	NA	NA	0.86	1.34E-02
235927_at	XPO1	exportin 1 (CRM1 homolog, yeast)	0.86	5.71E-02
224998_at	CMTM4	CKLF-like MARVEL transmembrane domain containing 4	0.86	3.07E-02
228188_at	FOSL2	FOS-like antigen 2	0.86	1.80E-02
202888_s_at	ANPEP	alanyl (membrane) aminopeptidase	0.87	2.77E-02
235392_at	NA	NA	0.87	2.25E-02
223218_s_at	NFKBIZ	nuclear factor of kappa light polypeptide gene enhancer in B-cells inhibitor, zeta	0.87	1.85E-02
206805_at	SEMA3A	sema domain, immunoglobulin domain (Ig), short basic domain, secreted, (semaphorin) 3A	0.87	2.50E-02
235061_at	PPM1K	protein phosphatase, Mg2+/Mn2+ dependent, 1K	0.87	2.25E-02
221745_at	DCAF7	DDB1 and CUL4 associated factor 7	0.88	1.85E-02
223475_at	CRISPLD1	cysteine-rich secretory protein LCCL domain containing 1	0.88	2.46E-02

...continuous on the next page

Probe set ID	Gene symbol	Gene name	logFc	adj. p-value
212533_at	WEE1	WEE1 homolog (S. pombe)	0.88	5.20E-02
200901_s_at	M6PR	mannose-6-phosphate receptor (cation dependent)	0.88	1.34E-02
239367_at	BDNF	brain-derived neurotrophic factor	0.89	1.18E-02
227040_at	NHLRC3	NHL repeat containing 3	0.89	3.46E-02
201490_s_at	PPIF	peptidylprolyl isomerase F	0.89	1.80E-02
209892_at	FUT4	fucosyltransferase 4 (alpha (1,3) fucosyltransferase, myeloid-specific)	0.89	1.45E-02
226038_at	LONRF1	LON peptidase N-terminal domain and ring finger 1	0.90	2.03E-02
235205_at	LOC346887	similar to solute carrier family 16 (monocarboxylic acid transporters), member 14	0.90	1.85E-02
226233_at	B3GALNT2	beta-1,3-N-acetylgalactosaminyltransferase 2	0.90	1.44E-02
219637_at	ARMC9	armadillo repeat containing 9	0.90	5.18E-02
201008_s_at	TXNIP	thioredoxin interacting protein	0.90	5.26E-02
1569290_s_at	GRIA3	glutamate receptor, ionotrophic, AMPA 3	0.90	2.08E-02
210807_s_at	SLC16A7	solute carrier family 16, member 7 (monocarboxylic acid transporter 2)	0.91	4.84E-02
212343_at	YIPF6	Yip1 domain family, member 6	0.91	1.18E-02
236179_at	CDH11	cadherin 11, type 2, OB-cadherin (osteoblast)	0.91	1.56E-02
226085_at	CBX5	chromobox homolog 5	0.91	2.22E-02
232021_at	GXYLT1	glucoside xylosyltransferase 1	0.91	3.16E-02
230003_at	NA	NA	0.92	1.18E-02
207147_at	DLX2	distal-less homeobox 2	0.92	1.44E-02
200900_s_at	M6PR	mannose-6-phosphate receptor (cation dependent)	0.92	2.10E-02
218976_at	DNAJC12	DnaJ (Hsp40) homolog, subfamily C, member 12	0.92	1.79E-02
224847_at	CDK6	cyclin-dependent kinase 6	0.93	2.01E-02
212094_at	PEG10	paternally expressed 10	0.93	1.18E-02

...continuous on the next page

Probe set ID	Gene symbol	Gene name	logFc	adj. p-value
241866_at	SLC16A7	solute carrier family 16, member 7 (monocarboxylic acid transporter 2)	0.93	2.13E-02
212565_at	STK38L	serine/threonine kinase 38 like	0.93	4.80E-02
230766_at	GART	phosphoribosylglycinamide formyltransferase, phosphoribosylglycinamide synthetase, phosphoribosylaminoimidazole synthetase	0.94	1.85E-02
1555167_s_at	NAMPT	nicotinamide phosphoribosyltransferase	0.94	4.86E-02
227568_at	HECTD2	HECT domain containing 2	0.94	1.77E-02
205609_at	ANGPT1	angiopoietin 1	0.94	2.57E-02
226430_at	RELL1	RELT-like 1	0.95	1.82E-02
222880_at	AKT3	v-akt murine thymoma viral oncogene homolog 3 (protein kinase B, gamma)	0.95	2.34E-02
212624_s_at	CHN1	chimerin (chimaerin) 1	0.95	5.02E-02
224848_at	CDK6	cyclin-dependent kinase 6	0.95	3.60E-02
235518_at	SLC8A1	solute carrier family 8 (sodium/calcium exchanger), member 1	0.97	1.18E-02
228325_at	KIAA0146	KIAA0146	0.97	1.44E-02
210829_s_at	SSBP2	single-stranded DNA binding protein 2	0.97	2.16E-02
213469_at	PGAP1	post-GPI attachment to proteins 1	0.97	1.56E-02
238045_at	TMEM65	transmembrane protein 65	0.97	1.45E-02
1554018_at	GPNMB	glycoprotein (transmembrane) nmb	0.97	1.82E-02
244881_at	LMLN	leishmanolysin-like (metallopeptidase M8 family)	0.98	1.18E-02
231001_at	FIBIN	fin bud initiation factor homolog (zebrafish)	0.99	3.45E-02
225009_at	CMTM4	CKLF-like MARVEL transmembrane domain containing 4	0.99	1.85E-02
236826_at	TTC39B	tetratricopeptide repeat domain 39B	0.99	1.39E-02
218817_at	SPCS3	signal peptidase complex subunit 3 homolog (S. cerevisiae)	0.99	1.80E-02
228466_at	NA	NA	1.00	1.39E-02
221765_at	UGCG	UDP-glucose ceramide glucosyltransferase	1.00	1.77E-02
239903_at	NA	NA	1.00	4.14E-02

...continuous on the next page

Probe set ID	Gene symbol	Gene name	logFc	adj. p-value
223854_at	PCDHB10	protocadherin beta 10	1.00	2.55E-02
238546_at	SLC8A1	solute carrier family 8 (sodium/calcium exchanger), member 1	1.01	1.39E-02
205941_s_at	COL10A1	collagen, type X, alpha 1	1.01	3.60E-02
229800_at	DCLK1	doublecortin-like kinase 1	1.01	1.39E-02
241925_x_at	NA	NA	1.01	1.39E-02
203787_at	SSBP2	single-stranded DNA binding protein 2	1.02	1.88E-02
225429_at	PPP6C	protein phosphatase 6, catalytic subunit	1.02	1.18E-02
204881_s_at	UGCG	UDP-glucose ceramide glucosyltransferase	1.02	4.09E-02
206061_s_at	DICER1	dicer 1, ribonuclease type III	1.02	2.01E-02
219338_s_at	LRRC49	leucine rich repeat containing 49	1.02	1.45E-02
228391_at	CYP4V2	cytochrome P450, family 4, subfamily V, polypeptide 2	1.02	3.49E-02
224645_at	EIF4EBP2	eukaryotic translation initiation factor 4E binding protein 2	1.03	1.18E-02
203666_at	CXCL12	chemokine (C-X-C motif) ligand 12	1.03	1.18E-02
209267_s_at	SLC39A8	solute carrier family 39 (zinc transporter), member 8	1.03	2.01E-02
213229_at	DICER1	dicer 1, ribonuclease type III	1.03	2.43E-02
202856_s_at	SLC16A3	solute carrier family 16, member 3 (monocarboxylic acid transporter 4)	1.04	1.80E-02
235907_at	TMEM33	transmembrane protein 33	1.04	1.18E-02
203284_s_at	HS2ST1	heparan sulfate 2-O-sulfotransferase 1	1.04	1.44E-02
227963_at	NA	NA	1.04	1.56E-02
206118_at	STAT4	signal transducer and activator of transcription 4	1.05	1.74E-02
213006_at	CEBPD	CCAAT/enhancer binding protein (C/EBP), delta	1.05	1.56E-02
223541_at	HAS3	hyaluronan synthase 3	1.05	1.81E-02
224851_at	CDK6	cyclin-dependent kinase 6	1.06	2.26E-02
217739_s_at	NAMPT	nicotinamide phosphoribosyltransferase	1.07	1.85E-02
214981_at	POSTN	periostin, osteoblast specific factor	1.08	2.01E-02
204491_at	PDE4D	phosphodiesterase 4D, cAMP-specific	1.08	2.96E-02

...continuous on the next page

Probe set ID	Gene symbol	Gene name	logFc	adj. p-value
235780_at	PRKACB	protein kinase, cAMP-dependent, catalytic, beta	1.09	1.18E-02
202282_at	HSD17B10	hydroxysteroid (17-beta) dehydrogenase 10	1.10	3.04E-02
235348_at	ABHD13	abhydrolase domain containing 13	1.11	1.39E-02
204774_at	EVI2A	ecotropic viral integration site 2A	1.11	2.23E-02
203435_s_at	MME	membrane metallo-endopeptidase	1.12	5.86E-02
229744_at	SSFA2	sperm specific antigen 2	1.12	1.18E-02
228540_at	QKI	quaking homolog, KH domain RNA binding (mouse)	1.12	3.02E-02
242594_at	BOD1L	biorientation of chromosomes in cell division 1-like	1.13	2.27E-02
203946_s_at	ARG2	arginase, type II	1.13	2.01E-02
228481_at	NA	NA	1.15	3.07E-02
228962_at	PDE4D	phosphodiesterase 4D, cAMP-specific	1.16	4.53E-02
227084_at	DTNA	dystrobrevin, alpha	1.16	1.49E-02
202855_s_at	SLC16A3	solute carrier family 16, member 3 (monocarboxylic acid transporter 4)	1.18	2.26E-02
1559496_at	PPA2	pyrophosphatase (inorganic) 2	1.18	1.18E-02
228493_at	NA	NA	1.19	1.18E-02
241342_at	TMEM65	transmembrane protein 65	1.20	8.22E-03
203989_x_at	F2R	coagulation factor II (thrombin) receptor	1.20	2.66E-02
217428_s_at	COL10A1	collagen, type X, alpha 1	1.21	2.78E-02
226189_at	ITGB8	integrin, beta 8	1.22	1.18E-02
210998_s_at	HGF	hepatocyte growth factor (hepapoietin A; scatter factor)	1.23	4.08E-02
1561615_s_at	SLC8A1	solute carrier family 8 (sodium/calcium exchanger), member 1	1.24	2.44E-02
210997_at	HGF	hepatocyte growth factor (hepapoietin A; scatter factor)	1.25	2.34E-02
227929_at	NA	NA	1.26	1.87E-02
202499_s_at	SLC2A3	solute carrier family 2 (facilitated glucose transporter), member 3	1.26	4.63E-02
205608_s_at	ANGPT1	angiopoietin 1	1.26	1.18E-02

...continuous on the next page

Probe set ID	Gene symbol	Gene name	logFc	adj. p-value
217738_at	NAMPT	nicotinamide phosphoribosyltransferase	1.27	1.45E-02
202498_s_at	SLC2A3	solute carrier family 2 (facilitated glucose transporter), member 3	1.28	5.68E-02
1552508_at	KCNE4	potassium voltage-gated channel, Isk-related family, member 4	1.30	4.32E-02
222088_s_at	NA	NA	1.30	5.81E-02
209198_s_at	SYT11	synaptotagmin XI	1.31	1.18E-02
222379_at	KCNE4	potassium voltage-gated channel, Isk-related family, member 4	1.31	5.48E-02
209197_at	SYT11	synaptotagmin XI	1.32	1.18E-02
228186_s_at	RSPO3	R-spondin 3 homolog (Xenopus laevis)	1.32	2.78E-02
227368_at	NA	NA	1.34	1.34E-02
1568611_at	NA	NA	1.34	1.88E-02
210755_at	HGF	hepatocyte growth factor (hepapoietin A; scatter factor)	1.35	2.91E-02
204748_at	PTGS2	prostaglandin-endoperoxide synthase 2 (prostaglandin G/H synthase and cyclooxygenase)	1.36	1.85E-02
239835_at	KBTBD8	kelch repeat and BTB (POZ) domain containing 8	1.38	1.18E-02
208096_s_at	COL21A1	collagen, type XXI, alpha 1	1.39	4.21E-02
228817_at	ALG9	asparagine-linked glycosylation 9, alpha-1,2-mannosyltransferase homolog (S. cerevisiae)	1.40	1.18E-02
1554997_a_at	PTGS2	prostaglandin-endoperoxide synthase 2 (prostaglandin G/H synthase and cyclooxygenase)	1.41	1.49E-02
205475_at	SCRG1	stimulator of chondrogenesis 1	1.42	3.87E-02
235004_at	RBM24	RNA binding motif protein 24	1.44	1.80E-02
212636_at	QKI	quaking homolog, KH domain RNA binding (mouse)	1.48	1.62E-02
225496_s_at	SYTL2	synaptotagmin-like 2	1.49	1.34E-02
232914_s_at	SYTL2	synaptotagmin-like 2	1.53	1.18E-02
232000_at	TTC39B	tetratricopeptide repeat domain 39B	1.57	1.39E-02
207148_x_at	MYOZ2	myozenin 2	1.58	8.22E-03

...continuous on the next page

Probe set ID	Gene symbol	Gene name	logFc	adj. p-value
224680_at	TMED4	transmembrane emp24 protein transport domain containing 4	1.65	8.22E-03
205113_at	NEFM	neurofilament, medium polypeptide	1.67	5.68E-02
244360_at	FBXL17	F-box and leucine-rich repeat protein 17	1.69	1.16E-02
213222_at	PLCB1	phospholipase C, beta 1 (phosphoinositide-specific)	1.70	1.80E-02
213782_s_at	MYOZ2	myozenin 2	1.75	8.22E-03

Journal Publications

- Schlegelmilch K, Keller A, Zehe V, **Hondke S**, Schilling T, Jakob F, Klein-Hitpass L,Schütze N, "WISP1 is an important survival factor in human mesenchymal stromal cells.", *Gene*, 10;551(2):243-54, Nov. 2014

- Krüger JP, **Hondke S**, Endres M, Pruss A, Siclari A, Kaps C, "Human platelet-rich plasma stimulates migration and chondrogenic differentiation of human subchondral progenitor cells.", *Journal of orthopaedic research*, vol. 30, pp. 845-52, Jun. 2012

- Stoll C, John T, Conrad C, Lohan A, **Hondke S**, Ertel W, Kaps C, Endres M, Sittinger M, Ringe J, Schulze-Tanzil G, "Healing parameters in a rabbit partial tendon defect following tenocyte/biomaterial implantation.", *Biomaterials*, vol. 32, pp. 4806-15, Jul. 2011

Oral Presentation

- **Hondke S**, Hilpert S, Zehe V, Schlegelmilch K, Keller A, Schütze N, "WISP1 and -3 affect cell survival in human mesenchymal stem cells (hMSCs) and TC28a2 chondrocytes", *3rd International Conference "Strategies in Tissue Engineering"*, Würzburg - Germany, May 2012

Poster Presentation

- **Hondke S**, Hilpert S, Zehe V, Schlegelmilch K, Keller A, Wiesner S, Schütze N, "Funktionsaufklärung von WISP3 Protein in humanen Chondrozyten und humanen mesenchymalen Stammzellen.", *Osteology Congress*, Basel - Swiss, Mar. 2012
  received **Poster price** from the DVO (umbrella association osteology)

- **Hondke S**, Zehe V, Schlegelmilch K, Keller A, Wiesner S, Schütze N, "WISP3 beeinflusst das Überleben von humanen Chondrozyten und mesenchymalen Stammzellen.", *Osteology Congress*, Weimar - Germany, Mar. 2013

- **Hondke S**, Zehe V, Schlegelmilch K, Wiesner S, Keller A, Schütze N, "WISP3 affects cell survival in human chondrocytes and mesenchymal stem cells.", *American Society for Bone and Mineral Research - Annual Meeting*, Baltimore - USA, Oct. 2013

- **Hondke S**, Zehe V, Schlegelmilch K, Wiesner S, Keller A, Schütze N, "WISP3 - an important survival factor in human chondrocytes and mesenchymal stem cells.", *TERMIS EU Congress*, Genoa - Italy, Jun. 2014